Department of
Industry and Resources

REPORT
104

# GEOCHEMISTRY OF VOLCANIC ROCKS OF THE NORTHERN PILBARA CRATON WESTERN AUSTRALIA

by R. H. Smithies, D. C. Champion,
M. J. Van Kranendonk and A. H. Hickman

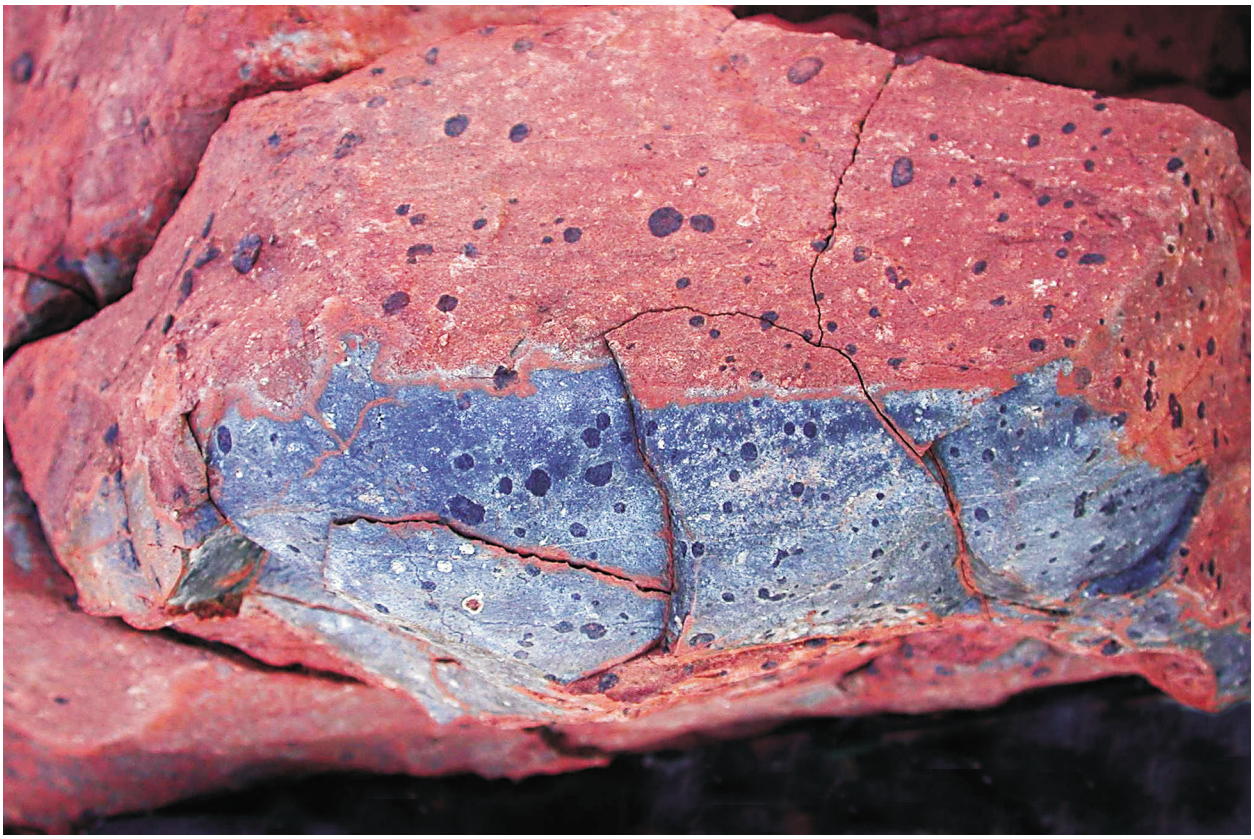

Geological Survey of Western Australia


GEOLOGICAL SURVEY OF WESTERN AUSTRALIA

REPORT 104

# GEOCHEMISTRY OF VOLCANIC ROCKS OF THE NORTHERN PILBARA CRATON

by
R. H. Smithies, D. C. Champion[1], M. J. Van Kranendonk, and A. H. Hickman

[1] Geoscience Australia, GPO Box 378, Canberra, ACT 2601

Perth 2007

**REFERENCE**
**The recommended reference for this publication is:**
SMITHIES, R. H., CHAMPION, D. C., VAN KRANENDONK, M. J., and HICKMAN, A. H., 2007, Geochemistry of volcanic rocks of the northern Pilbara Craton, Western Australia: Western Australia Geological Survey, Report 104, 47p.

**National Library of Australia**
**Cataloguing-in-publication entry**

(Geochemistry of volcanic rocks of the northern Pilbara Craton, Western Australia)

**Bibliography.**
**ISBN 978-1-74168-122-2 (web)**

1. Geochemistry — Western Australia — Pilbara
2. Volcanic ash, tuff, etc. — Western Australia — Pilbara
3. Rocks, Igneous — Analysis
I. Smithies, Robert Hugh, 1962–
II. (Title. (Series: Report (Geological Survey of Western Australia); 104).

552.06

**ISSN 0508–4741**

**Grid references in this publication refer to the Geocentric Datum of Australia 1994 (GDA94). Locations mentioned in the text are referenced using Map Grid Australia (MGA) coordinates, Zones 50 and 51. All locations are quoted to at least the nearest 100 m.**

Copy editor: J. F. Johnston
Cartography: A. Blake, S. Dowsett
Desktop publishing: K. S. Noonan

**Published 2007 by Geological Survey of Western Australia**
**This Report is published in digital format (PDF), and is available online at www.doir.wa.gov.au/GSWA/publications.**
**Laser-printed copies can be ordered from the Information Centre for the cost of printing and binding.**

**Further details of geological publications and maps produced by the Geological Survey of Western Australia are available from:**
Information Centre
Department of Industry and Resources
100 Plain Street
EAST PERTH, WESTERN AUSTRALIA 6004
Telephone: +61 8 9222 3459 Facsimile: +61 8 9222 3444
**www.doir.wa.gov.au/GSWA/publications**

**Cover photograph:**

Mafic globules within a basalt at the transition zone between the tholeiitic basalts and the F1 series, Coonterunah Subgroup, Warrawoona Group. Specimen is from a locality about 6.8 km south-southwest of Table Top Well (MGA Zone 50 711949E 7663602N)

# Contents

# Appendices



# Figures



# Table

# Geochemistry of volcanic rocks of the northern Pilbara Craton

by

**R. H. Smithies, D. C. Champion[1], M. J. Van Kranendonk, and A. H. Hickman**

## Abstract

New geochemical data are presented for 438 whole-rock samples of volcanic rocks from both the East Pilbara Terrane and the West Pilbara Superterrane of the Archean Pilbara Craton. The samples include the full range of volcanic rock types observed in the craton, cover the full c. 3.52 – 2.93 Ga depositional range of the greenstone units within the craton, and are representative of the volcanic lithological units within all of the major tectonic units of the craton.

Komatiites in the East Pilbara Terrane include both Al-depleted and Al-undepleted types, whereas those in the West Pilbara Superterrane are typically Al-undepleted. Basalts in the older (3.52 – 3.23 Ga) sequences (Pilbara Supergroup) of the East Pilbara Terrane can be subdivided into a high-Ti group ($TiO_2$ >0.8 wt%) and a low-Ti group ($TiO_2$ <0.8 wt%). The mantle source for both groups was typically less depleted than a N-MORB source. The low-Ti basalts show a general decrease in incompatible trace element compositions throughout the depositional history of the Pilbara Supergroup that likely reflects an increasingly refractory source. The high-Ti group shows no evolutionary trends over the same period and is likely derived from a series of mantle plumes. Most primitive high- and low-Ti magmas erupted essentially free of significant input from felsic crust. Nevertheless, individual basalt units do show compositions that reflect at least some interaction with felsic crust. However, neither the degree of contamination nor the proportion of contaminated rocks appears to increase significantly with decreasing age.

The geochemical diversity of the felsic volcanic rocks within the Pilbara Supergroup (East Pilbara Terrane) appears to increase with decreasing age. These felsic sequences become generally more silicic and aluminium rich and have higher La/Yb ratios with decreasing age. This can be interpreted in terms of a general increase in the pressure of magma genesis with decreasing age, or an increasing contribution of a source component that was formed at high pressure. The felsic volcanic series more closely match compositions expected from extensively fractionated tholeiitic magmas accompanied by varying degrees of crustal contamination, rather than rocks of the Archean tonalite–trondjemite–granodiorite (TTG) series.

Younger (<3.2 – 2.95 Ga) basalts flank the northern part of the East Pilbara Terrane and basalts of an equivalent age form a significant part of the West Pilbara Superterrane. These basalts differ significantly from older basalts of the East Pilbara Terrane in having strongly enriched trace element signatures (e.g. high La/Sm, La/Nb) that are difficult to explain through assimilation of crust. They require an enriched-mantle source that is interpreted to have formed during an early subduction event (3.2 – 3.1 Ga). Included in this series of rocks are calc-alkaline basalts, Nb-enriched basalts, and boninites of the 3.12 Ga Whundo Group, interpreted to represent an intra-oceanic arc assemblage resulting from this subduction event.

KEYWORDS: Pilbara Craton, East Pilbara Terrane, West Pilbara Superterrane, Archean, geochemistry, volcanic rocks, magmatic fractionation, subduction enrichment, tectonic evolution

## Introduction

The 3.65 – 2.83 Ga Pilbara Craton (Fig. 1) was remapped between 1994 and 2004 by the Geological Survey of Western Australia (GSWA) and Geoscience Australia (GA) as part of a National Geoscience Mapping Accord. The program involved the production of thirty-one 1:100 000-scale map sheets and was designed to cover the full outcrop extent of greenstone belts in the Pilbara Craton, except for inliers exposed through younger rocks of the Mount Bruce Supergroup in the area between Nullagine and Balfour Downs. The program integrated extensive petrological, geochronological, mineralization, and geochemical studies, and provides a firm basis for further geoscientific work in the region.

As part of the geological studies within the region, an extensive program of whole-rock geochemistry was carried out in 2002, sampling all of the major volcanic units of the Pilbara Craton older than the 2.77 – 2.63 Ga Fortescue Group. Where possible, volcanic units were sampled along traverses perpendicular to strike, and as much of the exposed stratigraphic range as outcrop allowed

[1] Geoscience Australia, GPO Box 378, Canberra, ACT 2601

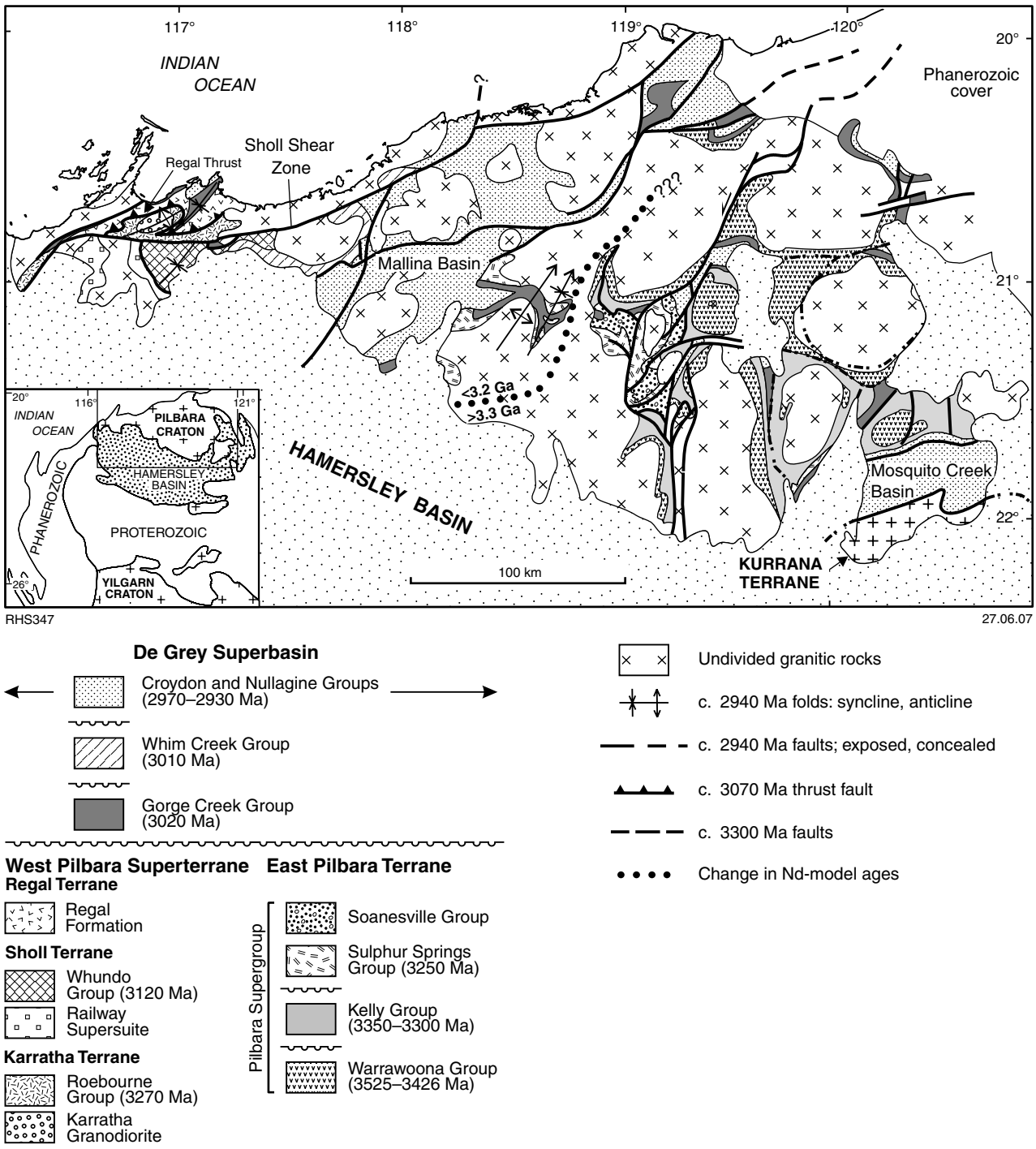


**Figure 1. Location of the East Pilbara Terrane, West Pilbara Superterrane, and the Mallina Basin within the northern Pilbara Craton, Western Australia**

was sampled within each specific unit. The localities of traverses (and other sampling regions) are presented in Figure 2. The results of this program supplement and update those of earlier sampling programs carried out by GSWA and the former Bureau of Mineral Resources, now GA (see Glikson and Hickman, 1981), the data for which are not widely available and lack the precision and accuracy that modern analytical techniques permit for key trace elements.

The purpose of this geochemical project was primarily to:

- identify the geochemical characteristics of the 3.52–2.93 Ga supracrustal sequences;
- identify any diagnostic compositional features that may help to assign isolated outcrops to an established stratigraphy; and
- obtain additional evidence on tectonic settings of volcanic formations.

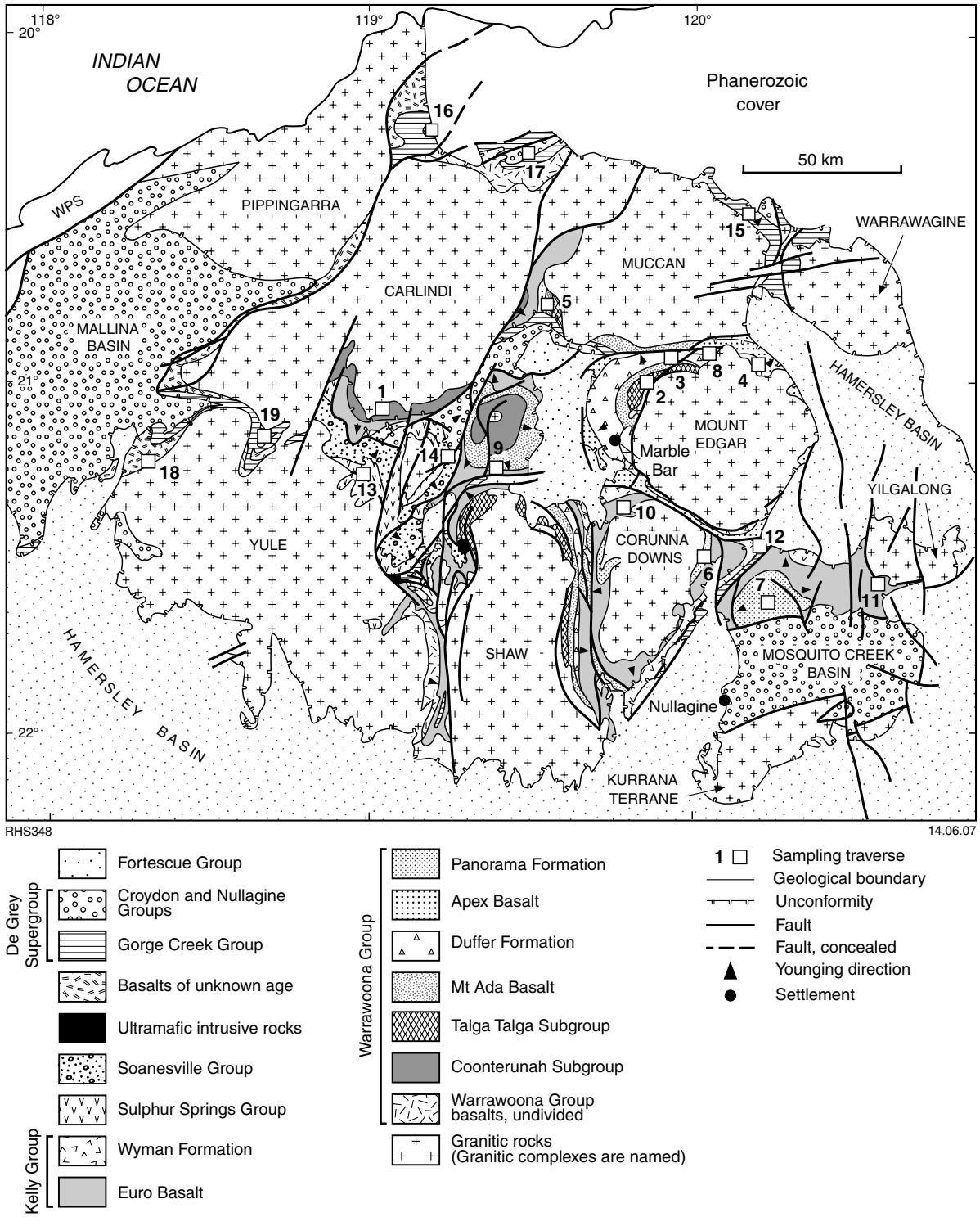


Figure 2. The localities of major sampling traverses throughout the East Pilbara Terrane: 1. Coonterunah Subgroup, Warrawoona Group and Euro Basalt, Kelly Group; East Strelley greenstone belt. 2. North Star Basalt, Warrawoona Group; Marble Bar greenstone belt. 3. Mount Ada Basalt and Duffer Formation, Warrawoona Group; Marble Bar greenstone belt. 4. Apex Basalt, Warrawoona Group; Marble Bar greenstone belt. 5. Apex Basalt, Warrawoona Group; Warralong greenstone belt. 6. Euro Basalt, Kelly Group and Panorama Formation, Warrawoona Group; Sandy Creek area, Kelly greenstone belt. 7. Panorama Formation, Warrawoona Group; McPhee greenstone belt. 8. Panorama Formation, Warrawoona Group; Kittys Gap area, Marble Bar greenstone belt. 9. Panorama Formation, Warrawoona Group; Panorama ridge, Panorama greenstone belt (North Pole Dome). 10. Euro Basalt, Kelly Group; Camel Creek area, northwest Kelly greenstone belt. 11. Euro Basalt, Kelly Group; Mount Elsie greenstone belt. 12. Charteris Basalt, Kelly Group; northeast Kelly greenstone belt. 13. Kunagunarrina Formation, Sulphur Springs Group; Pincunah greenstone belt. 14. Honeyeater Basalt, Soanesville Group; Soanesville greenstone belt. 15. Coonieena Basalt Member, Bookingarra Formation, Croydon Group; Shay Gap greenstone belt (Mallina Basin). 16. Bookingarra Formation, Croydon Group; Ord Ranges (Mallina Basin). 17. Bookingarra Formation, Croydon Group; Goldsworthy area (Mallina Basin). 18. Unassigned greenstones; Pilbara Well greenstone belt. 19. Unassigned greenstones; Wodgina greenstone belt. WPS = West Pilbara Superterrane

For this study, 438 new whole-rock analyses were obtained from ultramafic, mafic, and felsic volcanic rocks (Appendix 1, in digital format) covering most of the geographical extent and depositional age range of the supracrustal sequences within the Pilbara Craton.

This Report presents the entire new geochemical dataset and describes and compares the geochemical characteristics of specific lithostratigraphic units. The geological and tectonic significance of some subsets of the data have already been published (Smithies 2002; Smithies et al., 2004a,b, 2005a,b), and sections of this Report summarize interpretations in those publications.

The Report is essentially divided into three parts, and the approach used in describing the geochemistry of the units in each varies as follows:

(i) The volcanic rocks of the East Pilbara Terrane are grouped, independent of stratigraphic position, into the major lithological types — 'komatiites and komatiitic basalts', 'basaltic rocks' and 'felsic volcanic rocks and felsic series'. This approach was adopted here because there is very little compositional variation between the major lithological types from formation to formation;

(ii) Volcanic rocks of the West Pilbara Superterrane are described by formation because the geochemistry of the volcanic rocks in each formation is distinctive;

(iii) Mafic volcanic rocks of the Mallina Basin are described in terms of the major lithological types — 'basaltic rocks' and 'boninite-like rocks'.

## Nomenclature and terminology

Rock nomenclature used here follows the IUGS classification (Le Maitre, 2002) with the following exceptions:

- Under the IUGS scheme the term 'basalt' is applied to mafic volcanic rocks with $SiO_2$ <52 wt% (anhydrous); however, a large percentage of mafic rocks within the greenstone successions of the Pilbara Craton have between 52 and 55 wt% $SiO_2$ (anhydrous). Although these are widely regarded as basalts, and are informally referred to as basalts, they should be classified as basaltic andesites according to the IUGS classification. For the purposes of the following Report, we use the terms 'basaltic' and 'basalt' to describe a rock within the silica range of basalt and basaltic andesite.
- The term 'siliceous high-magnesian basalt' (Sun et al., 1989) has been used for a class of Archean and Proterozoic mafic igneous rocks, generally in the basaltic andesite silica range, characterized by high MgO contents (and high $Mg^{\#}$ [$Mg^{\#} = (Mg^{2+}/(Mg^{2+}+Fe^{tot})$ where all Fe is as $Fe^{2+}$]) and unusually high concentrations of Th and light rare earth elements.
- Komatiite is used for an ultramafic volcanic rock with >18 wt% MgO and with olivine-spinifex textures, or ultramafic volcanic rocks spatially associated with rocks with such textures.
- Komatiitic basalt is used for volcanic rocks with between 10 and 18 wt% MgO, irrespective of texture.

Unless otherwise stated, all quoted silica values have been calculated on an anhydrous basis. Measured values for loss on ignition (LOI) are given in the data tables. Iron concentrations are given as total iron ($\Sigma$Fe = all Fe calculated as $Fe_2O_3$). Normalization of trace element concentrations is against primitive mantle (PM) values of Sun and McDonough (1989), unless otherwise stated, and is denoted (for example) as $[La/Yb]_{PM}$. In places, normalization against normal mid-oceanic ridge basalt (N-MORB) compositions (Sun and McDonough, 1989) has also been used and is denoted (for example) as $[La/Yb]_N$. Chondritic values used are also those of Sun and McDonough (1989). Other abbreviations used include:

- LILE — large ion lithophile elements (e.g. Cs, K, Rb, Sr, Ba)
- HFSE — high field strength elements (e.g. Nb, Ta, Zr, Hf, Ti)
- REE — rare earth elements (La–Lu)
- LREE — light rare earth elements (e.g. La, Ce)
- MREE — middle rare earth elements (e.g. Gd, Tb)
- HREE — heavy rare earth elements (e.g. Yb, Lu)

Pilbara Craton nomenclature used herein follows that outlined in Van Kranendonk et al. (2006) for all stratigraphic units and tectonic elements.

## Analytical details

Care was taken to ensure samples were fresh and contained no visible veins or alteration. Nevertheless, some of the mafic and ultramafic rocks sampled show low degrees of carbonate alteration and silicification. All samples have also been recrystallized at greenschist facies, as is typical of Archean supracrustal rocks. Metamorphism and hydrothermal alteration can result in mobility of some major elements (particularly Si, Na, K, and Ca, but also Fe) and trace elements (particularly the LILE). However, the REE and HFSE are generally immobile under these conditions (e.g. Arndt et al., 2001) and so these elements are most useful in describing primary (magmatic) compositional variations of the volcanic rocks presented here.

Major elements were determined by wavelength-dispersive XRF spectrometry on fused disks using methods similar to those of Norrish and Hutton (1969). Precision is better than ±1% of the reported values. LOI was determined by gravimetry after combustion at 1100°C. Fe abundances were determined by digestion and electrochemical titration using a modified methodology based on Shapiro and Brannock (1962). The trace elements Ba, Cr, Cu, Ni, Sc, V, Zn, and Zr were determined by wavelength-dispersive XRF spectrometry on a pressed pellet using methods similar to those of Norrish and Chappell (1977), whereas Cs, Ga, Nb, Pb, Rb, Sr, Ta, Th, U, Y, and the REE were analysed by ICP–MS (Perkin Elmer ELAN 6000) using methods similar to those of Eggins et al. (1997), but on solutions obtained by dissolution of fused glass disks (Pyke, 2000). Precision for trace elements is better than ±10% of the reported values. Details of standards used for major and trace element analysis are given in Morris and Pirajno (2005).

# Regional geology

The Pilbara Craton is divided into the 3.65 – 3.17 Ga East Pilbara Terrane, the 3.27 – 3.17 Ga West Pilbara Superterrane, and >3.2 – 3.18 Ga Kurrana Terrane (Van Kranendonk et al., 2006). Each of these terranes (Fig. 3) is characterized by unique lithostratigraphy, structural map patterns, geochemistry, and tectonic histories (Van Kranendonk et al., 2002, 2006). The West Pilbara Superterrane amalgamated with the East Pilbara Terrane at c. 3.07 Ga, whereas the Kurrana Terrane amalgamated with the East Pilbara Terrane at 2.905 Ga. These three principal elements of the craton are unconformably overlain, and separated, by dominantly coarse clastic sedimentary rocks of the De Grey Supergroup (Van Kranendonk et al., 2002) that were deposited in five basins across the craton between 3.02 – 2.93 Ga (Figs 1 and 2). Widespread and voluminous suites of geochemically varied granitic rocks were emplaced across the craton from ~3.65 – 2.83 Ga (Van Kranendonk et al., 2006). Unless otherwise cited, age data quoted herein are referenced in Van Kranendonk et al. (2002).

## East Pilbara Terrane

The East Pilbara Terrane (Fig. 3) includes the Pilbara Supergroup comprising four demonstrably autochthonous volcano-sedimentary groups deposited between c. 3.52 and 3.20 Ga (Van Kranendonk and Morant, 1998; Van Kranendonk et al., 2002, 2006). The maximum *preserved* thickness of the supergroup is ~20 km. Recent detailed geological mapping and extensive sensitive high-resolution ion microprobe (SHRIMP) geochronology has revealed no stratigraphic repetitions (Van Kranendonk et al., 2001, 2002).

The stratigraphically lowest Warrawoona Group is up to 12 km thick and was formed through continuous volcanism from 3.525 to 3.426 Ga. The bulk of this succession comprises pillow basalt and komatiitic basalt. Less common felsic volcanic formations are typically dacite-dominated deposits locally several km thick (e.g. in the Coucal, Duffer, and Panorama Formations). Much thinner and typically tuffaceous felsic volcanic units are locally present in some of the mafic formations. Volcanic rocks were erupted as several (ultra)mafic–felsic volcanic cycles of ~15 m.y. duration (Hickman and Van Kranendonk, 2004). Four subgroups are recognized. From base to top these are the 3.525 – 3.498 Ga Coonterunah, 3.490 – 3.477 Ga Talga Talga, 3.474 – 3.463 Ga Coongan, and 3.458 – 3.426 Ga Salgash Subgroups. This early period of crustal growth was accompanied by sodic granite magmatism emplaced as a sheeted sill complex in the mid-crust. Warrawoona Group volcanism closed with Panorama Formation andesitic to rhyolitic volcanism in several stratigraphically and compositionally distinct centres from 3.458 to 3.426 Ga.

A 75 m.y. hiatus in volcanism following Warrawoona Group volcanism was marked by deposition of the Strelley Pool Chert across a regional unconformity (Buick et al., 1995; Van Kranendonk et al., 2002). This formation represents the base of the newly defined Kelly Group (Van Kranendonk et al., 2006) and comprises lower fluviatile to shallow-marine conglomerates and quartzite, and upper stromatolitic marine carbonates (Van Kranendonk et al., 2002, 2003). The conformably overlying Euro Basalt consists of a ≤1.5 km-thick basal unit of komatiite and up to 5 km of overlying, interbedded komatiitic basalt and tholeiitic basalt that was erupted in ~20 m.y. from 3.35 to 3.315 Ga. This was followed at c. 3.325 – 3.315 Ga by voluminous, high-$K_2O$ felsic volcanism (Wyman Formation) and genetically related, voluminous monzogranitic plutonism (3.324 – 3.294 Ga) of crustal origin (Collins 1993; Barley and Pickard, 1999). Basaltic volcanism continued with eruption of the Charteris Basalt.

The 3.27 – 3.23 Ga Sulphur Springs Group was deposited across an unconformity (Van Kranendonk, 2000). This group consists of a komatiitic through rhyolitic volcanic succession, up to 4 km thick, capped by <30 m of silicified epiclastic and siliciclastic rocks (Van Kranendonk and Morant, 1998; Buick et al., 2002). The group is intruded by the syn-volcanic Strelley Monzogranite, a $K_2O$-rich subvolcanic laccolith (Brauhart, 1999; Van Kranendonk, 2000). Felsic volcanism was coeval with widespread monzogranite plutonism of the Cleland Supersuite across the East Pilbara Terrane (Van Kranendonk et al., 2002).

The Sulphur Springs Group is disconformably overlain by the undated clastic sedimentary rocks of the Soanesville Group, comprising banded iron-formation, sandstone, and shale. The upper part of the group includes komatiitic basalt (Honeyeater Basalt) and banded iron-formation.

## West Pilbara Superterrane

The West Pilbara Superterrane (Fig. 3) is a collage of three fault-bounded tectono-stratigraphic terranes, each with a unique stratigraphic succession (Hickman, 1997, 2004; Smith, 2003; Van Kranendonk et al., 2006). Two of the terranes are separated by the 1 km-wide Sholl Shear Zone, a long-lived, re-activated suture. North of the Sholl Shear Zone is the Karratha Terrane, comprising the 3.27 – 3.25 Ga Roebourne Group of ultramafic to felsic volcanic and sedimentary rocks and contemporaneous subvolcanic intrusions including the Karratha Granodiorite. These rocks have Nd-model ages as old as 3.49 Ga, similar to the East Pilbara Terrane (Smith et al., 1998; Sun and Hickman, 1998).

The Karratha Terrane is in contact with structurally overlying, 3.5 km-thick, MORB-like basalts (Ohta et al., 1996) of the undated Regal Formation across the Regal Thrust (Hickman, 1997, 2004).

South of the Sholl Shear Zone is the 3.12 Ga Whundo Group, a >10 km-thick succession of bimodal basaltic to felsic volcanic and volcaniclastic rocks (Hickman, 1997). Together with co-magmatic granitic rocks of the Railway Supersuite, these rocks form the exotic Sholl Terrane (Hickman, 2004; Smithies et al., 2005a; Van Kranendonk et al., 2006). Neither the base nor the top of the group is preserved. The stratigraphic sequence contains no sedimentary material of continental provenance. This,

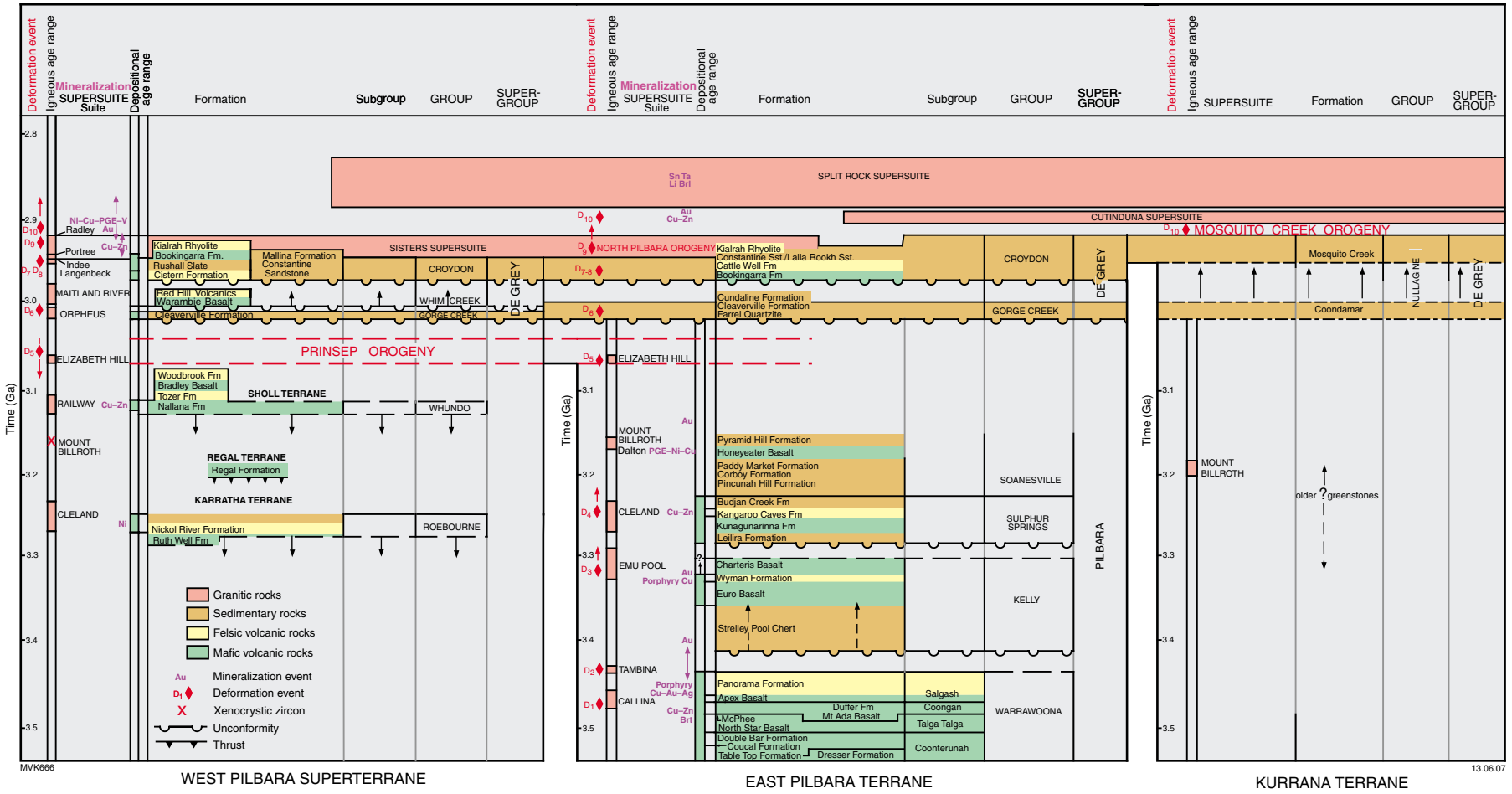


**Figure 3. Stratigraphy, geochronology, and events in the East Pilbara Terrane and the (combined) West Pilbara Superterrane and Mallina Basin (after Van Kranendonk et al., 2006)**

together with geochemical evidence, including juvenile $\varepsilon_{Nd(3130\ Ma)}$ values of ~+2 to +3 on volcanic rocks, suggests that the group represents juvenile crust formed in an intraoceanic arc (Smithies et al., 2005a).

## De Grey Superbasin

The 3.02 – 2.93 Ga De Grey Supergroup spans the Pilbara Craton (Fig. 1) in five basins. At the base of the supergroup, c. 3.02 Ga clastic sedimentary rocks, chert, banded iron-formation, and minor felsic volcaniclastic rocks of the Cleaverville Formation (Hickman, 1997) of the Gorge Creek Group, unconformably overlies older tectono-stratigraphic terranes of the West Pilbara Superterrane. Rocks of this group extend eastward underneath younger clastic rocks of the supergroup, and across much of the East Pilbara Terrane, forming what is referred to as the Gorge Creek Basin.

The c. 3.01 Ga Whim Creek Group is a complex association of coeval felsic to mafic volcanic, intrusive, and volcaniclastic rocks that unconformably overlie the Whundo Group and Cleaverville Formation across the Sholl Shear Zone, and are interpreted to represent an intracontinental pull-apart basin (Barley, 1987; Van Kranendonk et al., 2006) or intra-continental arc (Pike and Cas, 2002). The group is disconformably overlain by the Croydon Group (De Grey Supergroup) of the Mallina Basin.

Coarse- to fine-grained siliciclastic sedimentary rocks of the regionally extensive Croydon Group in the Mallina Basin lie unconformably on West Pilbara Superterrane rocks (Smithies et al., 2001) as well as those of the East Pilbara Terrane. The c. 2.97 Ga Cistern Formation forms the base of the Croydon Group and contains abundant volcaniclastic material derived from the underlying Whim Creek Group. Rocks of the Cistern Formation show an upward increase in siliciclastic material and parallel decrease in grain size, culminating with the deposition of the Rushall Slate. The rocks are overlain by locally spinifex-textured and variolitic siliceous high-magnesian basalts (Sun et al., 1989) of the Louden Volcanics and the Mount Negri Volcanics (Hickman, 1997). Pike and Cas (2002) recognized peperite-like contacts where basalt locally intruded unlithified sediment, indicating that basaltic volcanism and clastic deposition in the upper part of the group overlapped in time. Similar volcanic rocks occur along the northern and northeastern margins of the East Pilbara Terrane, and include the Coonieena Basalt.

Mallina Basin clastic sedimentary rocks were deposited as a series of submarine fans (Eriksson, 1982), with detrital zircon age patterns very similar to a mix of East Pilbara Terrane and West Pilbara Superterrane crust (Smithies et al., 2001). Gravity modelling (GSWA, unpublished data), and other data indicate a preserved thickness of no more than ~5 km. Coarse clastic rocks of the Croydon Group (De Grey Supergroup) lie unconformably on older rocks of the East Pilbara Terrane in dismembered remnants of the Lalla Rookh Basin. Deposition was largely in a fluviatile environment, with local lacustrine settings (Eriksson et al., 1994), preceding, or contemporaneous with, regional sinistral transpression at 2.94 – 2.93 Ga (Van Kranendonk and Collins, 1998).

The Mosquito Creek Basin lies unconformably on the East Pilbara Terrane in the southeast of the craton. The basin consists of the lower, undated Coondamar Formation (Farrell, 2006) of mafic schists and fine-grained metasedimentary rocks with dominantly mafic detritus. This formation is in fault contact with the Kurrana Terrane to the south, and does not come into contact with the East Pilbara Terrane to the north. The overlying Mosquito Creek Formation of fine- to coarse-grained siliciclastic sedimentary rocks was deposited at ≤ c. 2.926 Ga (Bagas et al., 2005). Penetrative deformation, granite intrusion, and shear-hosted Au mineralization in the basin occurred at 2.905 Ga (Huston et al., 2002).

# East Pilbara Terrane and the De Grey Superbasin in the east Pilbara

Several sampling traverses of the volcanic rocks were completed throughout the East Pilbara Terrane (Fig. 2 and Table 1). The primary aims of this sampling were to:

- characterize the lithological and compositional range of volcanic rock types in the Pilbara Supergroup; and
- determine if there is any systematic compositional variation in particular rock types (basalts and felsic volcanic rocks) with time.

Samples were also collected from two localities (Pilbara Well and Wodgina greenstone belts) where the stratigraphic position of the rocks was poorly constrained, with the aim of using geochemical information to help clarify their stratigraphic position.

Data from previous sampling of the Sulphur Springs Group (Van Kranendonk, unpublished data; see also Fig. 2) has also been added to Table 1 and these data are included within the discussion of the geochemistry of the Warrawoona Group rocks (below).

## Traverse geology

### Warrawoona Group

#### *Coonterunah Subgroup*

Samples were collected from three sections through the c. 3.525 – 3.498 Ga Coonterunah Subgroup of the Warrawoona Group in the East Strelley greenstone belt. The major traverse (traverse 1 on Fig. 2: MGA Zone 50 717483E 7667755N to 715646E 7662881N) was approximately 5 km long. This traverse was more or less perpendicular to depositional layering, which typically dips at a moderate to steep angle to the south and, based on well-preserved facing indicators (pillow structures and graded beds within volcaniclastic units), consistently faces to the south. Mapping gave no indication of any large-scale structural repetition of the sequence. This traverse started at the stratigraphically lowest exposed

**Table 1. Stratigraphic units sampled during this program — from oldest to youngest**

| *Unit* | *Rock types* | *Locality/traverse (Fig. 1)* | *Number* |
|---|---|---|---|
| Coonterunah Subgroup | Komatiite–dacite | East Strelley | 59 |
| North Star Basalt | Basalt | Talga Talga | 3 |
| Mount Ada Basalt | Basalt | Talga Talga | 18 |
| Duffer Formation | Basalt–dacite | Talga Talga | 32 |
| Apex Basalt | Basalt | Bamboo Creek | 20 |
| Panorama Formation | Rhyolite | Kittys Creek | 4 |
| | Basalt–dacite | McPhee Dome | 6 |
| | Volcaniclastic sandstone | Panorama Ridge | 3 |
| | Andesite–rhyolite | Sandy Creek | 10 |
| Euro Basalt | Basalt | Mount Elsie | 10 |
| | Basalt | Sandy Creek | 20 |
| | Komatiite–basalt | Camel Creek | 16 |
| | Basalt | East Strelley | 9 |
| Charteris Basalt | Basalt | Charteris Creek | 7 |
| | Komatiite | Kittys Gap | 1 |
| Coonieena Basalt | Basalt | Shay Gap | 10 |
| Paradise Plains Formation | Basalt | Ord Range | 1 |
| | | Goldsworthy Syncline | 2 |
| Unknown | Basalt | Pilbara Well | 7 |
| | Basalt | Wodgina | 5 |

part of the Coonterunah Subgroup, within the Table Top Formation, and ended at the top of the middle stratigraphic unit — the Coucal Formation. The upper unit — the Double Bar Formation — was not sampled. Two shorter traverses (beginning at MGA Zone 50 711949E 7663602N and at 730751E 7669202N) were restricted to the Coucal Formation.

The exposed base of the Coonterunah Subgroup in the area of the main traverse included a unit of interleaved vesicular tholeiitic basalts and thin (1–5 m scale) vesicular and spinifex-textured komatiite flow units. These units are overlain by a thick sequence of locally vesicular and pillowed tholeiitic flows with rare interflow accumulations of carbonate-rich sandstone and siltstone, chert, and quartzite. The boundary between the tholeiitic basalt pile of the Table Top Formation and the overlying felsic volcanic rocks of the Coucal Formation is a transition zone, containing basaltic rocks with geochemical and textural evidence for limited mingling with felsic magmas. Tholeiitic basalt does not reoccur above this transition zone.

The overlying Coucal Formation is dominated by andesitic to dacitic volcanic and volcaniclastic units. These include massive plagioclase porphyry, feldspar-phyric vitric tuff, and, near the top of the unit, multiple stacks of ~5 m-thick coarse- to fine-grained graded beds, each capped by a 0.5 – 1 m-thick layer of silicified ash (banded chert). Two compositional series are recognized: C-F1 volcanic rocks range from andesite to dacite and dominate the lower half of the sequence; C-F2 volcanic rocks range from basalt to andesite and dominate the upper half.

### North Star Basalt

Three samples were collected from the c. 3.49 Ga North Star Basalt in the Talga Talga anticline of the Marble Bar greenstone belt (traverse 2 on Fig. 2). This formation is typically poorly exposed in this area or extensively carbonate altered, or both. The samples were from a small exposure of amphibolite, which varied locally in texture from vesicular to variolitic to massive.

### Mount Ada Basalt

A ~3.5 km-long, northwest-trending traverse in the Talga Talga anticline of the Marble Bar greenstone belt (traverse 3 on Fig. 2 starting at MGA Zone 50 794012E 7678757N) sampled the full stratigraphic extent of the c. 3.47 Ga Mount Ada Basalt, and included 18 samples of basalt (traverse 3 on Fig. 2). In this area, the Mount Ada Basalt includes basalts that vary from massive to either highly vesicular or highly variolitic. In rare cases, the rocks are both vesicular and variolitic (there are no consistent compositional differences between vesicular, variolitic, or massive units). Pillow structures are locally common, as are flow-top breccias. Poorly sorted volcaniclastic conglomerate layers form a minor component. Carbonate alteration is locally pervasive.

### Duffer Formation

The c. 3.474 – 3.463 Ga Duffer Formation was sampled along two north-trending traverses 3.9 and 2.7 km in length (traverse 3 on Fig. 2, starting at MGA Zone 50 793980E 7678838N to 795124E 7682702N and 804358E 7680233N to 804895E 7682991N) in the Talga Talga anticline of the Marble Bar greenstone belt. The traverses were perpendicular to steeply north-dipping and north-facing depositional layering. As with the Coonterunah Subgroup, a knowledge of the geochemistry of the Duffer Formation aids considerably in establishing a stratigraphy, and so a description of the general geology necessarily pre-empts some broad geochemical descriptions.

In the area of the traverses, the Mount Ada Basalt passes conformably into the Duffer Formation, which, at its base, comprises interbedded massive, pillowed to tuffaceous basalt and massive to graded coarse- to fine-grained plagioclase-porphyritic andesite and dacite. Two compositional types of basalts are recognized (B1, B2). Duffer B1 basalts are typically tholeiitic and compositionally similar to the Mount Ada Basalt. They are typically plagioclase-phyric and form massive flow units or less commonly tuffaceous volcaniclastic deposits. Duffer B2 basalts range from plagioclase-porphyritic pillowed flow units to, more commonly, graded and strongly feldspar-porphyritic medium- to fine-grained volcaniclastic deposits.

The andesitic to dacitic rocks interbedded with B1 and B2 basalts dominate the lower half of the Duffer Formation. They include a high proportion of medium- to fine-grained volcaniclastic material (typically graded tuff), although volcaniclastic conglomerate as well as one to 5 m-thick, ungraded units of coarse- to medium-grained plagioclase porphyry, welded plagioclase-porphyritic tuff, and feldspar porphyry sills also outcrop. These rocks can be divided geochemically into a minor group showing characteristics of fractionated tholeiites (D-F1) and a larger group having similarities to the associated Duffer B2 basalts (D-F2).

The upper half of the Duffer Formation is typically composed of coarser grained, more coherent crystal tuffs and massive plagioclase-porphyritic rocks. These D-F3 rocks are compositionally distinct (more enriched) from the underlying D-F2 rocks. Pillowed units of D-B2 basalts are interbedded with the D-F3 sequence.

### Apex Basalt

Samples of the Apex Basalt were collected from a ~3 km-long, southwest-trending traverse in the northeastern part of the Marble Bar greenstone belt (traverse 4 on Fig. 2). This traverse started near the Bamboo Creek gold mine (at MGA Zone 51 207376E 7684966N). In this area, the Apex Basalt varies from weakly to highly vesicular and commonly pillowed basalt. Varioles up to 3 cm in diameter are locally abundant. Interflow mafic sedimentary rocks and basaltic conglomerates, flow-top breccias, and hyaloclastite deposits occur locally, but are never abundant. Carbonate alteration is locally pervasive. A shorter (~1 km) northwest-trending traverse to the north of the Coongan River in the Warralong greenstone belt (traverse 5 on Fig. 2, starting at MGA Zone 50 762792E 7697413N) sampled three pillowed basalts and a single sample of spinifex-textured komatiite that also belong to the Apex Basalt.

### Panorama Formation

In contrast to the felsic sequences within the Coonterunah Subgroup and Duffer Formation, the Panorama Formation comprises several regionally and compositionally distinct volcanic centres that erupted within a very broad time span, from 3.458 to 3.426 Ga. Two traverses were sampled: at Sandy Creek in the Kelly greenstone belt, 45 km southeast of Marble Bar (traverse 6 on Fig. 2, starting at MGA Zone 51 193347E 7623838N), and at McPhee Dome in the McPhee greenstone belt, 60 km east-southeast of Marble Bar (traverse 7 on Fig. 2, starting at MGA Zone 51 203552E 7606833N). Samples were also taken from Kittys Gap, 50 km northeast of Marble Bar, in the Marble Bar greenstone belt, and from Panorama Ridge (North Pole Dome), 40 km west of Marble Bar, in the Panorama greenstone belt (traverses 8 and 9 respectively, on Fig. 2).

Four samples of quartz- and feldspar-phyric vitric rhyolite were collected within a small area near Kittys Gap (traverse 8, starting at around MGA Zone 51 195080E 7686342N). Three samples of quartz- and feldspar-porphyritic rhyolite were taken from Panorama Ridge (traverse 9, starting at MGA Zone 50 750907E 7646839N), where they are interbedded with lesser amounts of poorly sorted volcanolithic sandstone. All samples from Kittys Gap and Panorama Ridge have been silicified.

Samples of Panorama Formation collected from various points throughout the McPhee Dome (see Appendix 1 for locality details) included plagioclase-phyric, vesicular, and locally pillowed basaltic rocks and andesites, plagioclase-porphyritic dacite and plagioclase-phyric vitric dacite.

In the Sandy Creek area, the Panorama Formation can be subdivided into distinct lower and upper stratigraphic portions. The lower stratigraphy is dominated by interbedded dacitic to rhyolitic lavas and volcaniclastic rocks. No basalt was observed and andesite is restricted to the lower part of the sequence and is rare. Coherent lavas include 5 to 30 m-thick layers of plagioclase-porphyritic vitric dacite and rhyolite. These are interbedded with lava breccias, clast-supported grain-flow breccias, graded pyroclastic flows, and hyaloclastite breccia. Eight samples of coherent lava facies were collected from the lower region. The upper stratigraphy is poorly exposed but appears dominated by volcaniclastic and epiclastic deposits, with significantly fewer coherent lavas (two sampled) compared to the lower regions.

## Kelly Group

### Euro Basalt

The Euro Basalt is the most voluminous and most widely exposed mafic unit of the Pilbara Supergroup and was sampled in several regions. In the Sandy Creek traverse of the Kelly greenstone belt (traverse 6 on Fig. 2), the Euro

Basalt was sampled along a ~3 km east-northeasterly trending traverse that started approximately 50 m east of the basal contact marked by the Strelley Pool Chert, which overlies felsic volcanic rocks of the Panorama Formation (at MGA Zone 51 195187E 7623120N). The section is dominated by basaltic rocks, which are typically vesicular and show well-preserved pillow structures. The central part of the traverse encountered komatiitic basalts with well-developed fine-grained pyroxene-spinifex textures. Twenty basalts and five komatiitic basalts were collected.

The Euro Basalt was also sampled near Camel Creek along a ~7 km northwest-trending traverse (starting at MGA Zone 50 790406E 7635204N) in the northeastern part of the Kelly greenstone belt (traverse 10 on Fig. 2). The geology along this traverse differed from that of the Sandy Creek traverse in that komatiitic basalt units were found near the base and top, rather than in the middle of the stratigraphy. Nine basaltic rocks and seven komatiitic basalts were sampled.

A short (~400 m) southeast-trending traverse to the south of Coucal Creek (starting at MGA Zone 50 714831E 7661854N), in the East Strelley greenstone belt, sampled the Euro Basalt where it unconformably overlies the Coonterunah Subgroup (traverse 1 on Fig. 2). The traverse encountered no komatiites or komatiitic basalts, and the nine samples collected were all of variably vesicular pillowed basalt.

Ten samples, including eight basaltic rocks and two komatiitic basalts were taken from various localities in the Mount Elsie greenstone belt (see Appendix 1 for locality details), on Eastern Creek* (traverse 11 on Fig. 2).

One sample of komatiite was collected to the south of Kittys Gap (at MGA Zone 51 199664E 7687761), in the Marble Bar greenstone belt (traverse 8 on Fig. 2). This rock contains less MgO (see below) than many other rocks classified here as komatiitic basalt. However, this is likely to be a result of alteration (mainly silicification) and the coarse olivine (sheath)-spinifex textures correctly identify this rock as komatiite.

The Charteris Basalt was sampled along a ~1 km northeast-trending traverse on Mount Edgar (starting at MGA Zone 51 203947E 7623276N), in the northeastern part of the Kelly greenstone belt (traverse 12 on Fig. 2). The area of the traverse was dominated by locally vesicular pillow basalt, in places with a poorly developed pyroxene-spinifex texture. Volcanic brecciation appears to be a significant feature of the area. Seven samples of pillowed basalt were collected.

## Sulphur Springs Group

Two parallel traverses through the Kunagunarrina Formation of the Sulphur Springs Group were conducted in the Pincunah greenstone belt on Wodgina and North Shaw (traverse 13 on Fig. 2, MGA Zone 50, from 794220E 7646950N to 794600E 7648200N and from 796400E 7647750N to 797400E 7648350N). Both traverses sampled weakly metamorphosed mafic–ultramafic lavas across a lower unit of light-brown weathering basalt to komatiitic basalt (1 km thick) with local pyroxene-spinifex texture, a middle unit of dark-brown weathering basalt to komatiite (1 km thick) with variolitic, spinifex, and pillow textures, and an upper unit of pillowed basalt–andesite (300 m thick).

## Soanesville Group

Five samples of the Honeyeater Basalt of the Soanesville Group were collected from the type area in the Soanesville greenstone belt (traverse 14 on Fig. 2, near MGA Zone 50 734000E 7654000N). Samples were of well-preserved, dark-brown weathering, weakly metamorphosed (prehnite–pumpellyite grade) pillow basalts that have common marginal vesicles and local varioles.

## De Grey Supergroup

### *Bookingarra Formation*

The Coonieena Basalt Member of the Bookingarra Formation was sampled along two northeast-trending traverses in the Shay Gap greenstone belt (traverse 15 on Fig. 2); three samples were collected along one short (~0.5 km) traverse (starting at MGA Zone 51 208416E 7726344N) and seven samples were collected over a one-km traverse (starting at MGA Zone 51 206205E 7726586N). In the area of these traverses, the Coonieena Basalt Member was typically massive, but locally included vesicular layers and, more rarely, layers of variolitic basalt and of flow-top breccia.

Basaltic rocks in the lower stratigraphic levels of the Croydon Group in the Goldsworthy area include massive, brecciated, and pillowed varieties, as well as graded volcaniclastic sandstones. One sample of massive basalt directly underlying a graded volcaniclastic sandstone unit was collected from the Ord Ranges on De Grey (traverse 16 on Fig. 2). Two samples of massive basalt were taken from the Goldsworthy Syncline on Pardoo (traverse 17 on Fig. 2).

## Units of unknown stratigraphic position

### *Pilbara Well greenstone belt*

The Pilbara Well greenstone belt lies between the rocks of the Mallina Basin (Croydon Group) and the northwestern edge of the East Pilbara Terrane (traverse 18 on Fig. 2). The belt is dominated by variolitic and locally pillowed basalts and komatiitic basalts. Five basalts and two komatiitic basalts were sampled along a ~2-km northwest-trending traverse (starting at MGA Zone 50 632549E 7653107N).

### *Wodgina greenstone belt*

The Wodgina greenstone belt is isolated within granites of the Yule Granitic Complex, in the western part of the East Pilbara Terrane (traverse 19 on Fig. 2). Isolated outcrop of supracrustal rocks to the north suggests a possible continuation of, or correlation with, the Pilbara

* Capitalized names refer to standard 1:100 000 map sheets

Well greenstone belt. A short (~200 m), north-trending traverse (starting at MGA Zone 50 672485E 7659156N) was dominated by basalt, ranging from massive vesicular rock to chlorite–actinolite schist. Four massive rocks and one schistose rock were sampled.

# Geochemistry

The geochemistry of volcanic rocks of the Pilbara and De Grey Supergroups from the East Pilbara Terrane are described mainly in terms of major rock groups (ultramafic, mafic, and felsic). However, the felsic units of the Pilbara Supergroup prove to be lithologically very diverse and it is clear that at least some are genetically directly related to contemporaneous basalts — forming continuous geochemical trends between the two rock types. In such cases, the basaltic rocks are described alongside the felsic rocks as part of a 'felsic series'.

## Komatiites and komatiitic basalts

Mg-rich basaltic rocks (MgO up to ~12 wt%) at the exposed base of the Warrawoona Group were described by Green et al. (2000). Our data for the Coonterunah Subgroup indicate interlayered, vesicular tholeiitic basalts and thin (1–5 m scale) vesicular and spinifex-textured komatiite flow units in the basal Tabletop Formation. These are the oldest komatiites of the Pilbara Craton. They have $SiO_2$ from 45.5 to 49.4 wt%, MgO from 22 to 30 wt%, $Mg^{\#}$ from 79 to 85, and flat normalized trace element patterns (Fig. 4) with values typically between 0.9 to 2.4 times primitive mantle values (~3 to 6 times chondritic) and $[Ce/Yb]_{PM}$ ~0.9. With near-chondritic Gd/Yb ratios (1.1 – 1.3) and $Al_2O_3/TiO_2$ ratios between 20 and 24, these rocks are Al-undepleted komatiites (Nesbitt et al., 1979). Komatiites and komatiitic basalts in the remaining, stratigraphically higher, units of the Warrawoona Group are also predominantly Al-undepleted (Fig. 5).

Komatiites and komatiitic basalts in the stratigraphically overlying Kelly Group (Euro Basalt) are both Al-depleted and Al-undepleted. Al-undepleted rocks occur at Kittys Gap and in the basal part of the Camel Creek traverse, and have low incompatible trace element concentrations and flat normalized trace element patterns that are indistinguishable from those of the Al-undepleted komatiites in the Coonterunah Subgroup. Samples from the Sandy Creek traverse and from the Mount Elsie greenstone belt are also Al-undepleted, but with higher normalized-trace element patterns and lower La(Ce)/Sm ratios. Al-depleted rocks ($Al_2O_3/TiO_2$ ~6) are restricted to the stratigraphically highest parts of the Camel Creek traverse and are LREE-enriched compared to all of the other komatiites and komatiitic basalts.

## Basaltic rocks

The geochemistry of various mafic rocks within the Pilbara Supergroup has previously been described by Glikson and Hickman (1981), Brauhart (1999), Green et al. (2000), Arndt et al. (2001), Bolhar et al. (2002), Van Kranendonk and Pirajno (2004), and Smithies et al. (2005b). These basaltic rocks follow tholeiitic trends and Smithies et al. (2005b) showed that they could be subdivided, irrespective of age, into a high-Ti group ($TiO_2$ >0.8 wt%) and a low-Ti group ($TiO_2$ <0.8 wt%). High- and low-Ti basalts are interbedded and cannot be distinguished in the field. Compared to the low-Ti basalts, the high-Ti basalts also have high concentrations of HFSE and REE (Fig. 6), are generally more Fe-rich, have very low $Al_2O_3/TiO_2$ (18.7 – 8.9) and high Gd/Yb ratios (1.12 – 2.23). The high-Ti group accounts for 65% of basaltic rocks within the Pilbara Supergroup. Glikson and Hickman (1981) showed that some of the lower basalt formations in the Pilbara Supergroup showed a progressive upward decrease in HFSE and REE. Smithies et al. (2005b) confirmed that this was also the case for the tholeiitic basalts in the lower Tabletop Formation of the Coonterunah Subgroup.

To facilitate comparison between basaltic groups of different ages and to minimize scatter attributable to variable degrees of fractionation or partial melting, trace element concentrations plotted in Figure 6 were recalculated to values expected at 9 wt% MgO [e.g. $Nb_{(9)}$] by extrapolating constant-slope trend lines based on the gradient of the linear regression for each group (see supplementary dataset in Smithies et al. (2005b) for statistical data related to these extrapolations). This approach assumes minimal redistribution of MgO during low-grade metamorphism. However, these recalculations do not significantly change trends or abundance patterns observed within the uncorrected data set.

### *Warrawoona Group*

The primitive basaltic rocks of the Warrawoona Group are generally thought to be derived from a series of mantle plumes (Arndt et al., 2001; Van Kranendonk et al., 2002; Van Kranendonk and Pirajno, 2004). According to Smithies et al. (2005b), the high-Ti basalts have compositional affinities with Al-depleted (or Barberton-type) komatiites and komatiitic basalts that formed during high-pressure melting in particularly hot mantle plumes. The mantle source for both the high- and low-Ti basalts was depleted (Green et al., 2000; Arndt et al., 2001), but typically not as depleted as a N-MORB source (Condie, 2005), although Smithies et al. (2005b) noted that sources more depleted than a N-MORB source could have produced some of the younger low-Ti tholeiites. Some of the basalts have compositions that reflect extensive contamination by felsic crust (possibly as much as 25% — Green et al., 2000), but the majority show little or no signs of contamination (Arndt et al., 2001; Bolhar et al., 2002). Smithies et al. (2005b) noted that there was no increase in the degree of contamination, or in the proportion of contaminated rock, with successively younger basaltic units of the Warrawoona Group.

Apart from variations in $TiO_2$, the individual basaltic units of the Warrawoona Group show considerable overlap in major element composition. For this reason, the discussion below concentrates mainly on variations in trace element concentrations.

Tholeiitic basaltic rocks in the Tabletop Formation at the base of the Coonterunah Subgroup fall into the

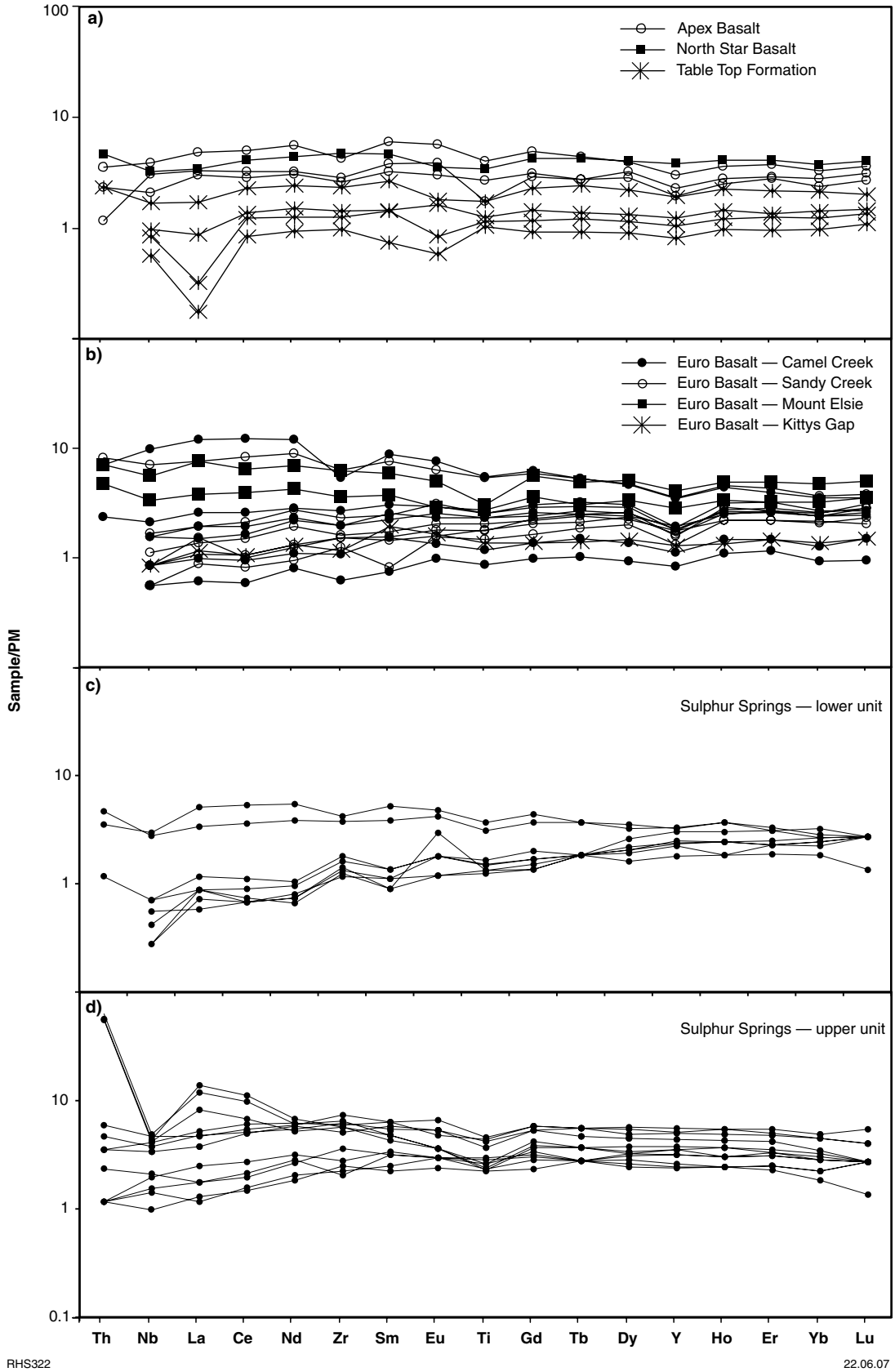


**Figure 4. Trace element plots normalized to primitive mantle for komatiites and komatiitic basalts of the Pilbara Supergroup. Normalizing factors after Sun and McDonough (1989)**

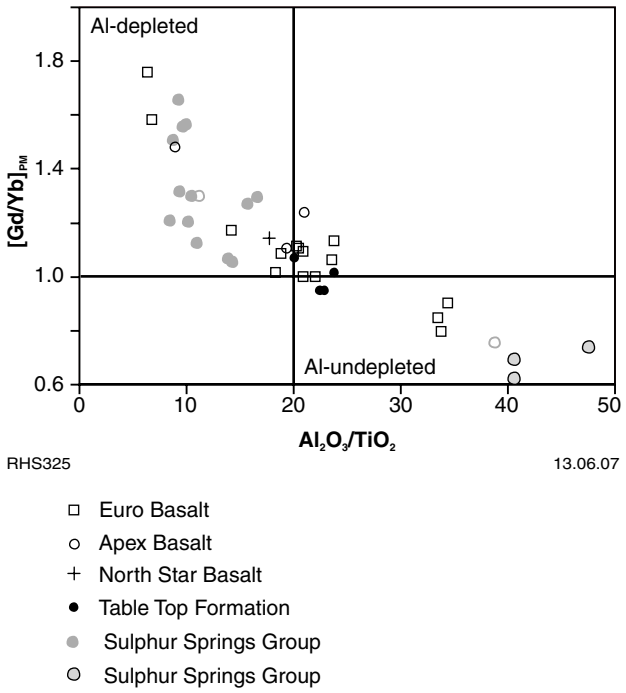


**Figure 5. $Al_2O_3/TiO_2$ ratios vs primitive mantle-normalized Gd/Yb ratios for komatiites and komatiitic basalts of the Pilbara Supergroup. Solid lines show primitive mantle values of respective ratios**

high-Ti group ($TiO_2$ >0.8 wt%). They show very weakly fractionated N-MORB-like trace element patterns which typically vary from 4 to 10 times primitive mantle values, with $[La/Yb]_{PM}$ from 0.8 to 2.0 (Fig. 7a). Most incompatible trace element ratios are correspondingly close to primitive mantle values, including $[La/Nb]_{PM}$ values that range from 0.89 to 1.66. $Mg^{\#}$ varies from 69 to values as low as 32 with very little change in $SiO_2$ values, which lie around 50.5 wt%. The most primitive rocks have Th/Nb and Nb/La ratios slightly lower than primitive mantle values, reflecting a slightly depleted source, but these ratios, and particularly Th/Nb, remain higher than N-MORB values. A single Nd-isotopic determination gives an $\varepsilon_{Nd}$ of +1.39, which is only slightly below the depleted mantle value of +2.37 at 3.51 Ga (assuming linear isotopic decay from an $\varepsilon_{Nd}$ of +10 at 4.56 Ga — Sun et al., 1995), and consistent with the La/Yb and La/Nb values of the basaltic rocks, which bracket primitive mantle values. These data indicate that the more primitive basalts in the upper part of the tholeiitic pile underwent very little interaction with felsic crust.

The transition zone between the tholeiitic basalts of the Tabletop Formation and the overlying felsic-dominated sequence (Coucal Formation) of the Coonterunah Subgroup includes basalts with higher concentrations of the more highly incompatible trace elements (Th, U, Nb, Zr, and LREE) than the underlying tholeiites. In terms of all major and trace elements, these basalts consistently plot between the compositional ranges for tholeiites and the interbedded and directly overlying felsic volcanic rock series. This stratigraphic interval is also notable for the presence of globules of basalt in andesite and of andesite in basalt, providing field evidence for some form of magma mingling. These basalts have crystallized from binary hybrid magmas.

Two samples of tholeiitic basalt from the North Star Basalt are high-Ti basalts with normalized trace element patterns (Fig. 7b) that completely overlap those of the tholeiitic basalt from the Coonterunah Subgroup, including $[La/Yb]_{PM}$ and $[La/Nb]_{PM}$ of 1.42 – 1.83 and 1.42 – 1.49 respectively.

Tholeiitic basalts from the Mount Ada Basalt are dominated by high-Ti compositions, but three low-Ti tholeiites were sampled. Normalized trace element patterns for the high-Ti basalts overlap extensively with those of the basalt from the Coonterunah Subgroup and North Star Basalt (Fig. 7), with a similar range in $[La/Yb]_{PM}$ (1.21 – 1.74) and $[La/Nb]_{PM}$ (1.20 – 1.65), but extend to higher concentrations (up to ~13 times primitive mantle values). The low-Ti basalts have lower incompatible trace element concentrations (generally <4 times primitive mantle values) than the high-Ti rocks (Fig. 7b), and show no negative Nb anomaly on primitive mantle-normalized plots. Low $[La/Yb]_{PM}$ (0.89 – 1.1) ratios and very low $[La/Sm]_{PM}$ (0.74 – 0.80) ratios reflect derivation from a significantly more depleted source than the source for the associated high-Ti rocks.

Tholeiitic basalts that are interleaved with felsic rocks of the Duffer Formation, but do not form part of either basalt – dacite felsic series (see below), are high-Ti tholeiites identical in trace element concentration and normalized patterns to the more trace element enriched high-Ti tholeiites of the underlying Mount Ada Basalt (Fig. 7d).

Tholeiitic basalts from the Apex Basalt are also dominated by high-Ti compositions; two low-Ti tholeiites were sampled. Normalized trace element patterns for the high-Ti basalts overlap extensively with those of the basalt from the underlying formations (Fig. 7e), and extend to similarly high concentration ranges as the Mount Ada Basalt (up to ~15 times primitive mantle values), but with wider ranges in $[La/Yb]_{PM}$ (0.87 – 2.2) and $[La/Nb]_{PM}$ (1.0 – 1.62). The low-Ti basalts have lower incompatible trace element concentrations (generally <4 times primitive mantle values) than the high-Ti rocks (Fig. 7e), and show no negative Nb anomaly on primitive mantle-normalized plots. Low $[La/Yb]_{PM}$ (0.77 – 0.89) ratios and very low $[La/Sm]_{PM}$ (0.73 – 0.84) ratios reflect derivation from a slightly more depleted source than the source for the associated high-Ti rocks.

### *Kelly Group*

The concentration ranges of incompatible trace elements, and the primitive mantle-normalized patterns, for high-Ti tholeiites from the Euro Basalt are almost identical to those of the Coonterunah Subgroup (Fig. 7f,g). The largest range in data are for the rocks from the Mount Elsie greenstone belt, whereas samples taken from the Camel Creek and Sandy Creek traverses have similarly low concentration ranges (i.e. relatively tightly constrained groups) at low concentrations (generally 4–7 times primitive mantle values). The low-Ti tholeiites of the Euro Basalt generally

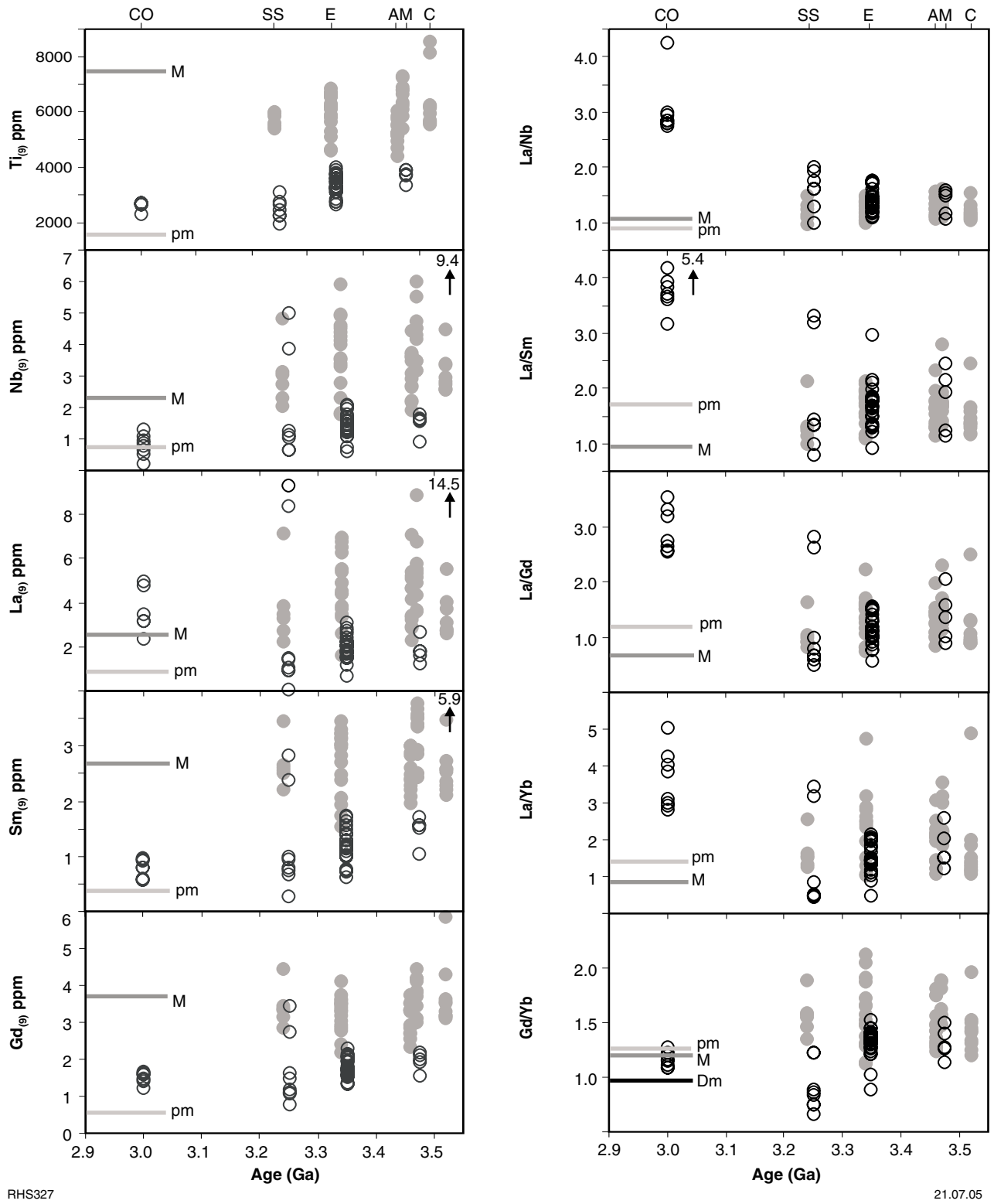


**Figure 6.** **Variations in the compositions of high-Ti basalts (grey circles) and low-Ti basalts (open circles) of the Pilbara Supergroup with time. C = Coonterunah Subgroup, M = Mount Ada Basalt, A = Apex Basalt, E = Euro Basalt, SS = Sulphur Springs Group, CO = Coonieena Basalt Member (Bookingarra Formation, Croydon Group, De Grey Supergroup). Values for N-MORB (M) and primitive mantle (pm) are from Sun and McDonough (1989). Trace element concentrations recalculated to values expected at 9 wt% MgO (e.g. $Ti_{(9)}$)**

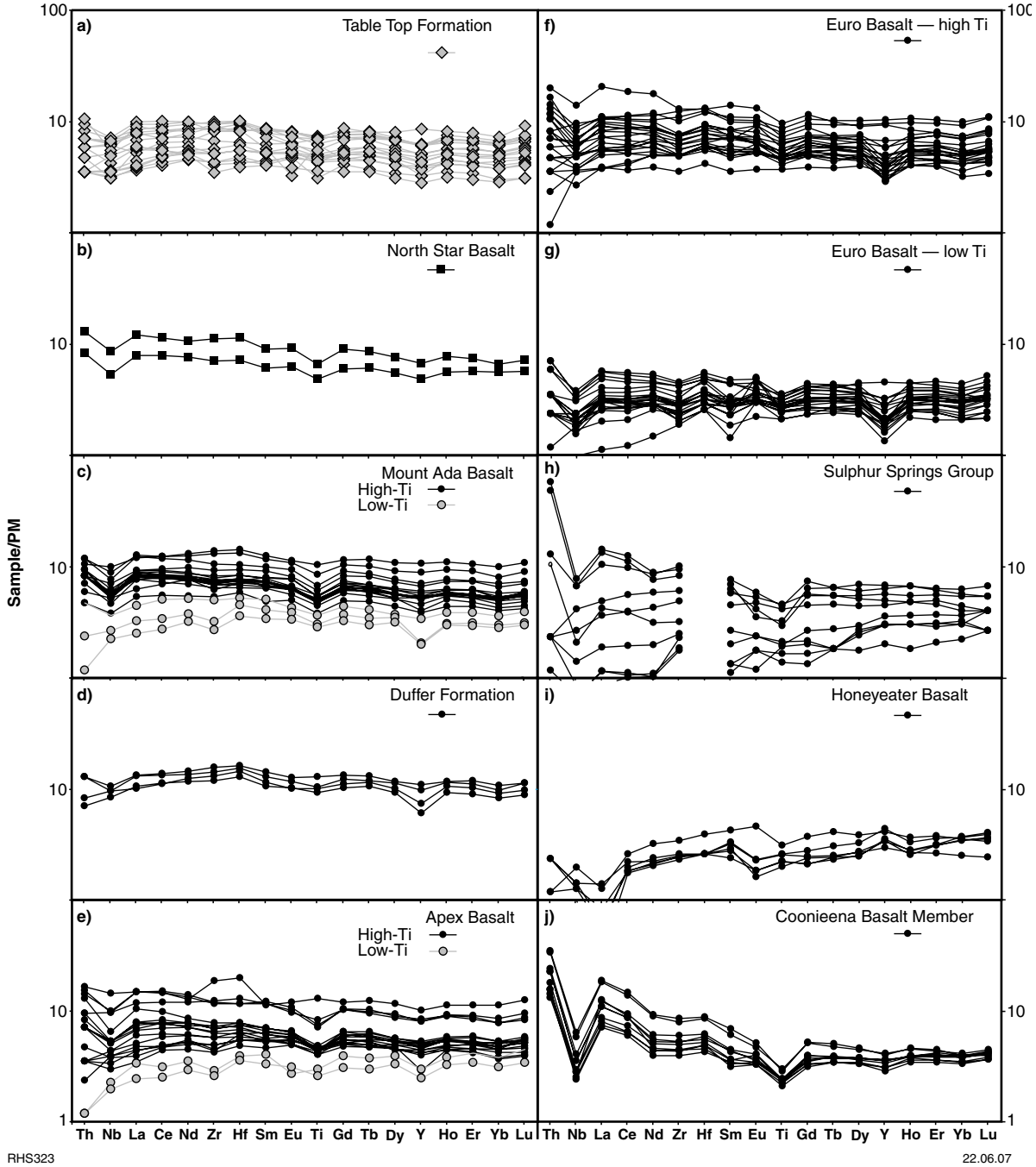


**Figure 7. Trace element plots normalized to primitive mantle for basalts of the Pilbara Supergroup. Normalizing factors after Sun and McDonough (1989)**

have lower incompatible trace element concentrations than the associated high-Ti tholeiites (Fig. 7) and have $[La/Yb]_{PM}$ ratios and $[La/Sm]_{PM}$ ratios as low as 0.36 and 0.6, respectively, reflecting a strongly depleted source.

### *Sulphur Springs Group*

Brauhart (1999) presented geochemical data on basaltic (basalt–andesite) to rhyolitic volcanic rocks from the Kangaroo Caves Formation of the Sulphur Springs Group around the Strelley Monzogranite. He showed that the basalt–andesite rocks, together with the more felsic components of the formation, could be divided into a basal suite of basalt–andesite (with andesite and rhyolite) that has Zr/Th <23.5, and an upper suite of basalt–andesite with Zr/Th >23.5. REE patterns for basalt–andesite show gentle slopes ($La_N/Yb_N$ = 1.97 – 6.42), with variably developed negative Eu anomalies, and almost flat HREE.

New data presented here were collected from an area to the west of the Strelley Monzogranite, across the late sinistral Lalla Rookh–Western Shaw Fault. These rocks are basalt, but yield a mixture of REE patterns (Fig. 7h), including a group with fractionated LREE and prominent negative Eu anomalies, another group with generally flat, but slightly depleted LREE, and a third group with what appears to be a mixture of the above two patterns, with fractionated LREE but with increasing MREE to HREE with increasing atomic weight. Field evidence for mingling between basalt and felsic melts (Brauhart, 1999; Van Kranendonk, 2000) may account for these diverse REE patterns.

All basaltic rocks from the Kangaroo Caves Formation show the same division into high-Ti and low-Ti groups, but with more extreme depletion in HFSE in the low-Ti group.

### Soanesville Group

Basaltic rocks of the Honeyeater Basalt (Fig. 7i) are typically low-Ti basalts. They have strongly LREE-depleted normalized trace element patterns very similar to those of the low-Ti basalts from the underlying Sulphur Springs Group.

### Croydon Group

The basaltic rocks of the Coonieena Basalt Member of the Bookingarra Formation have trace element concentration patterns that are very different to those of both high-Ti and low-Ti basalts in the lower parts of the Pilbara Supergroup (Fig. 7j). The Coonieena Basalt Member has flat primitive mantle-normalized HREE patterns, at similar concentrations (3–5 times primitive mantle values) to those in the low-Ti tholeiites, but show strongly fractionated patterns for the more highly incompatible elements, with very high $[La/Yb]_{PM}$ (2.0–4.7), $[La/Sm]_{PM}$ (2.0–3.5), and strongly developed negative Nb anomalies ($[La/Nb]_{PM}$ = 2.8–4.4; Fig. 6).

Basaltic rocks of the Croydon Group in the Goldsworthy area have very similar normalized trace element patterns to the rocks of the Coonieena Basalt Member (Fig. 8), but with slightly higher Th and LREE concentrations and correspondingly higher $[La/Yb]_{PM}$ (4.8–6.3).

### Samples of unknown stratigraphic position

Basaltic samples taken from the Pilbara Well greenstone belt show a wide range of incompatible trace element patterns (Fig. 8c):

- Three high-Ti samples show highly fractionated primitive mantle-normalized patterns with high concentrations of LREE (La 93 and 25 times primitive mantle values, respectively) and Th, compared to HREE (Yb ~4 times primitive mantle), high $[La/Yb]_{PM}$ (4.3–6.0) and $[La/Sm]_{PM}$ (2.0–2.9), and well-developed negative Nb anomalies ($[La/Nb]_{PM}$ = 2.3–2.9);
- One high-Ti basalt has relatively flat primitive mantle-normalized patterns (3–6 times primitive mantle values);
- One sample of low-Ti basalt has very low concentrations of incompatible trace elements (1–2.5 times primitive mantle values), with a highly depleted normalized pattern ($[La/Yb]_{PM}$ = 0.5, $[Gd/Yb]_{PM}$ = 0.66).

Five low-Ti basaltic rocks from the Wodgina greenstone belt have low concentrations of incompatible trace elements (1.5–4.0 times primitive mantle values; Fig. 8b), with patterns reflecting rocks that are only slightly less depleted ($[La/Yb]_{PM}$ = 0.52–0.79, $[Gd/Yb]_{PM}$ = 0.72–0.98) than the strongly depleted sample from the Pilbara Well greenstone belt.

Regional mapping suggests a possible continuation of stratigraphy from the Pincunah greenstone belt (Sulphur Springs Group) to the Wodgina and Pilbara Well greenstone belts heading from east to west. The Sulphur Springs Group has an unusually high proportion of basaltic rocks with highly depleted trace element patterns (Appendix 1; Brauhart, 1999; Smithies et al., 2005b). Significantly, these basaltic rocks show a wide range of incompatible trace element patterns that is almost identical to the range shown by the rocks from the Pilbara Well greenstone belt (Fig. 9). No other single unit within the Pilbara Supergroup shows this compositional diversity, supporting a lithostratigraphic correlation between these rocks.

### Secular compositional trends

Smithies et al. (2005b) showed that high- and low-Ti basalts show distinctly different trends through the c. 500 m.y. depositional history of the Pilbara Supergroup (Fig. 6). The low-Ti basalts show an overall decrease in $Ti_{(9)}$, $Nb_{(9)}$, $Zr_{(9)}$, $La_{(9)}$, $Sm_{(9)}$, $Gd_{(9)}$, and $Yb_{(9)}$ with decreasing age to 3.2 Ga. These decreases correspond with a general increase in maximum $Mg^{\#}$. Minimum values for La/Nb ratios show no trend with age. However, minimum values for ratios of La/Sm, La/Gd, La/Yb, and Gd/Yb typically lie between primitive mantle and N-MORB values for basalts in the stratigraphically lower part of the Warrawoona Group, but systematically decrease to values below N-MORB values (i.e. more depleted than N-MORB) in the upper part of the Warrawoona Group and in the Kelly and Sulphur Springs Groups.

In contrast, there appears no clear evolutionary trend in any of these trace elements and ratios for the high-Ti rocks. Minimum La/Nb, La/Sm, La/Gd, La/Yb, and Gd/Yb ratios are typically greater than N-MORB values and there is no evidence that the source(s) for these rocks became more depleted with decreasing age.

### Possible tectonic settings inferred from the geochemistry of the basaltic rocks

Green et al. (2000) suggested that basalts in the Warrawoona Group assimilated large amounts of crustal material and on that basis argued for interaction with continental crust. However, Arndt et al. (2001) argued that the lower Warrawoona Group represents a Paleoarchean analogue of oceanic plateau crust, erupted subaqueously and essentially free of any felsic crustal contamination.

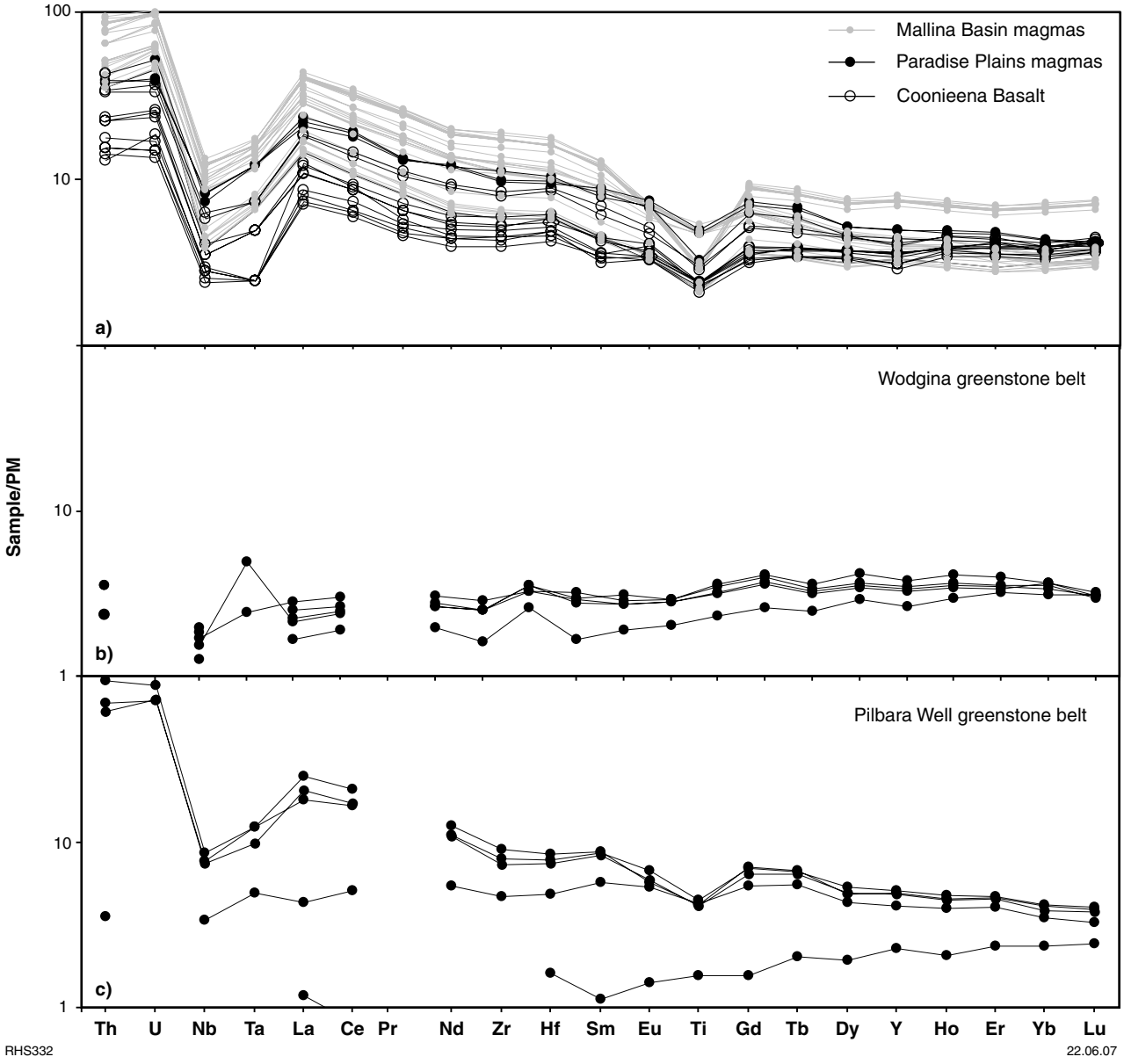


**Figure 8. Trace element plots normalized to primitive mantle comparing basalts from the Mallina Basin with those in the Goldsworthy area and from the Coonieena Basalt Member. Normalizing factors after Sun and McDonough (1989)**

Others have suggested that the Warrawoona Group was a volcanic plateau that was erupted onto continental crust (Van Kranendonk et al., 2002; Van Kranendonk and Pirajno, 2004). Low minimum La/Nb, La/Sm, and La/Yb ratios (N-MORB-like or lower) indicate that the most primitive high- and low-Ti magmas from throughout the Pilbara Supergroup erupted essentially free of significant input from felsic crust. Nevertheless, individual basalt units (high- and low-Ti) do show a range in La/Sm and La/Yb ratios and in LREE concentrations that likely reflects at least some interaction with felsic crust. However, neither the degree of contamination nor the proportion of contaminated rocks appears to increase significantly with decreasing age despite regional geological and geochronological evidence that large amounts of granitic material evolved throughout the depositional period of the group. The evidence from the Warrawoona and Kelly Groups cannot be used to support a setting similar to typical modern-day oceanic plateau crust or to continental crust, but rather a setting that incorporated aspects of both — possibly with similarities to the modern Kerguelen Plateau (Van Kranendonk and Pirajno, 2004).

The Coonieena Basalt and basalts in the Croydon Group (De Grey Supergroup) show a marked reversal of the compositional trends defined by the older low-Ti basalts of the Pilbara Supergroup. In particular, the very high La/Nb and La/Sm ratios suggest extensive contamination of the magmas by a crustal component (e.g. Arndt et al., 2001). Smithies et al. (2005b) noted that La/Nb ratios and Nb concentrations in the Coonieena Basalt and basalts in the Croydon Group are inconsistent with this crustal component simply being average exposed Archean Pilbara crust, but more likely reflect magma

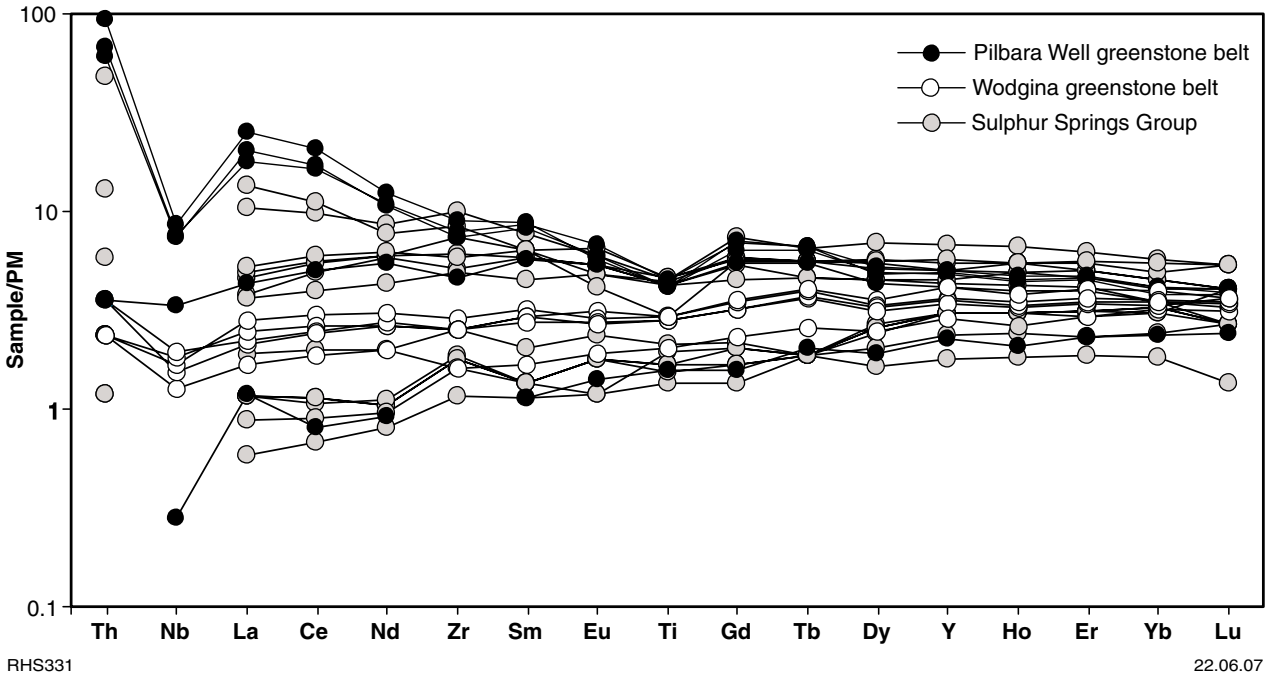


**Figure 9. Trace element plots normalized to primitive mantle comparing basalts from the Pilbara Well greenstone belt, the Wodgina greenstone belt, and from the Sulphur Springs Group. Normalizing factors after Sun and McDonough (1989)**

derivation from a refractory mantle source that was enriched by a subduction-derived component.

### *Use of geochemistry as an indication of stratigraphic affinity*

Although there are clear compositional variations in the geochemistry of basaltic rocks within the Pilbara Supergroup with time, the very large degree of compositional overlap shown by these rocks and, in particular, by rocks of the Warrawoona and Kelly Groups, greatly limits the use of geochemistry as a guide to stratigraphic affinity. It is clear that a single basalt sample could not be assigned to a specific stratigraphic unit, or even a general stratigraphic interval (e.g. lower, middle, upper) of the Pilbara Supergroup, based on geochemistry alone. An exception here might be for the Coonieena Basalt Member of the Bookingarra Formation (De Grey Supergroup), but even its characteristic Th- and LREE-enriched trace element patterns are approximated by the most LREE-enriched basalts from the Sulphur Springs Group, although at lower HREE concentrations and with lower La/Nb ratios.

However, the following two generalizations might be applicable:

1. strongly Th- and LREE-enriched rocks are more likely to come from the higher parts of the Pilbara Supergroup or De Grey Supergroup, and if the samples have La/Nb >2.5, they possibly correlate with the Bookingarra Formation of the Croydon Group, but if La/Nb <2.5, they are more likely to correlate with the Sulphur Springs Group;
2. the more depleted the source (i.e. samples with La/Yb, La/Sm, and Gd/Yb ratios lower than primitive mantle values), the more likely it is the samples will come from a stratigraphically higher part of the Pilbara Supergroup.

## Felsic volcanic rocks and felsic series

Cullers et al. (1993) have previously studied the geochemistry of the Duffer and Panorama Formations, and Brauhart (1999) has investigated the geochemical evolution of felsic volcanic rocks of the Sulphur Springs Group. Felsic rocks and rock series studied here are described from three stratigraphic intervals — all from the Warrawoona Group. In order of decreasing age, these are the Coucal Formation (Coonterunah Subgroup), the Duffer Formation, and the Panorama Formation. The Coucal Formation includes two mafic to felsic rock series (C-F1 and C-F2). The Duffer Formation includes a minor group of felsic volcanic rocks with characteristics of fractionated tholeiites (D-F1), a more voluminous mafic to felsic rock series (D-F2), and an overlying, voluminous group of distinctly trace element-enriched rocks (D-F3). The proportion of basaltic lava directly interbedded with the felsic volcanic and volcaniclastic layers of the Warrawoona Group decreases with decreasing age. However, the geochemical diversity of the felsic rocks appears to increase with decreasing age. Thus, the felsic volcanic sequences sampled from the Panorama Formation contained very few interbedded mafic rocks, but each discrete felsic volcanic centre has a unique compositional range.

Rocks belonging to the two volcanic series in the upper sequences of the Coucal Formation (C-F1 and

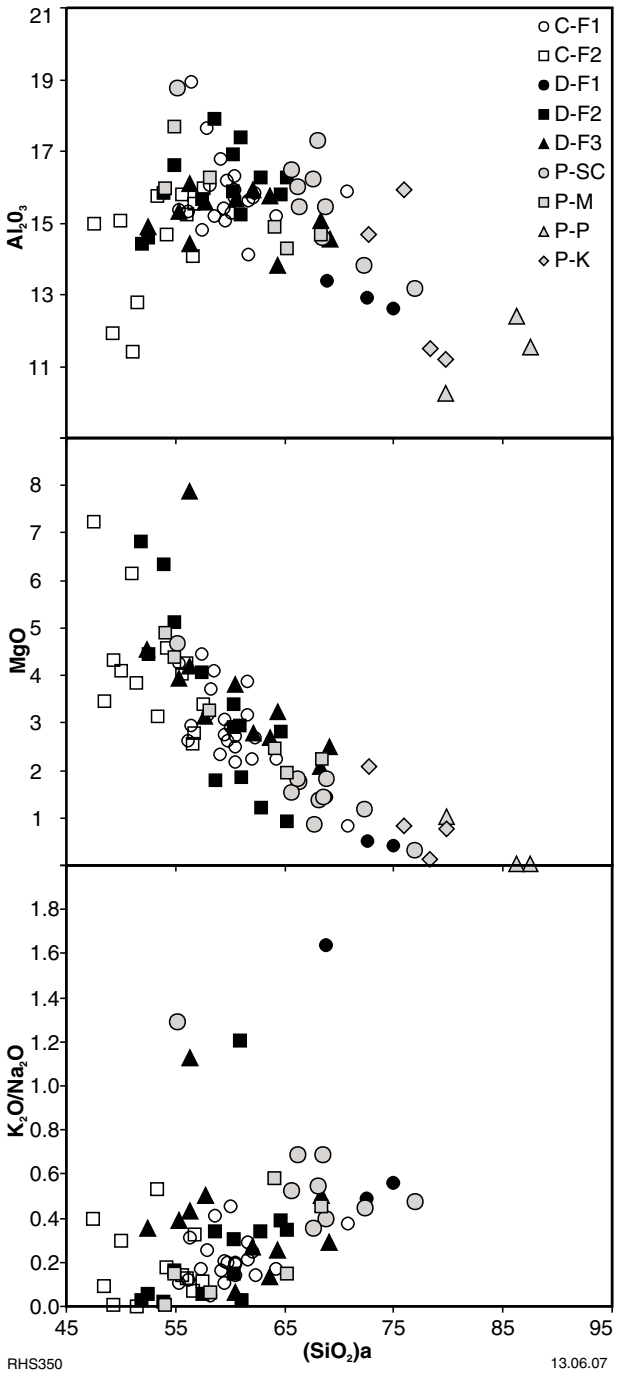


**Figure 10. Anhydrous $SiO_2$ vs $Al_2O_3$, MgO, and $K_2O/Na_2O$ for various felsic volcanic rock series of the Coucal Formation, Coonterunah Subgroup (C-F1 and C-F2); Duffer Formation (D-F1–3); and Panorama Formation (P). P-SC = Sandy Creek traverse; P-M = McPhee Dome traverse; P-P = Panorama Ridge; P-K = Kittys Gap**

C-F2) are not readily distinguishable from each other in the field, but are compositionally distinct (Fig. 10). The C-F1 rocks range from andesite to dacite with silica typically between 55 and 65 wt% (one sample at 71 wt%), whereas C-F2 rocks range from basalt to andesite with a silica range of 47.5 to 57.5 wt%. The two groups overlap extensively in terms of $Al_2O_3$, MgO, $K_2O$, and $Na_2O$, and both groups typically are sodic, with a $K_2O/Na_2O$ range between 0.05 and 0.45. The C-F1 rocks typically have lower concentrations of $TiO_2$, ΣFe (as $Fe_2O_3$), and $P_2O_5$. A single sample of sodic dacite has unusually high concentrations of La (26 ppm) and high La/Yb ratios (27), and matches very closely compositions typical of Archean TTG (Fig. 11).

Basaltic rocks within the C-F2 series show considerable overlap in major element compositions with the underlying tholeiites of the Tabletop Formation, but range to slightly more evolved members with MgO as low as 2.5 wt% ($Mg^{\#}$ ~24) and $SiO_2$ as high as 56 wt% (Fig. 10), and with significantly lower ranges in Cr and Ni. Concentration ranges for Yb also overlap extensively, but the more incompatible trace elements (e.g. La) are significantly enriched in the C-F2 basalts (Fig. 12), with very little overlap in La and Th concentrations. Values of La/Yb for the C-F2 basalts range from 3.2 to 6.5 (cf. 1.08 to 2.9 for the tholeiites), but La/Nb ratios are low (0.89 to 2.06) and similar to those of the tholeiitic basalts.

The C-F1 andesites and dacites show wide ranges in La/Nb (1.95–2.72) and Th/Nb (0.34–0.76) ratios over a narrow range of Nb concentrations (8–13 ppm; Fig. 13). In contrast, C-F2 basalts and andesites have narrower ranges of La/Nb (1.35–1.66) and La/Th (0.04–0.28), at significantly lower Nb concentrations. They also have generally lower La/Yb ratios (3.2–6.8 cf. 6.6–10.7) but similar Gd/Yb ratios (1.6–2.5).

Compared to rocks of the D-F2 and D-F3 series, the D-F1 rhyolites are silicic (68.8–75 wt% $SiO_2$), and at 14 wt% have relatively low $Al_2O_3$ (Fig. 10), high $K_2O$ (>2.3) and $K_2O/Na_2O$ (~0.5 and higher), and have the highest ΣFe (as $Fe_2O_3$; 2.7–4.6 wt%), lowest MgO (Fig. 10), and correspondingly lowest $Mg^{\#}$ (22–38) at a given silica value. The D-F2 and D-F3 series of the Duffer Formation overlap extensively in silica range (D-F2 = 51.8–65; D-F3 = 52.4–68.8), and in concentration ranges of all other major elements except for $Al_2O_3$, which, for samples with >55 wt% $SiO_2$, is generally higher in the D-F2 series (>15.7 cf. <15.7 for D-F3; Fig. 10). Both series are sodic, with $K_2O/Na_2O$ generally <0.5.

Compared to the felsic volcanic rocks of the Coonterunah Subgroup, the D-F2 and D-F3 series are typically more silicic (Fig. 10). C-F2 and D-F3 have a similar low range in $Al_2O_3$, but both D-F2 and D-F3 generally have lower ΣFe, for a given silica value, than the C-F1 and C-F2 series.

The felsic rocks of the Panorama Formation range to higher silica values than those of the older formations (Fig. 10). Although rocks from Panorama Ridge and Kittys Gap are clearly silicified ($SiO_2$ 72.7–87.5 wt%), unsilicified rocks from the Sandy Creek area range between 54 and 76.9 wt% $SiO_2$ (with an average of 67.5 wt% $SiO_2$), compared with an average of 61.3 wt% $SiO_2$ for the non-basaltic rocks in D-F2 and D-F3. Rocks from the McPhee Dome area have compositional ranges that closely resemble those of the D-F3 series for most major elements except for CaO, which is typically higher in the McPhee Dome rocks. The Sandy Creek rocks have higher $Al_2O_3$ than the D-F2 and D-F3 series at a given silica value, and represent the most Al-rich series sampled. They also have a wide range of generally lower $Na_2O$ values (2.3–5.0 wt%),

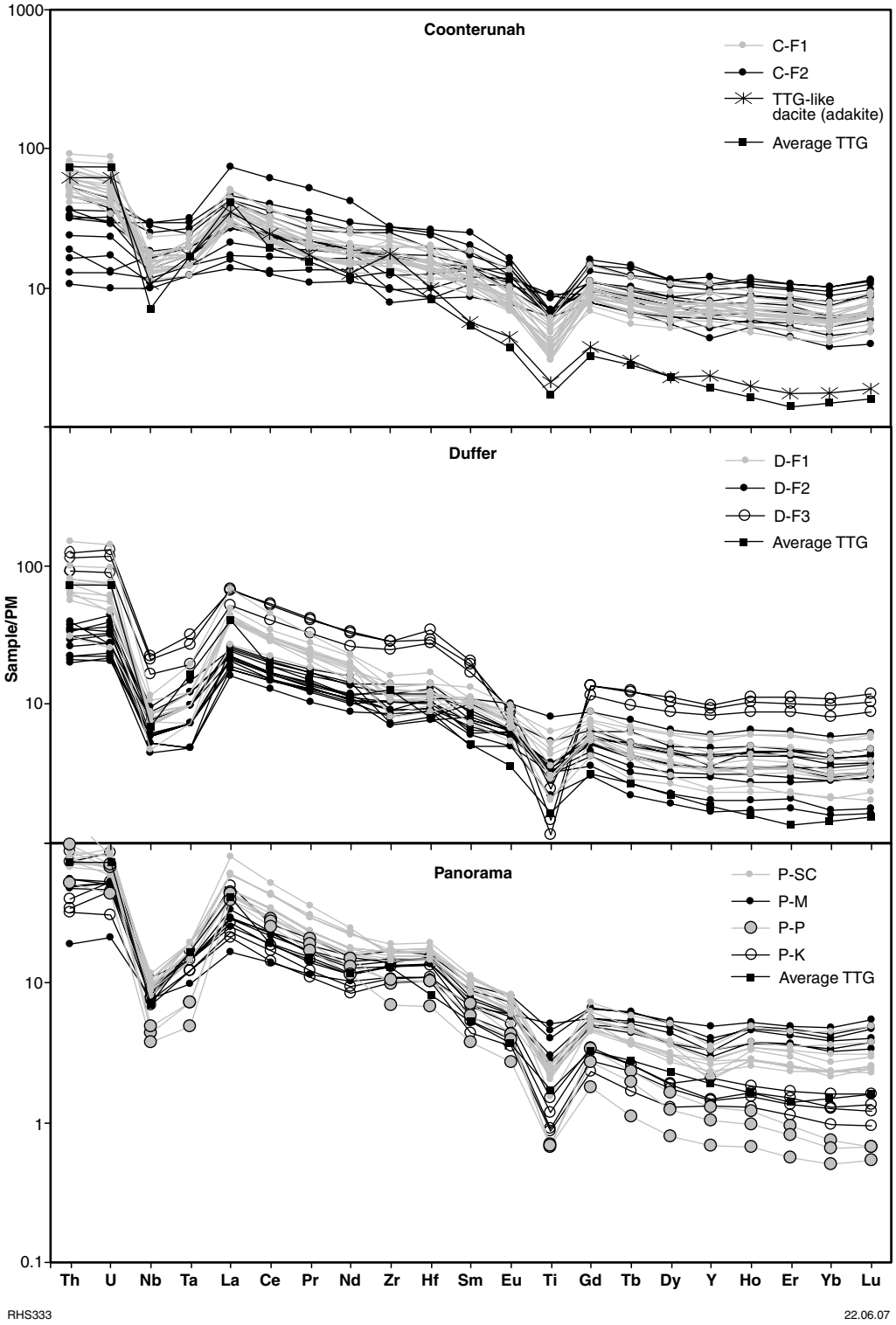


**Figure 11. Trace element plots normalized to primitive mantle for various felsic volcanic rock series of the Coucal Formation, Coonterunah Subgroup (C-F1 and C-F2 and TTG-like dacite); Duffer Formation (D-F1–3); and Panorama Formation (P). P-SC = Sandy Creek traverse; P-M = McPhee Dome traverse; P-P = Panorama Ridge; P-K = Kittys Gap. Average TTG is from Martin et al. (2005). Normalizing factors after Sun and McDonough (1989)**

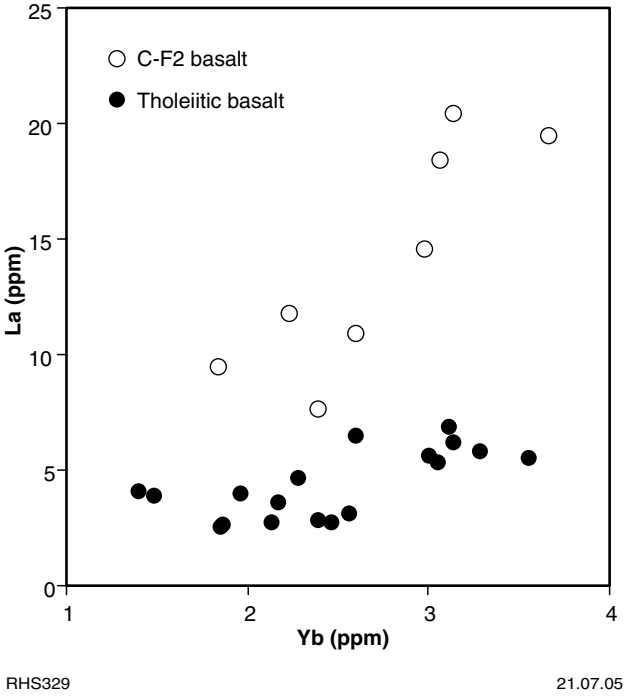


**Figure 12. Plot of Yb vs La for basalts of the Coonterunah Subgroup comparing C-F2 basalts of the Coucal Formation with underlying tholeiitic basalts of the Tabletop Formation**

and correspondingly higher CaO values (1.5–6.4) than the trend for D-F2 and D-F3, but are similar in this regard to rocks of the C-F1 series. The Sandy Creek and McPhee Dome rocks typically range to higher $K_2O/Na_2O$ (0.35–0.7) than series from the Coucal Formation and from the Duffer Formation. The very high $K_2O$ values (up to 8.2 wt%) and extremely low $Na_2O$ contents (<0.2 wt%) in the Panorama Ridge and Kittys Gap rocks are likely to be the result of alteration.

Trace element patterns normalized to primitive mantle show significant differences between the various felsic units/series of a particular age range, and between the various age groups (Fig. 11). For the Coonterunah Subgroup, the C-F1 series forms a tight array, whereas the C-F2 series shows a wider range of normalized data, but with more or less parallel patterns. The patterns for C-F1 and C-F2 overlap extensively, except for Th and U, the concentrations of which are generally significantly greater in the C-F1 series. The C-F1 series has significantly more fractionated patterns with higher average normalized Th/La (1.65 vs 0.91), La/Sm (3.02 vs 2.07) and La/Yb (6.24 vs 4.33), but with similarly low Gd/Yb (1.59) and with more-prominent Nb anomalies (average normalized La/Nb = 2.45 vs 1.67). The low La/Nb ratios for the C-F2 data do not change significantly with changing Nb and La concentrations. The C-F2 series has the least fractionated trace element patterns of all of the felsic units sampled from the Warrawoona Group.

The D-F1 rocks have the highest concentrations of highly incompatible trace elements of all the felsic units, but have MREE and HREE concentrations similar to those of the more enriched members of the C-F2 series and to tholeiitic basalts interlayered with the felsic rocks of the Duffer Formation. Compared to the felsic series from the Coonterunah Subgroup, the felsic series in the Duffer Formation have higher normalized La/Nb (~3.2 for D-F2 and 5.3 for D-F3). They are also notably depleted in HREE, and have more fractionated normalized trace element patterns (average $[La/Yb]_{PM}$ ~6.7 for D-F2 and ~13.3 for D-F3). In addition, whereas trace element patterns for each of the felsic series of the Coonterunah Subgroup are more or less parallel (i.e. little change in La/Yb for large change in Yb), the D-F2 series shows a large decrease in La/Yb and the D-F3 series a large increase in La/Yb, with increasing La.

The four different felsic volcanic rock groups from the Panorama Formation each show very different normalized trace element patterns and, in particular, have very different HREE concentrations (average normalized Yb concentrations ~0.6 for Panorama Ridge; ~1.3 for Kittys Gap; ~2.8 for Sandy Creek; ~3.3 for McPhee Dome). The Panorama Ridge rocks also have high normalized Gd/Yb ratios (~4.4) compared to all the other felsic volcanic rocks of the Warrawoona Group (Kittys Gap Gd/Yb ratio ~2.3, remainder <2). Except for the rocks from McPhee Dome,

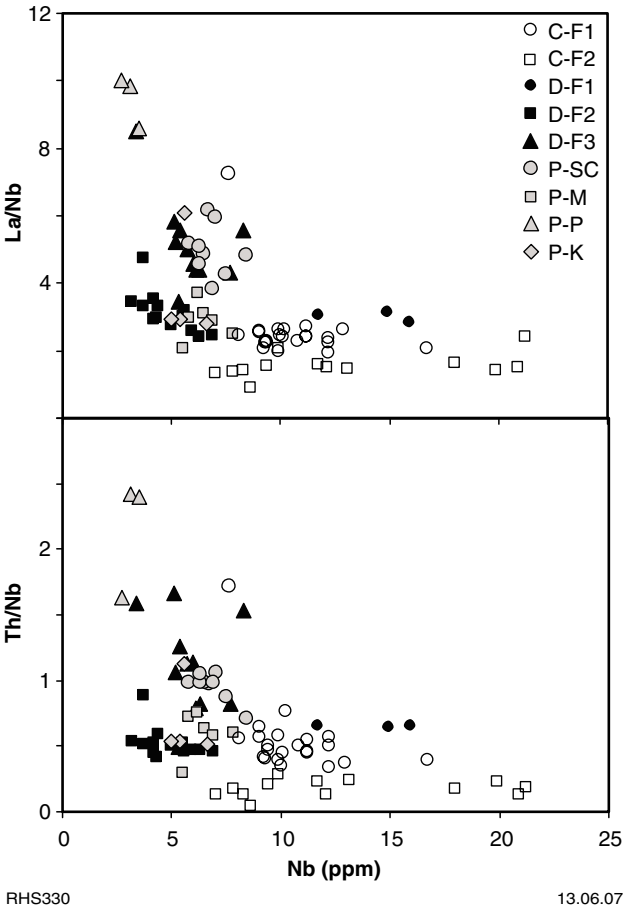


**Figure 13. Nb vs La/Nb and Th/Nb for various felsic volcanic rock series of the Coucal Formation, Coonterunah Subgroup (C-F1 and C-F2); Duffer Formation (D-F1–3); and Panorama Formation (P). P-SC = Sandy Creek traverse; P-M = McPhee Dome traverse; P-P = Panorama Ridge; P-K = Kittys Gap**

which have $[La/Yb]_{PM}$ ~8, the felsic volcanic groups from the Panorama Formation have the highest normalized La/Yb ratios (average ~19 for Sandy Creek; ~24 for Kittys Gap; and ~67 for Panorama Ridge) of all of the sampled felsic volcanic rocks of the Warrawoona Group. Felsic rocks from the Panorama Formation also have amongst the highest normalized La/Nb ratios.

### *Secular compositional trends*

The geochemical data for the felsic sequences of the Warrawoona Group show broad, though poorly defined, trends with decreasing age. In particular, the rocks become generally more silicic and aluminium rich (and possibly potassium rich), and have higher La/Yb and La/Nb ratios. Such trends could be interpreted in terms of a general increase in the pressure of magma genesis with decreasing age, or an increasing contribution of a source component that was formed at high pressure (e.g. TTG).

Intrusions with TTG-like compositions formed throughout the depositional period of the Warrawoona and Kelly Groups. However, it is interesting to note that, apart from a single TTG-like dacite found in the Coucal Formation, TTG-like magmas did not erupt until the Panorama Formation, where they form a (minor) component within the wide compositional range of felsic magmas that erupted at that time. One possible reason for this is that the high viscosity associated with the highly silicic magmas typical of the TTG series prevented them from rising significant distances through the thickening Pilbara crust.

The North Shaw Tonalite has compositions consistent with the Archean TTG series and its spatial and temporal relationship to the volcanic rocks of the Duffer Formation led Bickle et al. (1983) to suggest a genetic relationship. The geochemical data presented here clearly discount such a relationship (Fig. 11).

### *Use of geochemistry as an indication of stratigraphic affinity*

The felsic rocks of the Coonterunah Subgroup are distinguished from all other felsic volcanic rocks of the Warrawoona Group by such features as their unfractionated trace element patterns and relatively consistent La/Yb with varying La concentrations. However, the felsic rocks of the Duffer and Panorama Formations show too much compositional overlap for geochemistry to be confidently used as a basis for stratigraphic allocation.

# West Pilbara Superterrane and the De Grey Superbasin in the west Pilbara

## Roebourne Group — Ruth Well Formation

Four basaltic rocks, one komatiitic basalt, and two fine-grained peridotites were sampled from the Ruth Well Formation of the c. 3.27 – 3.25 Ga Roebourne Group, on the southeastern limb of the Roebourne Anticline, approximately 15 km south of Karratha (traverse 1 on Fig. 14). Arndt et al. (2001) also reported four analyses of rocks taken from the same region.

### Geochemistry

The basaltic rocks are generally tholeiitic, with concentrations of silica between 51.25 and 54.9 wt%, MgO between 5.1 and 11.2 wt%, ΣFe between 10.6 and 11.9 wt%, and $TiO_2$ between 0.88 and 1.41 wt%. MREE and HREE are unfractionated, with flat normalized patterns at 4 to 12 times primitive mantle values (Fig. 15). Concentrations of Th are up to 42 times primitive mantle values and the LREE are fractionated, with La at ~20 times primitive mantle values and $[La/Sm]_{PM}$ ratios from 1.6 to 2.0. There are significant depletions in Nb, with $[La/Nb]_{PM}$ ratios ~1.9. Two basalts, analysed by Arndt et al. (2001), are compositionally similar to those presented here. The enrichments in Th, U, and LREE clearly distinguish these basalts from rocks of the Regal Formation and tholeiites from the Whundo Group. Basaltic rocks with similar enrichments are found in the Whundo Group, but have calc-alkaline compositions and typically more pronounced Nb depletions ($[La/Nb]_{PM}$ = 1.7 – 2.6).

The peridotites have around 43 wt% $SiO_2$, 35 wt% MgO, $Mg^{\#}$ from 88 to 90, 2.5 wt% $Al_2O_3$, and 0.20 wt% $TiO_2$. Their Cr concentrations are 1775 and 4143 ppm, and Ni concentrations are 2232 and 2607 ppm. The two samples have very different normalized trace element patterns (Fig. 15). One sample (GSWA 160245) has a pattern that is more or less parallel to those of the associated basalts, but at significantly lower concentrations. This sample also has the highest Cr and Ni concentrations and is an olivine- and clinopyroxene-rich cumulate rock possibly related to the magmas from which the basalts crystallized. The second sample (GSWA 160242) has much flatter normalized trace element patterns, with values at ~0.5 to 1.0 times primitive mantle values, but with notable enrichments in Th (2.3 times primitive mantle), and is similar to komatiite samples analysed by Arndt et al. (2001). Sub-chondritic $Al_2O_3/TiO_2$ ratios (12–14), and Gd/Yb ratios (1.5 – 1.8) greater than chondritic values (~1.21; Fig. 16) for this sample are similar to the Al-depleted and Ti-enriched komatiites of Sproule et al. (2002).

No Nd-isotope data on the Ruth Well Formation were obtained during the present study; however, Arndt et al. (2001) presented Nd-isotope data for a single basalt [$\varepsilon_{Nd(3260\ Ma)}$ = +0.40] and a single komatiite [$\varepsilon_{Nd(3260\ Ma)}$ = +0.93].

## Whundo Group

Fifty-nine samples were analysed from the Whundo Group, including 50 samples within the compositional range of basalt to andesite and nine volcanic and volcaniclastic samples of rhyolitic composition (traverse 2 on Fig. 14). Sampling was primarily aimed at constraining the geochemical range of lithologies present, establishing a geochemical stratigraphy, and identifying any geochemical fingerprint that might help constrain the tectonic setting

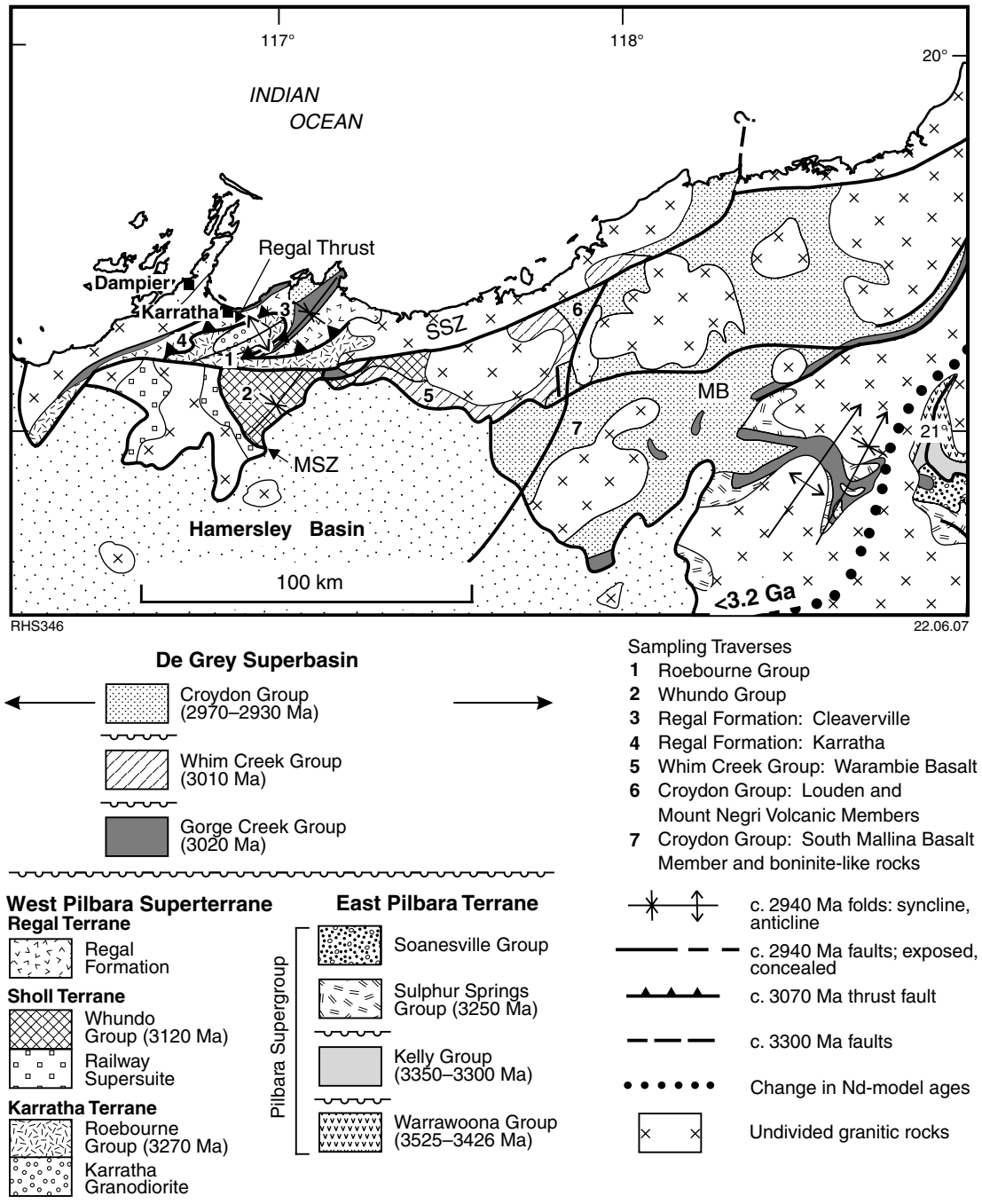


**Figure 14. The localities of major sampling traverses throughout the West Pilbara Superterrane. MSZ = Maitland Shear Zone, SSZ = Sholl Shear Zone, MB = Mallina Basin**

in which the group was deposited. Detailed results and interpretations of these data have been presented by Smithies et al. (2005a), from which the following summary is derived.

## Geochemical stratigraphy

The Whundo Group (Fig. 17) can be divided geochemically into three volcanic packages (Fig. 18). The lower volcanic package is dominated by calc-alkaline basaltic to andesitic lavas but includes ~1–10 m-thick flow units with boninite-like compositions (Smithies et al., 2004b), which are interbedded throughout and form up to ~15% of the package. This package forms the most deformed and metamorphosed part of the Whundo Group.

Tholeiitic lavas dominate the middle volcanic package but rare flows of boninite-like lavas persist into the lower parts of this package. Rocks compositionally transitional between these and overlying calc-alkaline lavas are found in the upper parts.

The upper volcanic package contains abundant calc-alkaline basaltic to dacitic flows of vesicular pillowed units intercalated with hyaloclastite, flow-top breccia,

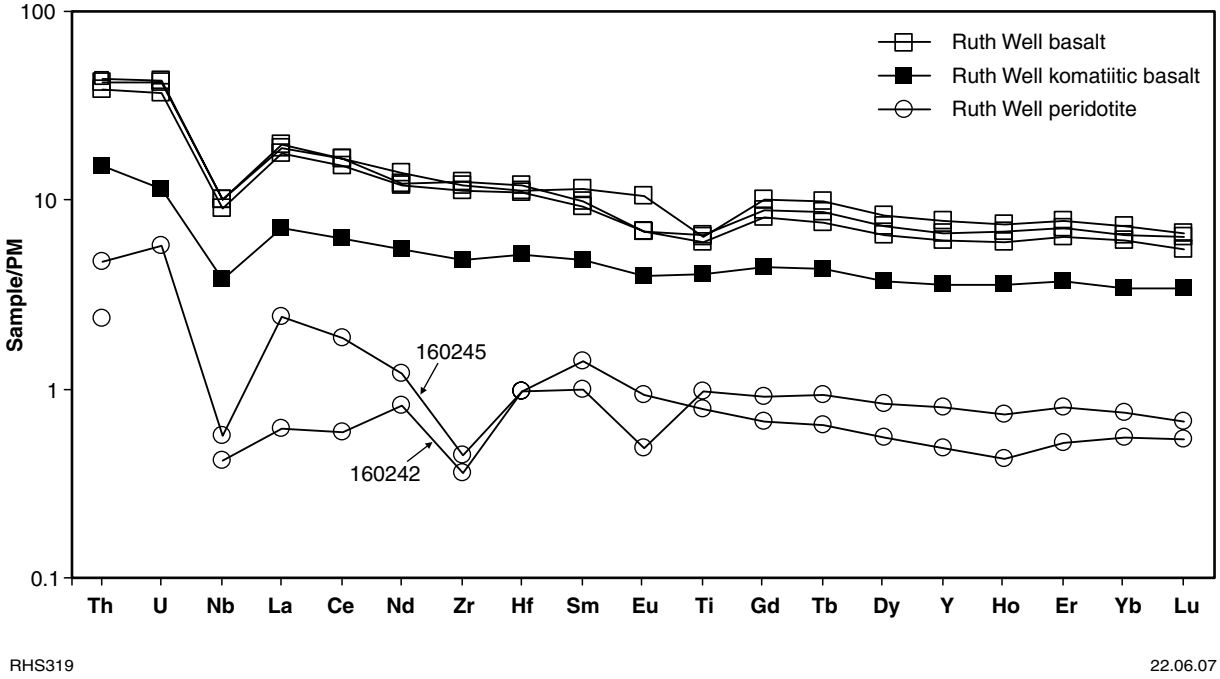


**Figure 15. Trace element plots normalized to primitive mantle for komatiites and komatiitic basalts of the West Pilbara Superterrane. Normalizing factors after Sun and McDonough (1989)**

and reworked volcaniclastic deposits. The area from which samples of these calc-alkaline rocks were taken is one of the few large areas within the Whundo region where extensive faulting or overprinting alteration are not significant.

Rocks clearly of a felsic volcanic origin first appear within the stratigraphically intermediate levels of the middle volcanic package and include laminated ash deposits, pumiceous breccia, and quartz–plagioclase-porphyritic flows. The proportion of felsic volcanic and volcaniclastic rocks increases upwards within the upper volcanic package and these rocks dominate the poorly preserved uppermost part of that package. Near the top of the upper volcanic package, felsic volcanic and volcaniclastic rocks are interbedded with minor flows of Nb-rich basalt and LREE-rich dacite.

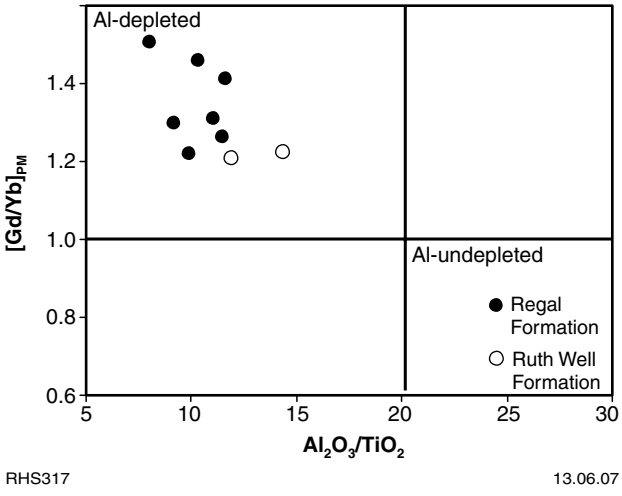


**Figure 16. $Al_2O_3/TiO_2$ ratios vs primitive mantle-normalized Gd/Yb ratios for komatiites of the West Pilbara Superterrane. Solid lines show mantle values of respective ratios**

## Geochemistry

### *Boninite-like rocks*

Boninites are rare, high-Mg basaltic to andesitic rocks typically with low Ti concentrations, high LILE concentrations, and with very high $Al_2O_3$/ $TiO_2$, low Gd/Yb, and high La/Gd compared to primitive mantle. In the Phanerozoic record they are confined to convergent margin settings (Crawford et al., 1989).

The Whundo Group boninite-like rocks have been described by Smithies et al. (2004b, 2005a) and range in $SiO_2$ content from 47.3 to 53.2 wt%, with an average $SiO_2$ value of ~52.5 wt%. They are the most primitive rocks of the Whundo Group, and their MgO concentrations range from 8.1 to 9.9 wt% and $Mg^{\#}$ ranges from 61 to 66. $TiO_2$ concentrations are low, between 0.3 and 0.5 wt%, whereas CaO and, particularly, $Al_2O_3$ are high, between 6.8–8.5 and 16.0–17.0 wt%, respectively. This results in high $Al_2O_3/TiO_2$ and $CaO/TiO_2$ ratios of 35–58 and 18–29 respectively, which distinguished these rocks from other basaltic rocks of the East Pilbara Terrane and West Pilbara Superterrane.

The Whundo Group boninite-like rocks form two geochemical groups (Fig. 19). One, referred to as 'evolved boninites', has higher incompatible trace element

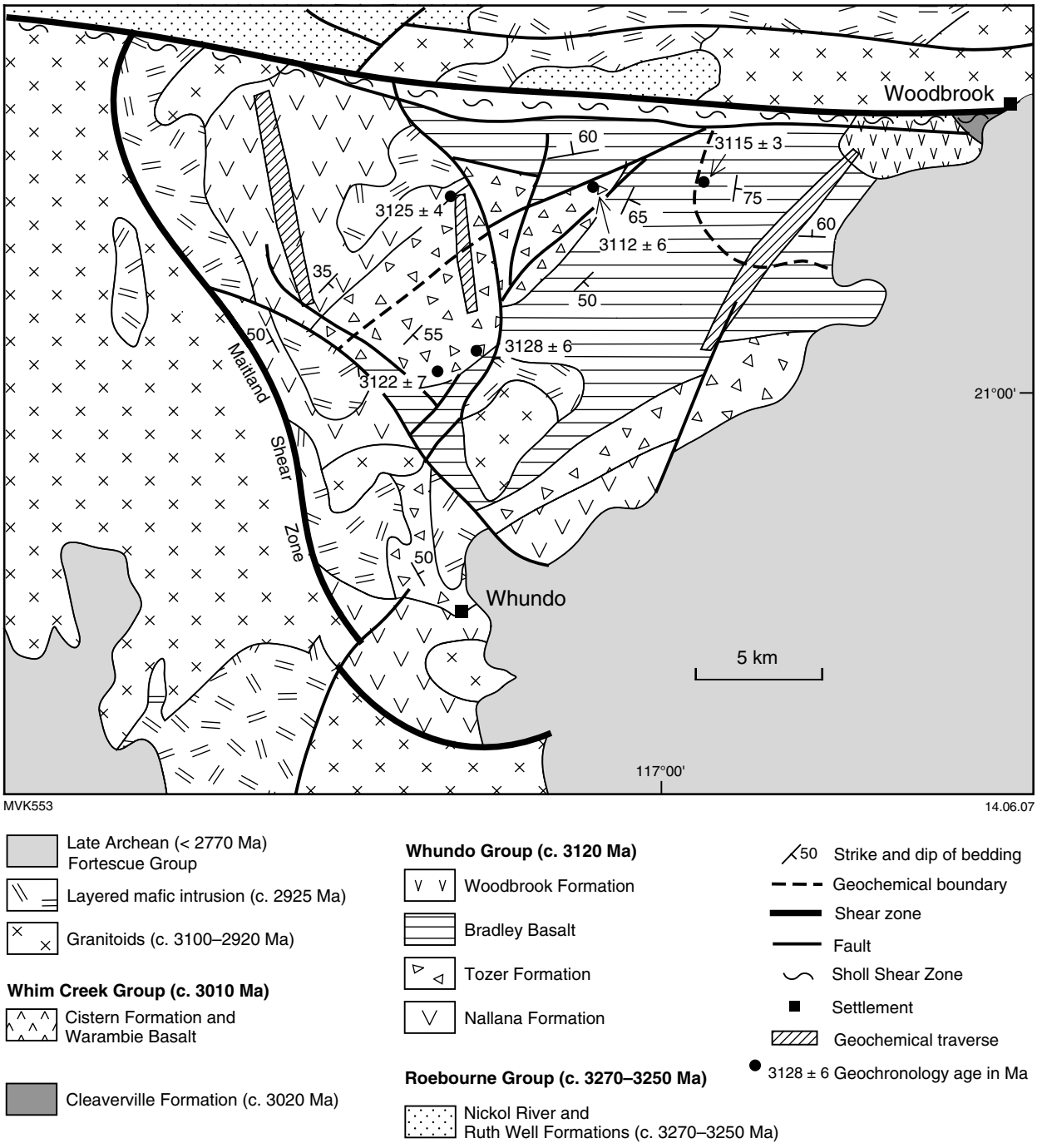


**Figure 17. Geological map of the Sholl Terrane, showing the location of geochemical traverses through the Whundo Group**

concentrations, is slightly more silicic, and has slightly lower $Mg^{\#}$ (61–63). Members of this group show strong enrichments in LREE and Th over middle to heavy REE, with primitive mantle-normalized La/Gd ratios ($[La/Gd]_{PM}$) between 2.63 and 2.02. They have moderate relative depletions of Eu, Nb, Ta, and Ti, slight Zr and Hf depletions, $[Gd/Yb]_{PM}$ between 0.98 and 0.82, and $[Yb/Sc]_{PM}$ from 1.14 to 0.85.

The second (primitive) group of boninitic rocks, with generally higher $Mg^{\#}$ (61–66), shows similar LREE and Th enrichment ($[La/Gd]_{PM}$ = 2.75 – 1.87) to the evolved boninites, but has lower $[Gd/Yb]_{PM}$ and $[Yb/Sc]_{PM}$, from 0.83 to 0.66 and 0.60 to 0.47, respectively. These rocks also show negative anomalies for Nb, Ta, and Zr (and Hf), but contrast with the evolved boninites in having slight positive Eu and Ti anomalies.

Compared to modern boninites, the Whundo boninite-like rocks are $SiO_2$ poor and $Al_2O_3$ rich, and have slightly elevated HREE concentrations, but otherwise closely match modern boninites, perhaps more so than any other Archean rocks thought to have a boninitic paragenesis (Smithies et al., 2004b).

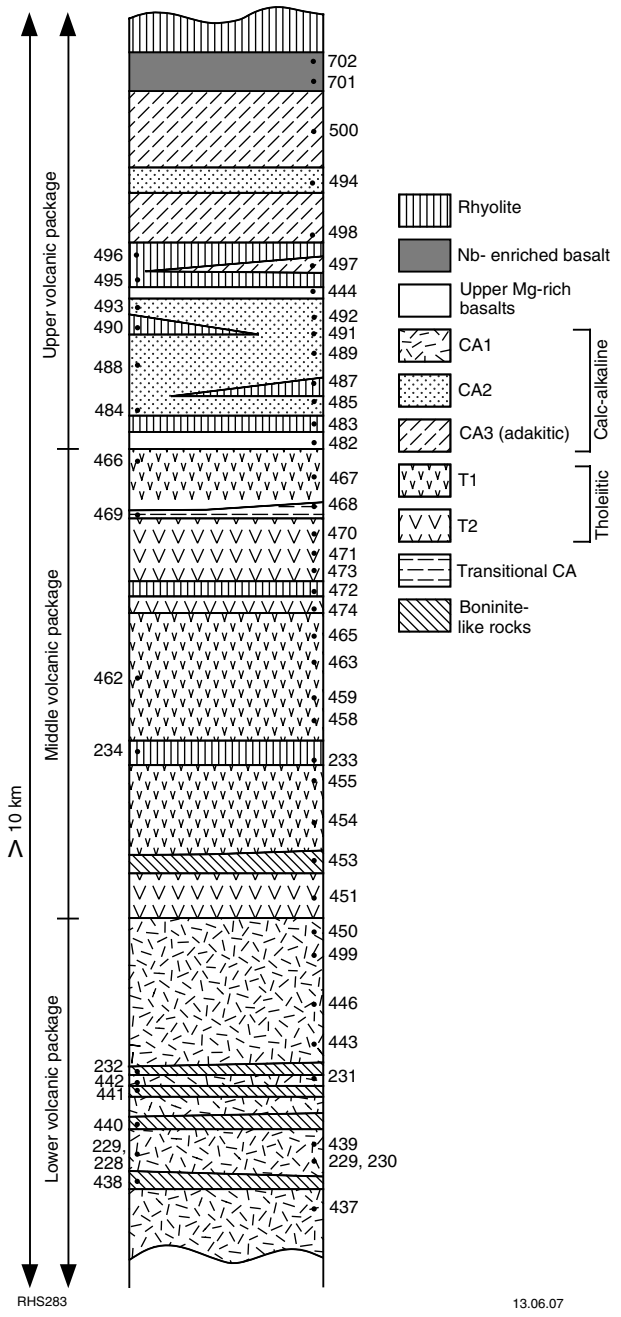


**Figure 18. Stratigraphy of the Whundo Group, showing relative proportions of units and position of specific samples. Sample numbers 4xx, are prefixed by 174 (i.e. 1744xx), 7xx are prefixed by 176, whereas numbers 2xx are prefixed by 180 (see Appendix 1)**

### *Tholeiites*

Tholeiitic volcanic rocks of the Whundo Group are dominantly basalts with $SiO_2$ <54 wt%, MgO >5 wt%, $Mg^{\#}$ >40 (Fig. 20), and $K_2O$ <0.5 wt%. The concentrations of MREE and HREE are between 1 to 2 times average N-MORB values (5–10 times primitive mantle; Fig. 19b), with only slightly fractionated $[Gd/Yb]_N$ (1.1–1.24). There are slight enrichments in the highly incompatible trace elements, with La and Th typically at concentrations of 2–3 and 5–8 times N-MORB, respectively. There are also small, but persistent, HFSE depletions, with $[La/Nb]_N$ between 1.1 and 1.26 ($[La/Nb]_{PM}$ 1.2–1.4) and $[Sm/Zr]_N$ between 1.01 and 1.13.

The tholeiites dominate the middle volcanic package and can be subdivided into two groups — T1 and T2. Flows of the second, less common, group (T2) are found at the base of the middle volcanic package, where they are overlain by boninite-like rocks, and at the transition between the middle and upper volcanic packages, where they are overlain by a short interval of T1 lavas prior to the onset of calc-alkaline volcanism (Fig. 18). The combination of slightly higher $Mg^{\#}$ (Fig. 20), lower $TiO_2$, V, Sc, and HREE, and more enriched incompatible trace element patterns (e.g. higher Th/Zr, Th/Yb, La/Sm, La/Yb) at lower trace element abundances (Fig. 19) distinguishes T2 lavas from T1 lavas. These compositional differences preclude a relationship between T1 and T2 via any simple liquid line of descent. La/Nb and Th/Nb ratios slightly higher than N-MORB values of 1.07 and 0.05 (Fig. 21) respectively, suggest either an enriched mantle source or minor crustal assimilation. The Nd-isotopic composition of the tholeiites ($\varepsilon_{Nd}$ ~+2.0) are slightly less radiogenic than depleted mantle ($\varepsilon_{Nd}$ ~+3.2 at 3.12 Ga). This permits a small crustal input to these rocks, but is not indicative of where that interaction may have occurred (mantle or crust).

### *Calc-alkaline rocks*

Calc-alkaline rocks of the Whundo Group can be broadly divided into four groups: CA1a and CA1b together form the bulk of the lower volcanic package (Fig. 18). The remainder (CA2 and CA3) form a major component of the upper volcanic package. All groups plot within, or straddle, the calc-alkaline field (Fig. 20) and, compared to the tholeiites, are depleted in HREE and distinctly enriched in incompatible trace elements, with higher La/Nb (Fig. 19c,d).

The two groups of calc-alkaline rocks in the lower volcanic package show a relatively large degree of compositional scatter (Fig. 20). These intercalated groups are only discriminated by geochemistry. The first group (CA1a) are andesites ($SiO_2$ from 56 to 60 wt%) and range in $Mg^{\#}$ from 52 to 64. The second group (CA1b) are dominantly basaltic ($SiO_2$ <56 wt%), and have lower $Mg^{\#}$ (44 to 55; Fig. 20) that suggest they are not parental to the CA1a andesites. Although their trace element abundance patterns are similar, the CA1a andesites have lower V (and Sc) and higher Th/Yb, Th/Nb, Th/La, and La/Sm ratios and generally higher Th, HFSE, and REE concentration than most of the CA1b basalts (Figs 19 and 20).

The CA2 flows of the upper volcanic package include some basaltic rocks but are mostly andesitic, with a $SiO_2$ range from 53 to 59 wt% and a range in $Mg^{\#}$ between 50 and 58. Their major element compositions lie between CA1a and CA1b (Figs 20 and 21) and their normalized trace element patterns and concentration range also closely resemble those rocks (Fig. 19). However, their magmatic associations differ; that is, CA2 lavas are interbedded

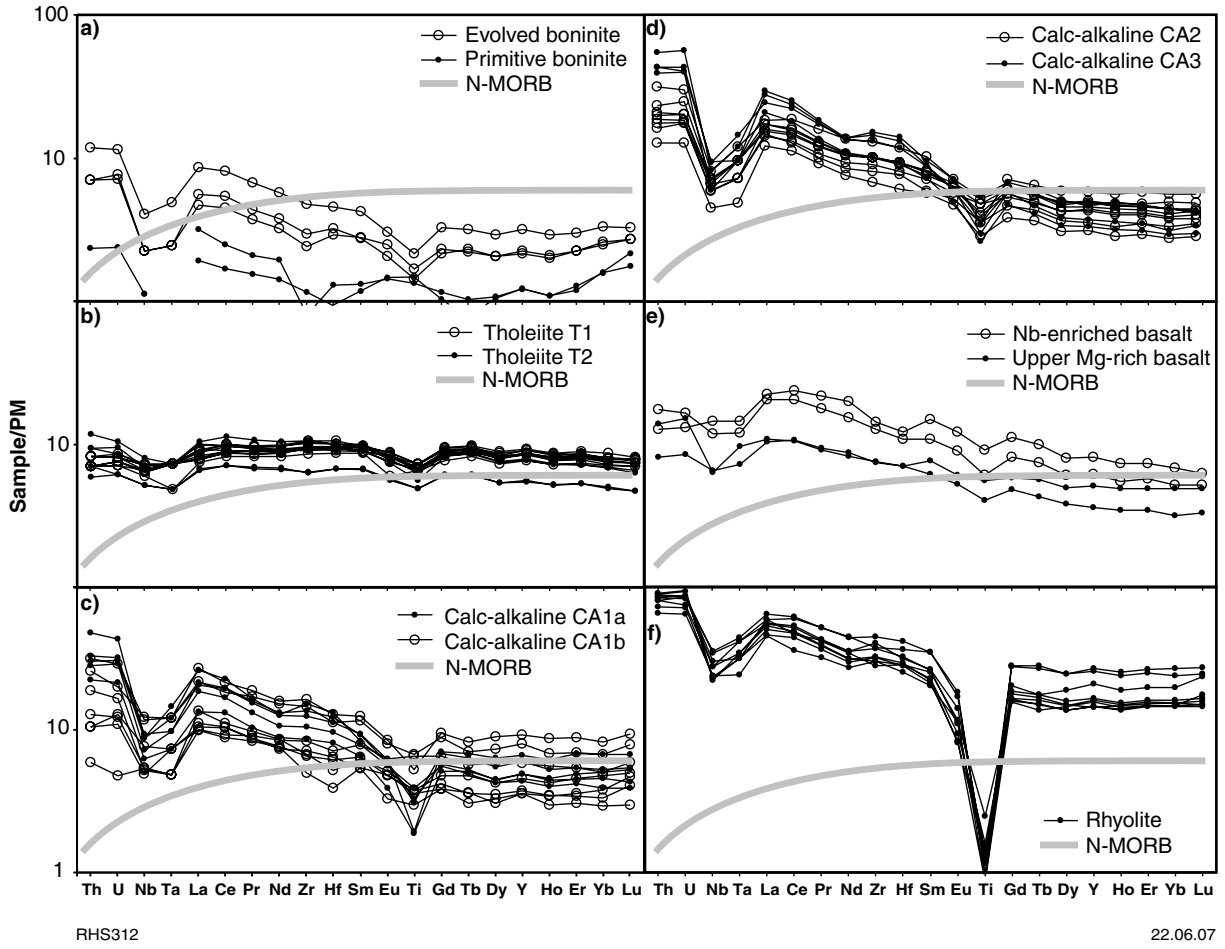


**Figure 19. Trace element plots normalized to primitive mantle for various volcanic rocks of the Whundo Group in the West Pilbara Superterrane. Normalizing factors after Sun and McDonough (1989)**

with locally abundant felsic lavas, whereas CA1 lavas are interbedded throughout with boninite-like rocks. This indicates that the CA2 lavas are not simply a structural repetition of the CA1 package.

Near the top of the upper volcanic package, felsic volcanic and volcaniclastic rocks are interbedded with andesitic to dacitic flows (CA3) and flows of unusually Nb-rich basalt. Compared to the other calc-alkaline lavas, the CA3 lavas are typically enriched in $SiO_2$ (>58 wt%), $Na_2O$ (2.1–5.6 wt%), LREE, and have higher La/Yb ratios (7.8–13.4 cf. 3.1–8) at similar $Mg^{\#}$ (38–57). They are unlikely to be genetically related to the associated rhyolites, which have much lower La/Yb (<6). Their compositions are similar to Phanerozoic adakites, which are felsic sodic magmas characterized by high La/Yb and Sr, and low HREE (Martin et al., 2005).

The calc-alkaline rocks have slightly lower initial $\varepsilon_{Nd}$ values ($\varepsilon_{Nd}$ ~+0.8 to +1.6) than the tholeiites ($\varepsilon_{Nd}$ ~+2.0 to +2.2), suggesting that the calc-alkaline rocks contain a slightly greater crustal component. The higher La/Nb at similar to lower Nb concentrations in the calc-alkaline rocks compared to the tholeiites (Fig. 21) indicates that the crustal material was very Nb poor. Importantly, exposed felsic crust of the Pilbara Craton typically has much higher Nb (~8 ppm) and La/Nb (~5) and so it is highly unlikely that the calc-alkaline rocks simply represent T1-type tholeiites with a greater component of assimilated Pilbara crust.

Two of the three stratigraphically lowest rocks of the upper volcanic package (GSWA 174468 and GSWA 174469 — 'transitional CA' rocks — Fig. 18) have compositions transitional between the evolved boninite-like rocks and CA2 lavas. These two lavas have $[Gd/Yb]_{PM}$ <1.0 and, along with the boninite-like rocks, preserve the only clear evidence of having been derived from a source more depleted than a N-MORB source.

### *Nb-enriched basalts*

Near the top of the upper volcanic package lie flow units of incompatible trace element-enriched basalt ($SiO_2$ = 51.3 to 53.5 wt%), interbedded with felsic and CA3 lavas (Fig. 18). These rocks have features transitional between the tholeiites and the calc-alkaline rocks. They are rich in ΣFe (10.5–13.8 wt%) and $TiO_2$ (1.3–2.0 wt%), and exhibit the strong LILE enrichments that characterize the calc-alkaline lavas. They are more Nb enriched (Nb = 8.6–10.5 ppm) than all tholeiites and most calc-alkaline rocks (Figs 19e and 21) and have the highest $P_2O_5$

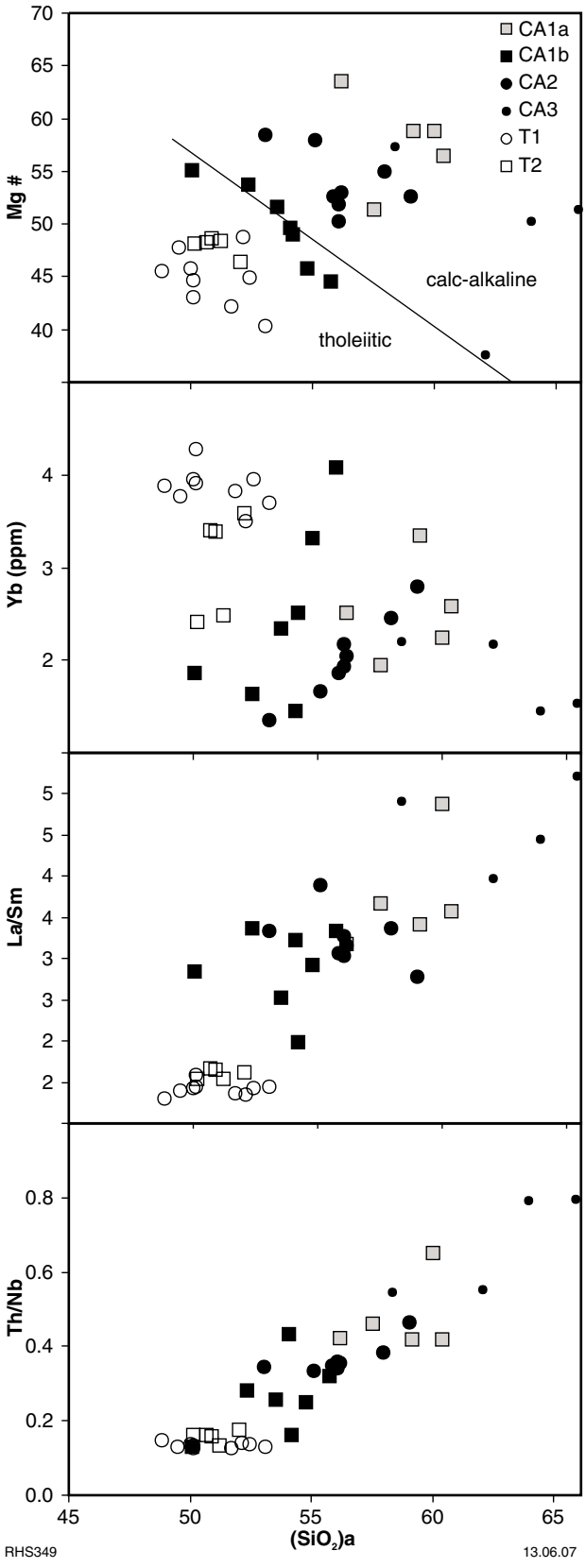


**Figure 20. Plot of anhydrous $SiO_2$ vs $Mg^{\#}$, Yb, La/Sm, and Th/Nb for various volcanic rocks of the Whundo Group in the West Pilbara Superterrane**

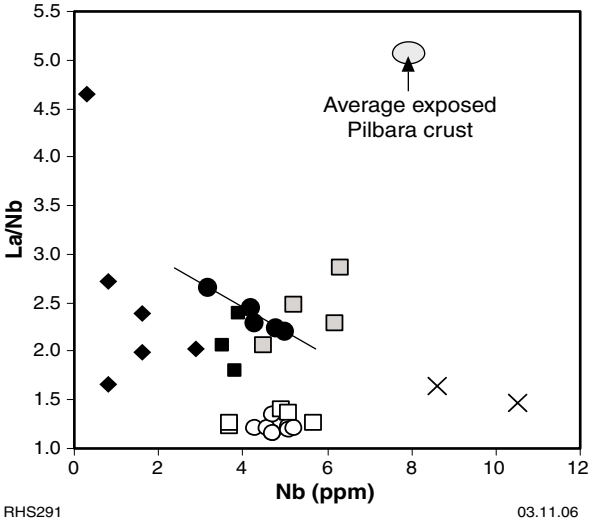


**Figure 21. Plot of Nb vs La/Nb for various volcanic rocks of the Whundo Group in the West Pilbara Superterrane (symbols as for Fig. 20, additional symbols are crosses = Nb-enriched basalts, solid diamonds = boninites)**

concentrations (0.34–0.45 wt%) of any rock within the Whundo Group. Two additional samples (GSWA 174482 and GSWA 174494 — referred to as 'Upper Mg-rich basalts') have similar trace element features (Fig. 19e) but are less enriched and have higher $Mg^{\#}$, MgO, and Cr concentrations.

### *Felsic rocks*

Felsic volcanic rocks within the Whundo Group form a compositionally coherent group of high-silica ($SiO_2$ >70 wt%), low- to medium-$K_2O$ rhyolites characterized by low $Al_2O_3$ (~11.4 wt%) and high $Na_2O/K_2O$ (~2.7) and ΣFe (~3.6 wt%). They have high HREE (Y from 60 to 130 ppm), Zr (300–500 ppm), and Nb (16–25 ppm) concentrations (Fig. 19f) coupled with low to moderate LILE concentrations. Their Nd-isotopic compositions ($\varepsilon_{Nd}$ ~+1.3 to +3.6; see Appendix 2) overlap the range for the tholeiites ($\varepsilon_{Nd}$ ~+2.0 to +2.2) and the calc-alkaline rocks ($\varepsilon_{Nd}$ ~+0.8 to +1.6). Smithies et al. (2005a) suggested these rocks evolved via extensive crystal fractionation or partial melting of a tholeiitic precursor contaminated by a component with a calc-alkaline composition.

## Tectonic implications and summary discussion

Smithies et al. (2005a) showed that there are numerous features of the Whundo Group that can be interpreted in terms of modern-style plate-tectonic processes. Whereas many of these features, taken individually, could be interpreted in terms of a range of processes not necessarily related to modern-style plate tectonics or to subduction, the combination of features provides a compelling case for a convergent-margin setting at 3.12 Ga. These features include:

- the fine- and broad-scale intercalation of discrete tholeiitic and calc-alkaline volcanic rocks;
- the presence of rocks with a strong boninite affinity near the base of the sequence;
- the presence of Nb-enriched basalts near the top of the sequence, and the close association of these with lavas of adakitic affinity;
- the recognition that assimilation of crust is an unlikely cause of LREE enrichments in the boninite-like lavas and calc-alkaline lavas;
- the identification of a range from depleted to undepleted and enriched source regions;
- mixing of source regions and/or primitive magmas derived from undepleted, depleted, calc-alkaline, and tholeiitic (MORB) sources, with distinct periods characterized by enhanced interaction and magmatic diversity;
- the recognition that the CA2 lavas, at least, are the result of flux melting; and
- the absence of any intervening sequences containing exotic 'continental' material.

The absence of evidence for basement material and of exotic 'continental' sedimentary material is most consistent with an intraoceanic-arc setting. Likewise, with Ce/Yb ratios mainly ~40 or less, the Whundo rocks correspond to the low Ce–Yb array of Hawkesworth et al. (1993), which distinguishes modern intra-oceanic arc basalts from continental-arc basalts.

# Regal Formation

The Regal Formation (Hickman, 1997) outcrops between Roebourne and Mount Regal, and is dominantly composed of amphibolite facies metabasalt. A second much smaller outcrop of the formation is on the Cleaverville Peninsula, where the metamorphic grade is lower greenschist facies. In both cases the formation consists of pillow basalt containing dolerite sills, and is stratigraphically overlain by the 3.02 Ga Cleaverville Formation of the Gorge Creek Group (De Grey Supergroup). In the larger outcrop area, the Regal Formation tectonically overlies the c. 3.27 to 3.25 Ga Roebourne Group and the 3.27 Ga Karratha Granodiorite across the Regal Thrust (Hickman, 2004). A sample of basalt from this formation gave a $T_{DM}$ model age of c. 3.16 Ga, very close to the assumed age of 3.2 Ga, and its $\varepsilon_{Nd}$ of ~+3.5 is close to depleted mantle values (3.2) at that time. Kiyokawa and Taira (1998) suggested that the outcrop at Cleaverville forms part of a subduction–accretion complex and that the basalt units occur in several thrust-bound slices. The geochemistry of basalts from the Cleaverville region has previously been studied by Ohta et al. (1996), who described them as LREE enriched, but otherwise MORB-like, and referred to them as Archean MORB (A-MORB).

A total of 38 samples of rocks mapped as part of the Regal Formation were analysed. The main population includes 15 basalts from a large outcrop 5–10 km south of Cleaverville (traverse 3 on Fig. 14). Ten samples were collected from an area immediately southeast of Karratha, including one sample of a serpentinized komatiite from the base of the section. Eight samples were collected from an area to the south of Dampier (Dampier Railway section — traverse 4 on Fig. 14). These included six samples from a sequence of olivine spinifex-textured komatiites and interlayered olivine cumulates, and two samples of structurally overlying basalt. Hickman (2001) interpreted the Dampier Railway section as lying near the stratigraphic base of the Regal Formation. A further two samples of basalt were taken from a roadside outcrop to the south, on PRESTON (Regal: Preston).

Except at Cleaverville (see above), the metamorphic grade of these rocks is typically around the lower amphibolite facies. At this grade, recrystallization of the basaltic rocks has resulted in fine- to medium-grained mineral assemblages, but vesicles and pillow structures are locally preserved. Greenschist facies assemblages occur locally, and in such areas vesicles and pillow structures are typically well preserved. Although the sampled komatiites have been metamorphosed to the lower amphibolite facies, these rocks commonly preserve all textural features characteristic of komatiite flows, including coarse olivine (sheath)-spinifex textures, random-spinifex textures, and olivine-cumulate textures.

The aims of sampling were to geochemically characterize the basalts of the Regal Formation using the samples from Cleaverville, and then to test the hypothesis that the samples from near Karratha, from the Dampier Railway section, and from PRESTON, might also belong to this formation. A further aim of this work was to compare geochemical features of the Regal Formation and the tholeiitic basalts of the Whundo Group to help clarify any possible relationship between these two units, which are separated by the major east-trending Sholl Shear Zone (Fig. 1). The outcrop of Regal Formation immediately south of Cleaverville is cut by a metamorphic isograd that separates greenschist facies basalts to the northwest from amphibolites to the southeast, and so a final aim of this sampling was to test if different metamorphic conditions affected the geochemical signature of the basalts.

## Geochemistry

The non-komatiitic rocks from all of the separate sampling localities and sections thought to be of Regal Formation rocks cannot be easily separated based on major and trace element geochemistry (e.g. Fig. 22). They are all tholeiitic, and 27 of the 32 samples are basalts, with silica between 48.9 and 52 wt%; the remaining five samples range up to 55.6 wt%. Concentrations of MgO lie between 3.6 and 7.9 wt%, ΣFe between 9.7 and 15.4 wt%, and $TiO_2$ between 0.65 and 1.51 wt%.

The concentrations of MREE and HREE are between 0.6 to 1.5 times average N-MORB values (~5 to 10 times primitive mantle; Fig. 23), with only slightly fractionated $[Gd/Yb]_N$ (1.1 – 1.27). There are slight enrichments in the highly incompatible trace elements (La and Th) and small but persistent HFSE depletions, with $[La/Nb]_N$ between 1.1 and 1.35. Only two Nd-isotopic data are available; one from a basalt in the Karratha section ($\varepsilon_{Nd(3200\ Ma)}$ ~+1.48), and one from a basalt in the Cleaverville section ($\varepsilon_{Nd(3200\,Ma)}$ ~+3.46).

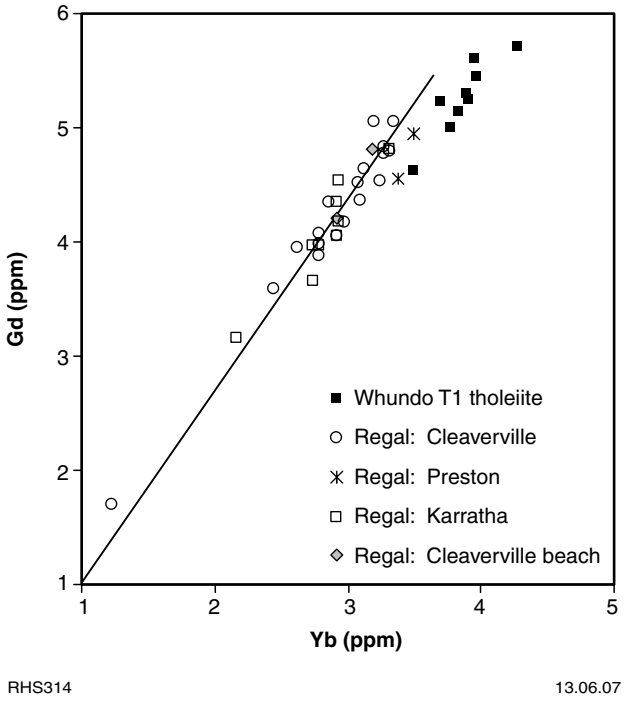


**Figure 22. Plot of Yb vs Gd comparing rocks from various outcrops of Regal Formation with tholeiitic basalts from the Whundo Group**

As with the basaltic rocks, there appear to be no compositional criteria for distinguishing the komatiitic rocks for the Dampier section from the single sample from the Karratha section (Fig. 23). As a group, these rocks have 43.5–46.3 wt% $SiO_2$, 27–36.9 wt% MgO, $Mg^{\#}$ from 84 to 89, 1.8–3.45 wt% $Al_2O_3$, 0.20–0.29 wt% $TiO_2$, 5229–1720 ppm Cr, and 2487 to 1489 ppm Ni. They have flat to slightly convex-upwards normalized trace element patterns with values typically between 0.6 to 2 times primitive mantle and with low $[La/Yb]_{PM}$ ratios ~0.9 to 3.8. With $Al_2O_3/TiO_2$ ratios (8–12) below chondritic values (~20) and Gd/Yb ratios (1.5–1.8) greater than chondritic values (~1.21; Fig. 16), these komatiites correspond to the Al-depleted and Ti-enriched komatiites of Sproule et al. (2002). Notably, the komatiitic rocks have generally higher La/Sm ratios (1.5–2.3) than the basalts (1.2–1.5). Only a single Nd-isotopic datum is available — the serpentinitic komatiite from the Karratha section giving an $\varepsilon_{Nd(3200\ Ma)}$ value of +0.56.

## Discussion

Since both fractional crystallization and crustal contamination should normally result in higher La/Sm ratios, the lower La/Sm ratios in the basalts (1.2–1.5) compared to the komatiites (1.5–2.3; Fig. 23) precludes a direct genetic relationship between the two rock types through any simple liquid line of descent, or any relationship to a common single mantle source component. The simplest interpretation is that the komatiites were more contaminated by felsic crust during magma ascent than the basalts, and this is supported by the less radiogenic Nd-isotopic composition of the komatiite.

The very close geochemical similarities between basalt samples from all of the individual localities and sections, and between the komatiitic rocks from the two sampled localities, is consistent with (though not proof of) the interpretation that all of these rocks belong to a single stratigraphic unit — the Regal Formation (Hickman, 1997; Figs 22 and 23).

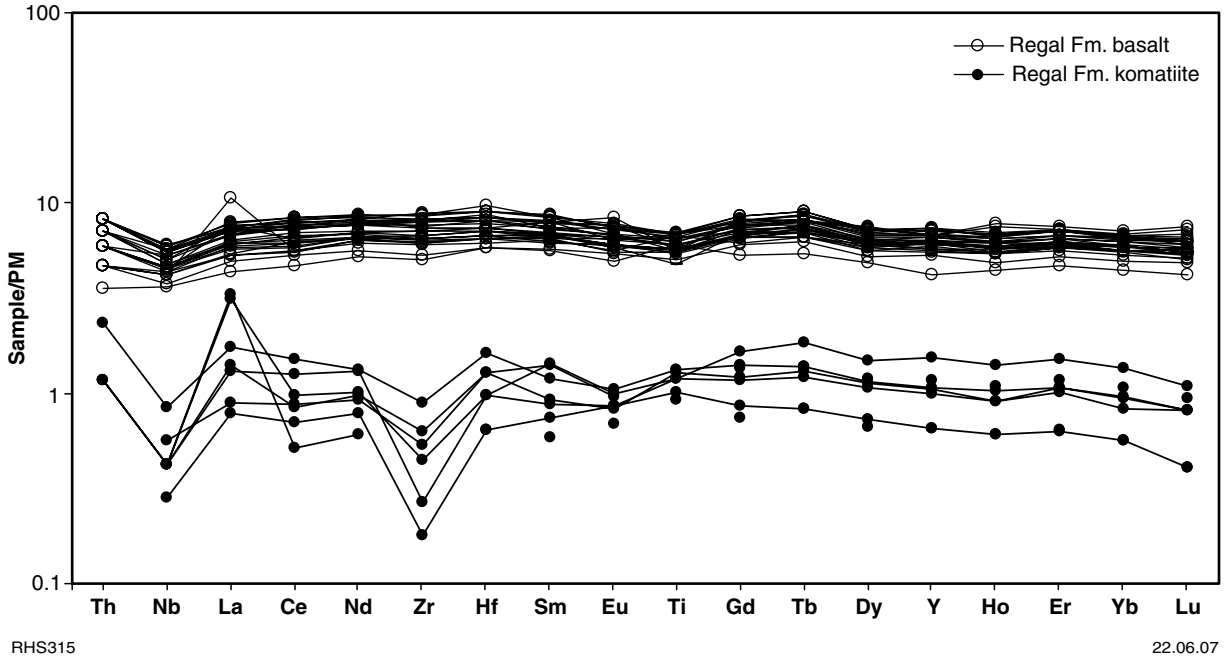


**Figure 23. Trace element plots normalized to primitive mantle for komatiites and basalts of the Regal Formation in the West Pilbara Superterrane. Normalizing factors after Sun and McDonough (1989)**

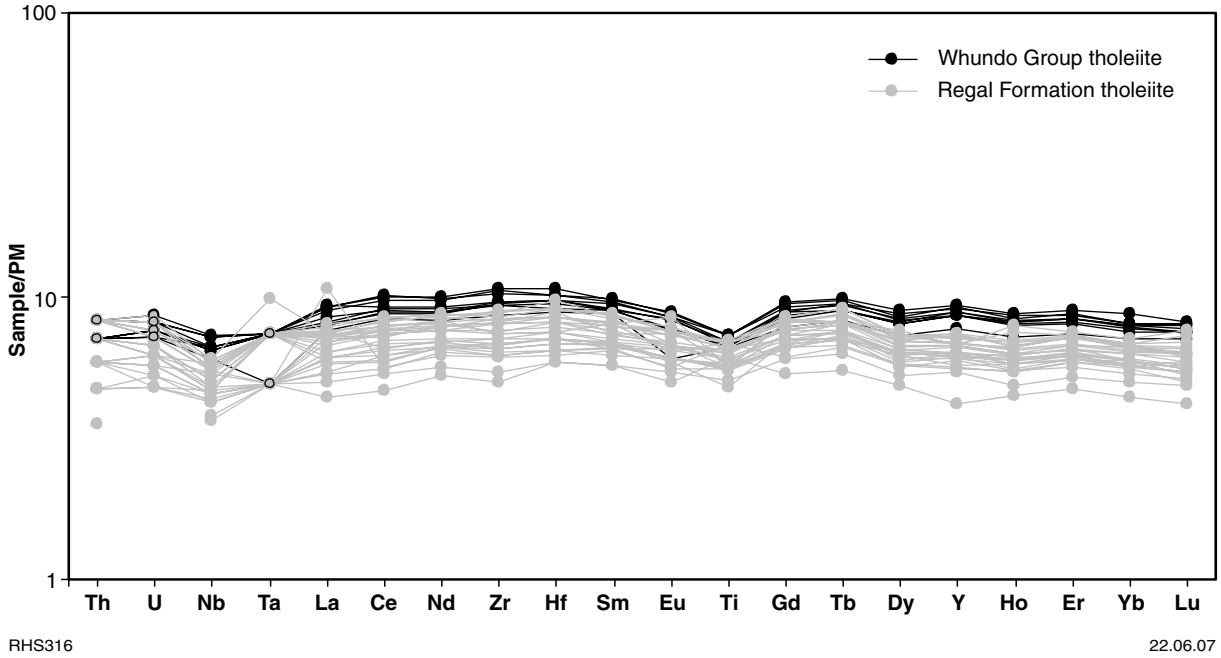


**Figure 24. Trace element plots normalized to primitive mantle comparing tholeiitic basalts from the Whundo Group and Regal Formation in the West Pilbara Superterrane. Normalizing factors after Sun and McDonough (1989)**

These basalts are also compositionally quite similar to the tholeiitic basalts from the Whundo Group (Whundo T1 in particular; Fig. 24). However, the latter have slightly, but persistently, higher MREE and HREE concentrations and lower Gd/Yb ratios (Fig. 22). The Whundo Group and Regal Formation also differ in terms of lithological association. Whereas the tholeiites of the Whundo Group are locally interlayered with calc-alkaline basalts, no such association is observed in the Regal Formation. The Whundo Group and Regal Formation are unlikely to be direct equivalents, although these data do not exclude a close temporal and spatial relationship.

When the amphibolite facies basalts are compared to the greenschist facies basalts, certain compositional differences emerge (Fig. 25). In particular, the amphibolite facies basalts tend to have higher MgO, ΣFe, Ni, Sc, and Cu and lower TiO, $Na_2O$, $P_2O_5$, LOI, Nb, Ta, Zr, Hf, Y, Th, U, and REE. Whereas differences in fluid mobile elements such as Fe and Na might be attributable to differing metamorphic grades, elements such as Zr, Nb, Th, and the HREE are not known to be mobile during low- to medium-grade metamorphism. When the data are plotted in terms of stratigraphic height (Fig. 25), trends to decreasing HREE with increasing height in the amphibolite facies rocks are mirrored within the greenschist facies rocks, and might be interpreted in terms of structural repetition of the sequence. However, trends for other elements (e.g. U) show continuous enrichment (or depletion) with stratigraphic height, irrespective of metamorphic facies. The most likely explanation for these trends is that the sampling traverse intersected two separate, internally fractionated, major magmatic cycles, and that the boundary between the two fortuitously coincides more or less with the metamorphic isograd separating the amphibolite and greenschist facies.

# De Grey Supergroup

## Whim Creek Group — Warambie Basalt

The Warambie Basalt forms the basal unit to the c. 3.01 Ga Whim Creek Group of the De Grey Supergroup. Two samples of this basalt were collected (traverse 5 on Fig. 14). The geochemistry of this unit was studied in more detail by Pike (2001). The two samples collected during the present study consistently fall into the range described by Pike (2001) and so the compositional ranges described here refer to the wider dataset of Pike (2001).

Rocks of the Warambie Basalt have 45–55 wt% $SiO_2$, 0.7 – 1.5 wt% $TiO_2$, 2–5 wt% MgO, 10–15 wt% ΣFe, and 2 – 4.5 wt% $Na_2O$. They are typically tholeiitic, but samples with higher $Na_2O$ are transitional to alkalic. Their normalized trace element patterns (Fig. 26) are moderately fractionated, with significant enrichments in Th (40 times N-MORB), Nb (3 times N-MORB) and LREE (La ~9 times N-MORB), depletions in HREE (Yb ~0.5 times N-MORB), and with $[La/Yb]_N$ ~16. Similarly LREE-enriched tholeiites are found in the Ruth Well Formation, but these have lower La/Nb ratios $[La/Nb]_N$ ratios ~1.7 cf. 3.2 for the Warambie Basalt) and are not HREE-depleted.

Given the low $Mg^{\#}$, the HREE depletions seen in these rocks are unlikely to be related to high-degree partial melting alone. They more likely relate to either derivation from a depleted mantle source region or to inclusion of a source component containing residual garnet (eclogite or a garnet-bearing mantle source), or both. Enrichments in Th and LREE reflect either assimilation of felsic crust or an enriched mantle source like those that feed modern subduction-related basaltic magmas. The evidence from the 3.13 Ga Whundo Group and from the c. 2.97 Ga

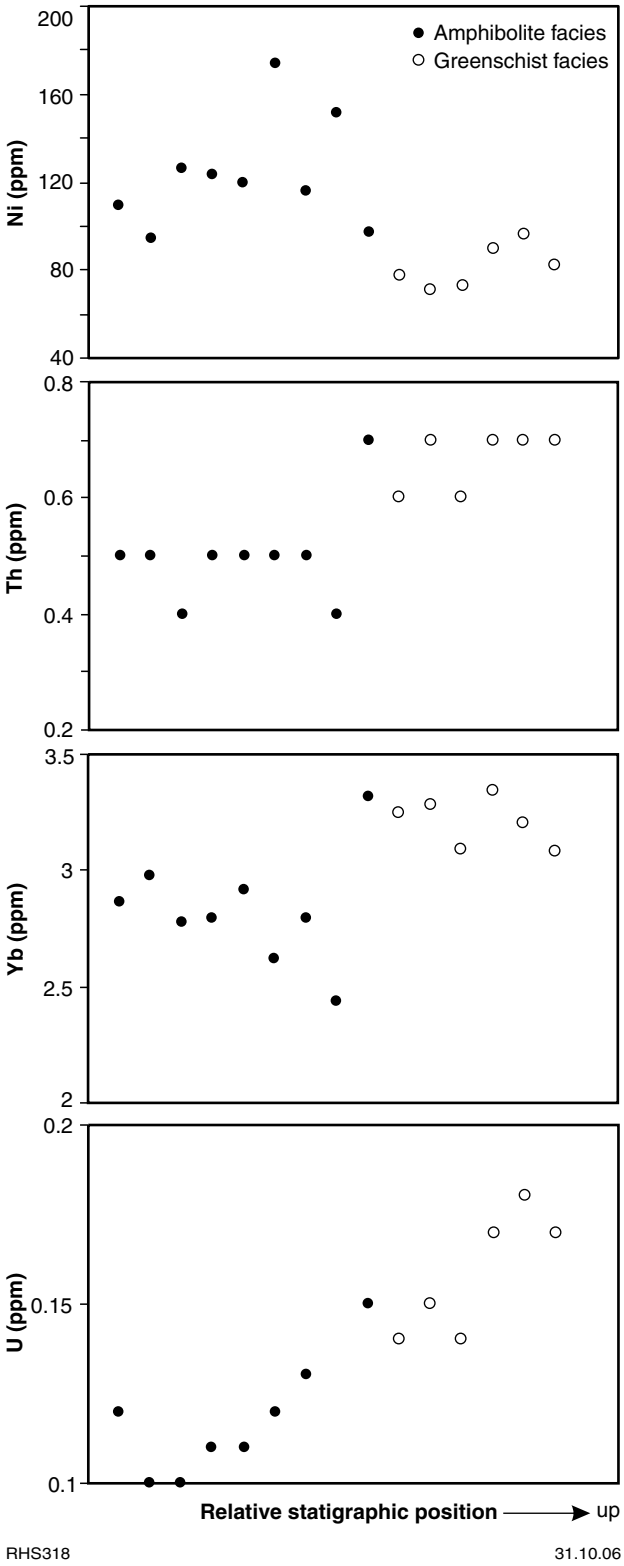


**Figure 25. Plots show compositional changes in tholeiitic basalts of the Regal Formation with stratigraphic height and metamorphic grade**

basalts in the Croydon Group that overlies the Whim Creek Group (see later) is that subduction-modified mantle sources underlay the region both before and after production of the Warambie Basalt (Smithies et al., 2004a; 2005a). Pike (2001) suggested that the Warambie Basalt is a tholeiitic arc basalt that has assimilated felsic crust, or felsic magma, during ascent. The normalized trace element patterns of the Warambie Basalt are very similar to those of the older CA3 basaltic rocks of the Whundo Group, which are interpreted to include a source component derived from slab melting (Smithies et al., 2005a). A similar petrogenesis for the Warambie Basalt might explain the high LREE without the need for assimilation of felsic crust. Alternatively, or in addition, the $Na_2O$- and Nb-rich compositions of the Warambie Basalt might reflect some form of rift-related environment, possibly linked to early evolution of the Whim Creek Basin.

## Croydon Group

Subaqueous flows of siliceous high-Mg basalt and of rocks that Arndt et al. (2001) called 'high-Si basalts' dominate the upper part of the Croydon Group in the northwestern part of the Mallina Basin and are collectively referred to as the Bookingarra Formation (area around traverse 6 on Fig. 14; Van Kranendonk et al., 2006). Here, the Mount Negri Volcanic Member of the Bookingarra Formation typically forms vesicular flow units with interlayered hyaloclastite deposits, whereas the Louden Volcanic Member of the Bookingarra Formation locally includes aphyric flow units and cumulate-textured units but is dominated by well-developed pyroxene-spinifex textures. In the southern parts of the Mallina Basin (area around traverse 7 on Fig. 14), subaqueous flows and hyaloclastite deposits of high-Si basalt (South Mallina Basalt Member of the Bookingarra Formation) form a widespread discontinuous layer within siliciclastic turbidite units and are interpreted as time correlatives of the Louden and Mount Negri Volcanic Members, as are LREE-enriched gabbros that intrude the turbidite units (Smithies et al., 2005b). Rocks with compositions similar to boninites also form a thin (~300 m) layer in the southern part of the basin, referred to as the Yareweeree Boninite Member of the Bookingarra Formation. The continuity of this thin layer in coarse-grained sedimentary rocks suggests it is a sill and so the textural evidence for rapid cooling probably indicates a high-level (sub-volcanic) intrusive origin (Smithies, 2002). The available geochronology suggests that all of this volcanic and sub-volcanic mafic magmatism occurred within the short interval between 2.955 Ga and 2.945 Ga (Smithies et al., 2005b). The geochemical sampling was aimed at identifying any potential genetic links between these diverse magma types.

The geochemistry of these rocks has been described in detail by Smithies et al. (2004a), from which the following section is summarized. A general conclusion of Smithies et al. (2004a) was that the LREE-enriched characteristic of these basaltic rocks resulted through partial melting of a subduction-enriched mantle source. Arndt et al. (2001) presented an alternative view that these rocks, like most other basaltic rocks referred to as siliceous high-Mg basalt (SHMB), derive their LREE-enriched

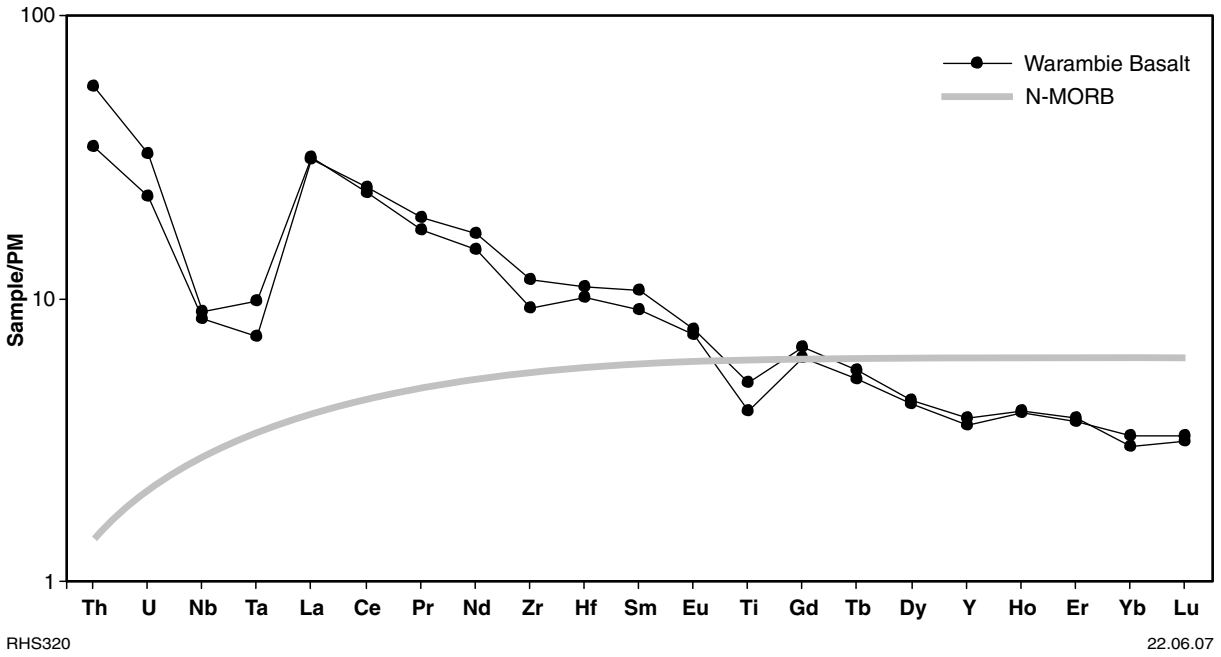


**Figure 26. Trace element plots normalized to primitive mantles for the Warambie Basalt in the West Pilbara Superterrane. Normalizing factors and N-MORB after Sun and McDonough (1989)**

characteristics through assimilation of felsic crust by a komatiitic magma.

### *Basaltic rocks*

Rocks of the Louden Volcanic Member have high $SiO_2$ (51–56 wt%), Th, and LREE concentrations and have been included within the class of Precambrian mafic rocks known as siliceous high-Mg basalt (Sun et al., 1989).

Sampling of the fine-grained and typically spinifex-textured Louden Volcanic Member revealed no rocks with MgO >9 wt%, although dyke rocks with well-developed olivine-cumulate textures have MgO up to ~18 wt%. Approximately one third of the samples studied by Arndt et al. (2001) have MgO >10 wt%, but many of these appear to be from cumulate layers (and ?dykes) including all samples with MgO >13 wt%.

The Mount Negri Volcanic Member and the South Mallina Basalt Member have lower MgO contents and $Mg^{\#}$ than the Louden Volcanic Member and higher Th, Zr, and LREE concentrations (Fig. 27). These rocks share moderate to low $TiO_2$ (0.39–0.66 wt%) and high $Al_2O_3/TiO_2$ (22.5–48.6), and have silica values between 53 and 59 wt%, comparable to modern continental flood basalts (Arndt et al., 2001).

On trace element diagrams normalized to primitive mantle (Fig. 27), the Louden Volcanic Member, LREE-rich gabbro, and the South Mallina Basalt Member show virtually identical patterns that include significant enrichments in Th, Zr, and LREE, with $[Th/Gd]_{PM}$ ~9–11 and flat normalized-HREE patterns. The Mount Negri Volcanic Member has more fractionated HREE concentrations ($[Gd/Lu]_{PM}$ ~1.8 cf. ~1.1 for the Louden Volcanic Member) but has virtually identical normalized trace element patterns to the other basaltic rocks for elements between Th and Gd (Fig. 27). On variation diagrams using La, Sm, and Zr, the Louden Volcanic Member, South Mallina Basalt Member, LREE-rich gabbros, and the Mount Negri Volcanic Member show a single linear trend with a constant slope that projects back to the origin (Fig. 28). Smithies et al. (2004a) used these similarities to suggest that the magmas were derived from a common mantle source region enriched in incompatible trace elements.

Despite the similar trace element patterns, absolute abundances of Th to Lu in the South Mallina Basalt Member are 2 to 3 times higher than those in both the Louden Volcanic Member and LREE-rich gabbros. There are also very subtle but persistent differences in such ratios as Nb/Th, Th/U, and Th/Nd. The South Mallina Basalt Member shows lower Ti/Zr and $Al_2O_3/TiO_2$ and, as well as some of the LREE-rich gabbros, has lower Cr than the Louden Volcanic Member.

### *Boninite-like rocks*

Boninite-like rocks from the Mallina Basin (Yareweeree Boninite Member) have been described in detail by Smithies (2002). Smithies et al. (2004b) compared these with boninite-like rocks from the Whundo Group as well as similar rocks reported from other Archean terrains. Samples of the Yareweeree Boninite Member from the Mallina Basin have $SiO_2$ between 52 and 54 wt%, $Mg^{\#}$ between 65 and 69, $TiO_2$ <0.3 wt%, and high $Al_2O_3/TiO_2$ (62–74) and $CaO/TiO_2$ (29–31). The concentrations of Th, Zr, and LREE are lower than in the Louden Volcanic Member, the high-Si basalts, and the LREE-rich gabbro, but are still strongly enriched (Fig. 27).

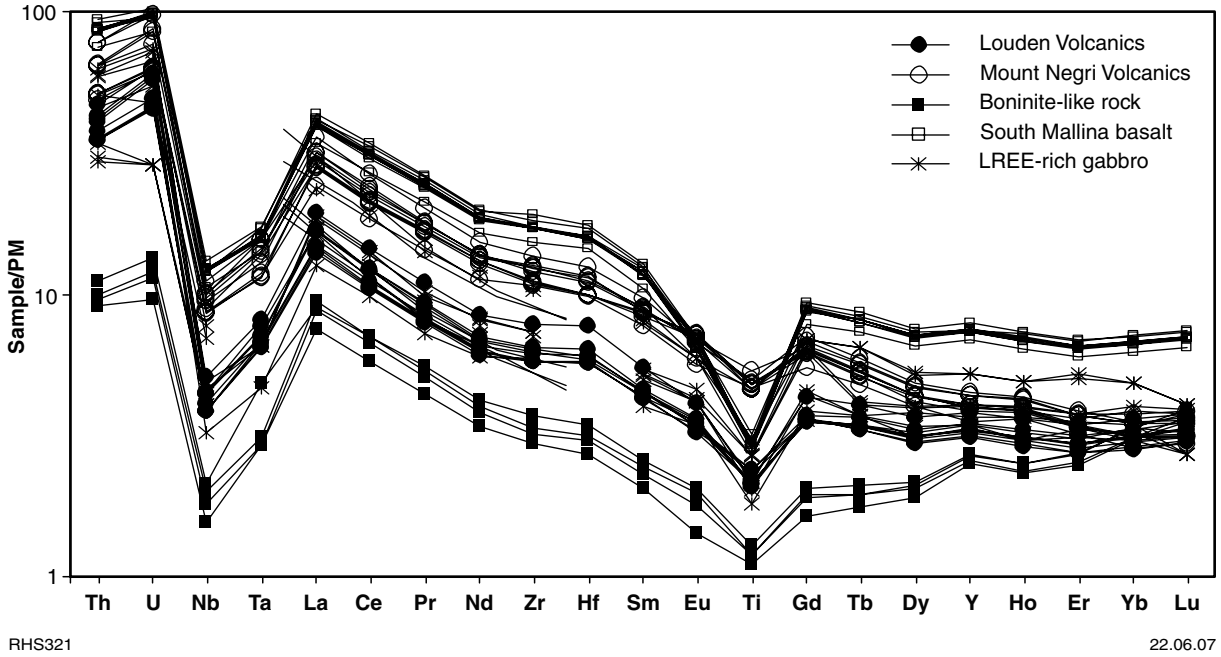


**Figure 27. Trace element plots normalized to primitive mantle for the basaltic rocks within the Mallina Basin. Normalizing factors after Sun and McDonough (1989)**

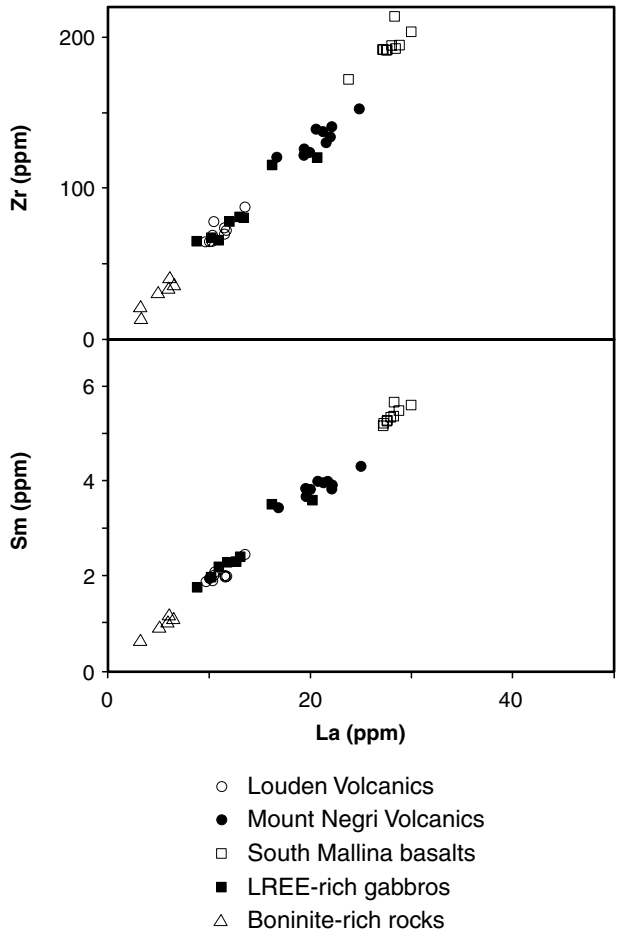


**Figure 28. Plots of La vs Zr and Sm for the basaltic rocks within the Mallina Basin**

Strongly fractionated LREE ($[La/Gd]_{PM}$ ~4.5) and HREE ($[Gd/Yb]_{PM}$ ~0.58) result in prominent 'U-shaped' normalized patterns, which are also a characteristic of Phanerozoic boninites (Crawford et al., 1989). Notably, on variation diagrams for La, Sm, and Zr (Fig. 28), the boninite-like rocks fall on the same linear trends defined by rocks of the Louden and Mount Negri Volcanic Members, South Mallina Basalt Member, and LREE-rich gabbros.

### *Nd-isotopic compositions*

The isotopic compositions of the Louden Volcanic and Mount Negri Volcanic Members are very similar with initial $\varepsilon_{Nd(2950\ Ma)}$ between -1.5 and -2.8 (Appendix 2). The data for two samples of the boninite-like rocks overlap this range but extend to more primitive values (-0.9 and -1.7), as do the data for the South Mallina Basalt Member (-0.6 to -1.0), and the LREE-rich gabbros (-0.5 and -1.5). These data, together with $T_{DM}$ model ages older than 3.2 Ga, clearly indicate the presence of an old (LREE-enriched) 'crustal' component within the rocks.

## Discussion

The mafic magmatism recorded within the Mallina Basin shows high primitive mantle-normalized $[La/Nb]_{PM}$ (>3) and $[La/Yb]_{PM}$ (>2), and non-radiogenic Nd-isotopic compositions ($\varepsilon_{Nd(2950\ Ma)}$ mostly <-1.0) suggesting the magmas incorporated a crustal component. Despite having intruded through compositionally diverse continental crust, they show a remarkably narrow range in La/Nb (~3.1), La/Sm (~5.3), La/Zr (~0.15), and a small range of $\varepsilon_{Nd(2950\ Ma)}$(-0.6 to -2.8) that is unlikely to be a result of assimilation of any single locally or regionally available

crustal component. The mafic magmas were most likely derived from a mantle source that incorporated a homogeneous mix of 'old-Pilbara crust' (i.e. >3.3 Ga, $\varepsilon_{Nd(2950\ Ma)}$ <-2.3, high La/Nb, Sm, and Zr) and crust that resembled c. 3.12 Ga greenstones of the Whundo Group ($\varepsilon_{Nd(2950\ Ma)}$ >-0.4, low La/Nb, Sm, and Zr) that outcrops to the northwest of the basin. Evidence for enrichment of Archean mantle source regions is typically extremely difficult to demonstrate and is primarily restricted to sequences that are c. 2.8 Ga or younger. However, the igneous rocks of the Mallina Basin show that such sources existed by c. 3.0 Ga. Subduction of oceanic crust, including compositionally homogenized sediment, is the most obvious model for this mantle enrichment, and possibly occurred during formation of the Whundo Group (Smithies et al., 2005a).

# Comparisons between mafic volcanic rocks in the West Pilbara Superterrane, East Pilbara Terrane, and Mallina Basin

Sequences of tholeiitic basaltic rocks in the West Pilbara Superterrane (i.e. in the Whundo Group and the Regal Formation) are restricted to high-Ti compositions and show a much narrower range in concentration of incompatible trace elements than high-Ti tholeiite sequences from the Pilbara Supergroup (cf. Figs 7 and 24). In particular, the Whundo Group and the Regal Formation do not include the Th- and LREE-rich high-Ti tholeiites found in the Pilbara Supergroup, with $[La/Yb]_{PM}$ restricted to values of less than 1.5 (cf. up to 2.2 for the Apex Basalt and 2.7 in the Euro Basalt). It is likely that this restricted range to lower Th and LREE concentrations reflects correspondingly lower degrees of interaction between the mafic magmas and felsic crust.

Strongly Th- and LREE-enriched compositions distinguish the Coonieena Basalt Member and the basaltic rocks in the Bookingarra Formation from the Goldsworthy area (De Grey Supergroup) from all other basalt units of the East Pilbara Terrane except, perhaps, the enriched rocks of the Sulphur Springs Group. The latter are associated with basalts with more strongly depleted trace element patterns. Such patterns are not seen associated with the former two groups of basaltic rocks, which are also characterized by generally higher $[La/Nb]_{PM}$ ratios (2.5 and higher) than the enriched rocks of the Sulphur Springs Group (<2.0). The Coonieena Basalt Member and other basaltic rocks of the Bookingarra Formation are more closely matched, in terms of their trace element patterns, by the Louden and Mount Negri Volcanic Members, and South Mallina Basalt Member (Fig. 8). The basaltic rocks in the Goldsworthy area and the Coonieena Basalt Member are, in fact, likely to be close stratigraphic correlatives of the basaltic rocks of the Mallina Basin. Because of these similarities, Smithies et al. (2005b) suggested that the Coonieena Basalt Member derived from the same subduction-enriched mantle source that produced the basaltic rocks of the Mallina Basin and, on this basis, the rocks have been incorporated together within the Croydon Group (Van Kranendonk et al., 2006).

# References


ARNDT, N., BRUZAK, G., and REISCHMANN, T., 2001, The oldest continental and oceanic plateaus: Geochemistry of basalts and komatiites of the Pilbara Craton, Australia, *in* Mantle Plumes: Their identification through time *edited by* R. E. ERNST and K. L. BUCHAN: Geological Society of America, Special Paper 352, p. 359–387.

BAGAS, L., FARRELL, T. R., and NELSON, D. R., 2005, The age and provenance of the Mosquito Creek Formation: Western Australia Geological Survey, Annual Review 2003–04, p. 62–70.

BARLEY, M. E., 1987, The Archaean Whim Creek Belt, an ensialic fault-bounded basin in the Pilbara Block, Australia: Precambrian Research, v. 37, p. 199–215.

BARLEY, M. E., and PICKARD, A. L., 1999, An extensive, crustally-derived, 3325 to 3310 Ma silicic volcanoplutonic suite in the eastern Pilbara Craton: evidence from the Kelly Belt, McPhee Dome, and Corunna Downs Batholith: Precambrian Research, v. 96, p. 41–62.

BICKLE, M. J., BETTENAY, L. F., BARLEY, M. E., CHAPMAN, H. J., GROVES, D. I., CAMPBELL, I. H., and de LAETER, J. R., 1983, A 3500 Ma plutonic and volcanic calc-alkaline province in the Archaean East Pilbara Block: Contributions to Mineralogy and Petrology, v. 84, p. 25–35.

BOLHAR, R., WOODHEAD, J. D., and HERGT, J. M., 2002, Continental setting inferred for emplacement of the 2.9 – 2.7 Ga Belingwe greenstone belt, Zimbabwe: Geology, v. 31, p. 295–298.

BRAUHART, C., 1999, Regional alteration systems associated with Archean volcanogenic massive sulphide deposits at Panorama, Pilbara, Western Australia: University of Western Australia, PhD Thesis (unpublished).

BUICK, R., BRAUHART, C. W., MORANT, P., THORNETT, J. R., MANIW, J. G., ARCHIBALD, N. J., DOEPEL, M. G., FLETCHER, I. R., PICKARD, A. L., SMITH, J. B., BARLEY, M. E., McNAUGHTON, N. J., and GROVES, D. I., 2002, Geochronology and stratigraphic relationships of the Sulphur Springs Group and Strelley Granite: a temporally distinct igneous province in the Archaean Pilbara Craton, Australia: Precambrian Research, v. 114, p. 87–120.

BUICK, R., THORNETT, J. R., McNAUGHTON, N. J., SMITH, J. B., BARLEY, M. E., and SAVAGE, M., 1995, Record of emergent continental crust ~3.5 billion years ago in the Pilbara Craton of Australia: Nature, v. 375, p. 574–577.

COLLINS, W. J., 1993, Melting of Archaean sialic crust under high $a_{H2O}$ conditions: genesis of 3300 Ma Na-rich granitoids in the Mount Edgar Batholith, Pilbara Block, Western Australia: Precambrian Research, v. 60, p. 151–174.

CONDIE, K. C., 2005, High field strength element ratios in Archean basalts: a window to evolving sources of mantle plumes?: Lithos, v. 79, p. 491–504.

CRAWFORD, A. J., FALLOON., T. J., and GREEN, D. H., 1989, Classification, petrogenesis and tectonic setting of boninites, *in* Boninites *edited by* A. J. CRAWFORD: London, United Kingdom, Unwin–Hyman, p. 1–49.

CULLERS, R. L., DiMARCO, M. J., LOWE, D. R., and STONE, J., 1993, Geochemistry of a silicified felsic volcanic suite from the early Archean Panorama Formation, Pilbara Block, Western Australia — an evaluation of depositional and post-depositional processes with special emphasis on the rare earth elements: Precambrian Research, v. 60, p. 99–116.

EGGINS, S. M., WOODHEAD, J. D., KINSLEY, L. P. J., MORTIMER, G. E., SYLVESTER, P., McCULLOCH, M. T., HERGT, J. M., and HANDLER, M. R., 1997, A simple method for the precise determination of >40 trace elements in geological samples by ICPMS using enriched isotope internal standardisation: Chemical Geology, v. 134, p. 311–326.

ERIKSSON, K. A., 1982, Geometry and internal characteristics of Archaean submarine channel deposits, Pilbara Block, Western Australia: Journal of Sedimentary Petrology, v. 52/2, p. 383–393.

ERIKSSON, K. A., KRAPEZ, B., and FRALICK, P., 1994, Archaean sedimentation: Earth-Science Reviews, v. 37, p. 1–88.

FARRELL, T., 2006, Geology of the Eastern Creek 1:100 000 sheet: Western Australia Geological Survey, 1:100 000 Geological Series Explanatory Notes, 33p.

GLIKSON, A. Y., and HICKMAN, A. H., 1981, Geochemistry of Archaean volcanic successions, eastern Pilbara Block, Western Australia: Australia Bureau of Mineral Resources, Geology and Geophysics, Record 1981/36, 56p.

GREEN, M. G., SYLVESTER, P. J., and BUICK, R., 2000, Growth and recycling of early Archaean continental crust: geochemical evidence from the Coonterunah and Warrawoona Groups, Pilbara Craton, Australia: Tectonophysics, v. 322, p. 69–88.

HAWKESWORTH, C. J., GALLAGHER, K., HERGT, J. M., and McDERMOTT, F., 1993, Mantle and slab contributions in arc magmas: Annual Review of Earth and Planetary Sciences, v. 21, p. 175–204.

HICKMAN, A. H., 1997, A revision of the stratigraphy of Archaean greenstone successions in the Roebourne–Whundo area — west Pilbara: Western Australia Geological Survey, Annual Review 1996–97, p. 76–81.

HICKMAN, A. H., 2004, Two contrasting granite–greenstone terranes in the Pilbara Craton, Australia: evidence for vertical and horizontal tectonic regimes prior to 2900 Ma: Precambrian Research, v. 131, p. 153–172.

HICKMAN, A. H., and VAN KRANENDONK, M. J., 2004, Diapiric processes in the formation of Archaean continental crust, East Pilbara Granite–Greenstone Terrane, Australia, *in* The Precambrian Earth: Tempos and Events *edited by* P. G. ERIKSSON, W. ALTERMANN, D. R. NELSON, W. U. MUELLER, and O. CATUNEAU: Amsterdam, Elsevier, p. 54–75.

HUSTON, D. L., SUN, S.-S., BLEWETT, R., HICKMAN, A., VAN KRANENDONK, M., PHILLIPS, D., BAKER, D., and BRAUHART, C., 2002, The timing of mineralization in the Archaean Pilbara Craton, Western Australia: Economic Geology, v. 97, p. 733–755.

KIYOKAWA, S., and TAIRA, A., 1998, The Cleaverville Group in the west Pilbara coastal granite–greenstone terrane of Western Australia: an example of a mid-Archaean immature oceanic island-arc succession: Precambrian Research, v. 88, p. 102–142.

Le MAITRE, R.W., (editor), 2002, Igneous rocks: a classification and glossary of terms. Recommendations of the International Union of Geological Sciences Subcommission on the Systematics of Igneous Rocks: Cambridge, Cambridge University Press, 236p.

MARTIN, H., SMITHIES, R. H., RAPP, R., MOYEN, J.-P., and CHAMPION, D., 2005, An overview of adakite, tonalite–trondhjemite–granodiorite (TTG), and sanukitoid: relationships and some implications for crustal evolution: Lithos, v. 79, p. 1–24.

MORRIS, P. A., and PIRAJNO, F., 2005, Mesoproterozoic sill complexes in the Bangemall Supergroup, Western Australia: geology, geochemistry, and mineralization potential: Western Australia Geological Survey, Report 99, 75p.

NESBITT, R. W., SUN, S.-S., and PURVIS, A. C., 1979, Komatiites: geochemistry and genesis: Canadian Mineralogist, v. 17, p. 165–186.

NORRISH, K., and CHAPPELL, B. W., 1977, X-ray fluorescence spectrometry, *in* Physical Methods in Determinative Mineralogy, 2nd edition *edited by* J. ZUSSMAN: London, Academic Press, p. 201–272.

NORRISH, K., and HUTTON, J. T., 1969, An accurate X-ray spectrographic method for the analysis of a wide range of geological samples: Geochimica et Cosmochimica Acta, v. 33, p. 431–453.

OHTA, H., MARUYAMA, S., TAKAHASHI, E., WATANABE, Y., and KATO, Y., 1996, Field occurrence, geochemistry and petrogenesis of the Archaean Mid-Oceanic Ridge Basalts (AMORBs) of the Cleaverville area, Pilbara Craton, Western Australia: Lithos, v. 37, p. 199–221.

PIKE, G., 2001, The facies architecture of two contrasting volcano-sedimentary basin successions from the Archaean Whim Creek Belt, North Pilbara Terrain, Western Australia: The intra-continental arc-related Whim Creek Group and plume-related, continental rift-hosted Bookingarra Group: Melbourne, Monash University, PhD thesis (unpublished).

PIKE, G., and CAS, R. A. F., 2002, Stratigraphic evolution of Archean volcanic rock-dominated rift basins from the Whim Creek Belt, west Pilbara Craton, Western Australia: Special Publication of the International Association of Sedimentologists, v. 33, p. 213–234.

PYKE, J., 2000, Minerals laboratory staff develops new ICP–MS preparation method: Australian Geological Survey Organisation, Research Newsletter, v. 33, p. 12–14.

SHAPIRO, L., and BRANNOCK, W. W., 1962, Rapid analysis of silicate, carbonate and phosphate rocks: United States Geological Survey, Bulletin 1144-A.

SMITH, J. B., 2003, The episodic development of intermediate to silicic volcano-plutonic suites in the Archaean West Pilbara, Australia: Chemical Geology, v. 194, p. 275–295.

SMITH, J. B., BARLEY, M. E., GROVES, D. I., KRAPEZ, B., McNAUGHTON, N. J., BICKLE, M. J., and CHAPMAN, H. J., 1998, The Sholl Shear Zone, West Pilbara: evidence for a domain boundary structure from integrated tectonic analyses, SHRIMP U–Pb dating and isotopic and geochemical data of granitoids: Precambrian Research, v. 88, p. 143–171.

SMITHIES, R. H., 2002, Archaean boninite-like rocks in an intracratonic setting: Earth and Planetary Science Letters, v. 197, p. 19–34.

SMITHIES, R. H., CHAMPION, D. C., and SUN, S.-S., 2004a, Evidence for early LREE-enriched mantle source regions: Diverse magmas from the c. 3.0 Ga Mallina Basin, Pilbara Craton, NW Australia: Journal of Petrology, v. 45, p. 1515–1537.

SMITHIES, R. H., CHAMPION, D. C., and SUN, S.-S., 2004b, The case for Archaean boninites: Contributions to Mineralogy and Petrology, v. 147, p. 705–721.

SMITHIES R. H., CHAMPION, D. C., VAN KRANENDONK, M. J., HOWARD, H. M., and HICKMAN, A. H., 2005a, Modern style subduction processes in the Mesoarchaean: geochemical evidence from the 3.12 Ga Whundo intraoceanic arc: Earth and Planetary Science Letters, v. 231, p. 221–237.

SMITHIES, R. H., NELSON, D. R., and PIKE, G., 2001, Development of the Archaean Mallina Basin, Pilbara Craton, northwestern Australia; a study of detrital and inherited zircon ages: Sedimentary Geology, v. 141–142, p. 79–94.

SMITHIES R. H., VAN KRANENDONK, M. J., and CHAMPION, D. C., 2005b, It started with a plume — early Archaean basaltic proto-continental crust: Earth and Planetary Science Letters, v. 238, p. 284–297.

SPROULE, R. A., LESHER, C. M., AYER, J. A., THURSTON, P. C., and HERZBERG, C. T., 2002, Spatial and temporal variations in the geochemistry of komatiites and komatiitic basalts in the Abitibi greenstone belt: Precambrian Research, v. 115, p. 153–186.

SUN, S.-S., and HICKMAN, A. H., 1998, New Nd-isotopic and geochemical data from the west Pilbara — implications for Archaean crustal accretion and shear zone development: Australian Geological Survey Organisation, Research Newsletter, June 1998.

SUN, S.-S., and McDONOUGH, W. F., 1989, Chemical and isotopic systematics of oceanic basalts: implications for mantle compositions and processes, *in* Magmatism in ocean basins *edited by* A. D. SAUNDERS and M. J. NORRY: Geological Society of London, Special Publication, v. 42, p. 313–345.

SUN, S.-S., NESBITT, R. W., and McCULLOCH, M. T., 1989, Geochemistry and petrogenesis of Archaean and early Proterozoic siliceous high-magnesian basalts, *in* Boninites *edited by* A. J. CRAWFORD: London, Unwin–Hyman, p. 149–173.

SUN, S.-S., WARREN, R. G., and SHAW, R. D., 1995, Nd isotope studies of granites from the Arunta Inlier, central Australia: constraints on geological models and limitation of the method: Precambrian Research, v. 71, p. 301–314.

VAN KRANENDONK, M. J., 2000, Geology of the North Shaw 1:100 000 sheet: Western Australia Geological Survey, 1:100 000 Geological Series Explanatory Notes, 89p.

VAN KRANENDONK, M. J., and COLLINS, W. J., 1998, Timing and tectonic significance of Late Archaean, sinistral strike-slip deformation in the Central Pilbara Structural Corridor, Pilbara Craton, Western Australia: Precambrian Research, v. 88, p. 207–232.

VAN KRANENDONK, M. J., HICKMAN, A. H., and COLLINS, W. J., 2001, Comment on "Evidence for multiphase deformation in the Archaean basal Warrawoona Group in the Marble Bar area, East Pilbara, Western Australia": Precambrian Research, v. 105, p. 73–78.

VAN KRANENDONK, M. J., HICKMAN, A. H., SMITHIES, R. H., NELSON, D. R., and PIKE, G., 2002, Geology and tectonic evolution of the Archaean North Pilbara terrain, Pilbara Craton, Western Australia: Economic Geology, v. 97, p. 695–732.

VAN KRANENDONK, M. J., HICKMAN, A. H., SMITHIES, R. H., WILLIAMS, I. R., BAGAS, L., and FARRELL T. R., 2006, Revised lithostratigraphy of Archean supracrustal and intrusive rocks in the northern Pilbara Craton, Western Australia: Western Australia Geological Survey, Record 2006/15, 57p.

VAN KRANENDONK, M. J., and MORANT, P., 1998, Revised Archaean stratigraphy of the North Shaw 1:100 000 sheet, Pilbara Craton: Western Australia Geological Survey, Annual Review 1997–98, p. 55–62.

VAN KRANENDONK, M. J., and PIRAJNO, F., 2004, Geological setting and geochemistry of metabasalts and alteration zones associated with hydrothermal chert ± barite deposits in the ca. 3.45 Ga Warrawoona Group, Pilbara Craton, Australia: Geochemistry: Exploration, Environment, Analysis, v. 4, p. 253–278.

VAN KRANENDONK, M. J., WEBB, G. E., and KAMBER, B. S., 2003, Geological and trace element evidence for a marine sedimentary environment of deposition and biogenicity of 3.45 Ga stromatolitic carbonates in the Pilbara Craton, and support for a reducing Archean ocean: Geobiology, v. 1(2), p. 91–108.

## Appendix 1

# Whole-rock geochemistry of rocks from the northern Pilbara Craton

Table of geochemical data for 438 whole-rock samples of volcanic rocks from the East Pilbara Terrane and West Pilbara Superterrane. Data are provided in a separate Excel spreadsheet in comma separated variable (csv) format.

## Appendix 2

# Nd-isotopic data

## References

ARNDT, N., BRUZAK, G., and REISCHMANN, T., 2001, The oldest continental and oceanic plateaus: Geochemistry of basalts and komatiites of the Pilbara Craton, Australia, *in* Mantle Plumes: Their identification through time *edited by* R. E. ERNST and K. L. BUCHAN: Geological Society of America, Special Paper 352, p. 359–387.

BICKLE, M. J., BETTENAY, L. F., CHAPMAN, H. J., GROVES, D. I., McNAUGHTON, N. J., CAMPBELL, I. H., and de LAETER, J. R., 1989, The age and origin of younger granitic plutons of the Shaw Batholith in the Archaean Pilbara Block, Western Australia: Contributions to Mineralogy and Petrology, v. 101, p. 361–376.

BICKLE, M. J., BETTENAY, L. F., CHAPMAN, H. J., GROVES, D. I., McNAUGHTON, N. J., CAMPBELL, I. H., and de LAETER, J. R., 1993, Origin of the 3500–3300 Ma calc-alkaline rocks in the Pilbara Archaean: isotopic and geochemical constraints from the Shaw Batholith: Precambrian Research, v. 60, p. 117–149.

BRAUHART, C. W., HUSTON, D. L., and ANDREW, A. S., 2000, Oxygen isotope mapping in the Panorama VMS district, Pilbara Craton, Western Australia: applications to estimating temperatures of alteration and to exploration: Mineralium Deposita, v. 35, p. 727–740.

McCULLOCH, M. T., 1987, Sm–Nd isotopic constraints on the evolution of Precambrian crust in the Australian continent, *in* Proterozoic lithospheric evolution *edited by* A. KROENER: American Geophysical Union Geodynamics Series, v. 17.

SMITH, J. B., BARLEY, M. E., GROVES, D. I., KRAPEZ, B., McNAUGHTON, N. J., BICKLE, M. J., and CHAPMAN, H. J., 1998, The Sholl Shear Zone, West Pilbara: evidence for a domain boundary structure from integrated tectonic analyses, SHRIMP U–Pb dating and isotopic and geochemical data of granitoids: Precambrian Research, v. 88, p. 143–171.

SUN, S-S., and HOATSON, M., 1992, Chemical and isotopic characteristics of parent magmas of the west Pilbara layered intrusions: implications for petrogenesis, magma mixing, and PGE mineralization in layered intrusions, *in* Petrology and Platinum-Group-Element geochemistry of Archaean layered mafic–ultramafic intrusions, West Pilbara Block, Western Australia *edited by* D. M. HOATSON, D. A. WALLACE, and S-S. SUN: Australian Geological Survey Organisation Bulletin 242.

TYLER, I. M., FLETCHER, I. R., de LAETER, J. R., WILLIAMS, I. R., and LIBBY, W. G., 1992, Isotope and rare earth element evidence for a late Archaean terrane boundary in the southeastern Pilbara Craton, Western Australia: Precambrian Research, v. 54, p. 211–229.

## Appendix 2.

| Sample | Easting | Northing | Unit | Lithology | Group/Suite/ Supersuite | Source of isotopic data | Age |
|---|---|---|---|---|---|---|---|
| M16 | unknown | unknown | Maddina Formation | basalt | Fortescue Group | Arndt et al. (2001) | 2690 |
| M17 | unknown | unknown | Maddina Formation | basalt | Fortescue Group | Arndt et al. (2001) | 2690 |
| J54 | unknown | unknown | Mount Jope | basalt | Fortescue Group | Arndt et al. (2001) | 2700 |
| J56 | unknown | unknown | Mount Jope | basalt | Fortescue Group | Arndt et al. (2001) | 2700 |
| J701 | unknown | unknown | Mount Jope | basalt | Fortescue Group | Arndt et al. (2001) | 2700 |
| J704 | unknown | unknown | Mount Jope | basalt | Fortescue Group | Arndt et al. (2001) | 2700 |
| J707 | unknown | unknown | Mount Jope | basalt | Fortescue Group | Arndt et al. (2001) | 2700 |
| J710 | unknown | unknown | Mount Jope | basalt | Fortescue Group | Arndt et al. (2001) | 2700 |
| K419 | unknown | unknown | Kylena Formation | basalt | Fortescue Group | Arndt et al. (2001) | 2720 |
| K94 | unknown | unknown | Kylena Formation | basalt | Fortescue Group | Arndt et al. (2001) | 2720 |
| 141945 | 117.68223 | 21.019724 | Opaline Well Intrusion | leucogranite | | GSWA/GA (unpubl.) | 2765 |
| R10 | unknown | unknown | Mount Roe Basalt | basalt | Fortescue Group | Arndt et al. (2001) | 2780 |
| R11 | unknown | unknown | Mount Roe Basalt | basalt | Fortescue Group | Arndt et al. (2001) | 2780 |
| R14 | unknown | unknown | Mount Roe Basalt | basalt | Fortescue Group | Arndt et al. (2001) | 2780 |
| R15 | unknown | unknown | Mount Roe Basalt | basalt | Fortescue Group | Arndt et al. (2001) | 2780 |
| R79 | unknown | unknown | Mount Roe Basalt | basalt | Fortescue Group | Arndt et al. (2001) | 2780 |
| SB584 | unknown | unknown | Spear Hill Monzogranite | monzogranite | Split Rock Supersuite | Bickle et al. (1989) | 2847 |
| SB593 | unknown | unknown | Cooglegong Monzogranite | monzogranite | Split Rock Supersuite | Bickle et al. (1989) | 2847 |
| 15207 | 119.3346 | 21.5486 | Cooglegong Monzogranite | monzogranite | Split Rock Supersuite | McCulloch (1987) | 2850 |
| 18481 | 119.4667 | 22.5833 | Cooglegong Monzogranite | muscovite–biotite granite | Split Rock Supersuite | Tyler et al. (1992) | 2850 |
| 18484 | 119.4667 | 22.5833 | Cooglegong Monzogranite | muscovite–biotite granite | Split Rock Supersuite | Tyler et al. (1992) | 2850 |
| 18487 | 119.4667 | 22.5833 | Cooglegong Monzogranite | muscovite–biotite granite | Split Rock Supersuite | Tyler et al. (1992) | 2850 |
| 98049100 | 118.9570 | 20.6799 | Kadgewarrina Monzogranite | granite | Split Rock Supersuite | GSWA/GA (unpubl.) | 2850 |
| 98049154 | 118.6797 | 20.9070 | Minamonica Monzogranite | granite | Split Rock Supersuite | GSWA/GA (unpubl.) | 2850 |
| 97045053 | 118.7883 | 21.2681 | Numbana Monzogranite | granite | Split Rock Supersuite | GSWA/GA (unpubl.) | 2850 |
| 98049219 | 118.9092 | 20.64205 | Tabba Tabba Monzogranite | granite | Split Rock Supersuite | GSWA/GA (unpubl.) | 2850 |
| 160725 | 118.7403 | 20.5477 | Carlindi Granitic Complex | muscovite leucogranite | Split Rock Supersuite | GSWA/GA (unpubl.) | 2850 |
| Y1-5 | unknown | unknown | Bamboo Springs Monzogranite | granodiorite–granite | Cutindunah Supersuite | Bickle et al. (1989) | 2908 |
| Y1-7 | unknown | unknown | Bamboo Springs Monzogranite | granodiorite–granite | Cutindunah Supersuite | Bickle et al. (1989) | 2908 |
| 83330136 | 116.8781 | 21.0947 | Munni Munni Intrusion | gabbronorite | Radley Suite | Sun and Hoatson (1992) | 2925 |
| 83330145 | 116.8762 | 21.1055 | Munni Munni Intrusion | olivine websterite | Radley Suite | Sun and Hoatson (1992) | 2925 |
| 85770179 | 116.8688 | 21.0915 | Munni Munni Intrusion | olivine gabbronorite | Radley Suite | Sun and Hoatson (1992) | 2925 |
| 84770042 | 116.8522 | 21.1163 | Munni Munni Intrusion | websterite | Radley Suite | Sun and Hoatson (1992) | 2925 |
| 84770003 | 116.8469 | 21.0955 | Munni Munni Intrusion | olivine websterite | Radley Suite | Sun and Hoatson (1992) | 2925 |
| 84770045 | 116.8425 | 21.1146 | Munni Munni Intrusion | plagioclase websterite | Radley Suite | Sun and Hoatson (1992) | 2925 |
| 84770045 | 116.8425 | 21.1146 | Munni Munni Intrusion | | Radley Suite | Sun and Hoatson (1992) | 2925 |
| 84770046 | 116.8425 | 21.1149 | Munni Munni Intrusion | orthopyroxenite block | Radley Suite | Sun and Hoatson (1992) | 2925 |
| 84770094 | 116.8111 | 21.1183 | Munni Munni Intrusion | mineralized websterite | Radley Suite | Sun and Hoatson (1992) | 2925 |
| 84770094 | 116.8111 | 21.1183 | Munni Munni Intrusion | | Radley Suite | Sun and Hoatson (1992) | 2925 |
| 84770048 | 116.8408 | 21.1155 | Munni Munni Intrusion | gabbronorite | Radley Suite | Sun and Hoatson (1992) | 2925 |
| 84770048 | 116.8402 | 21.1155 | Munni Munni Intrusion | | Radley Suite | Sun and Hoatson (1992) | 2925 |
| 84770052 | 116.8422 | 21.1227 | Munni Munni Intrusion | gabbronorite | Radley Suite | Sun and Hoatson (1992) | 2925 |
| 84770060 | 116.8427 | 21.1383 | Munni Munni Intrusion | gabbronorite | Radley Suite | Sun and Hoatson (1992) | 2925 |
| 84770061 | 116.8427 | 21.1399 | Munni Munni Intrusion | gabbronorite | Radley Suite | Sun and Hoatson (1992) | 2925 |
| 84770021 | 116.8497 | 21.1044 | Munni Munni Intrusion | clinopyroxenite | Radley Suite | Sun and Hoatson (1992) | 2925 |
| 83330141 | 116.8810 | 21.1082 | Munni Munni Intrusion | websterite | Radley Suite | Sun and Hoatson (1992) | 2925 |
| 85770172 | 116.8077 | 21.1192 | Munni Munni Intrusion | gabbronorite | Radley Suite | Sun and Hoatson (1992) | 2925 |
| 85770174 | 116.9194 | 20.9224 | Munni Munni Intrusion | plagioclase websterite | Radley Suite | Sun and Hoatson (1992) | 2925 |
| S9 | unknown | unknown | Garden Creek Monzogranite | granite–adamellite | Sisters Supersuite | Bickle et al. (1989) | 2925 |
| SB437 | unknown | unknown | Mulgandinnah Monzogranite | monzogranite | Sisters Supersuite | Bickle et al. (1989) | 2925 |
| SB450 | unknown | unknown | Pilga Monzogranite | monzogranite | Sisters Supersuite | Bickle et al. (1989) | 2925 |
| SB599 | unknown | unknown | Pinnacle Well region | granodiorite–granite | Sisters Supersuite | Bickle et al. (1989) | 2925 |
| JS42 | 116.9492 | 20.8892 | Sholl Shear zone | undeformed leucogranite | Sisters Supersuite | Smith et al. (1998) | 2925 |
| 118964 | 117.78254 | 20.847338 | Caines Well Monzogranite | monzogranite | Sisters Supersuite | GSWA/GA (unpubl.) | 2925 |
| 97045003 | 118.8843 | 21.1023 | Carlindi Granitic Complex | granite | Sisters Supersuite | GSWA/GA (unpubl.) | 2930 |
| 97045021 | 118.7183 | 21.0339 | Carlindi Granitic Complex | granite | Sisters Supersuite | GSWA/GA (unpubl.) | 2930 |
| 97045162 | 118.5773 | 21.2096 | Kangan Monzogranite | granite | Sisters Supersuite | GSWA/GA (unpubl.) | 2930 |
| 98049140 | 118.8765 | 21.3345 | Pincunah Monzogranite | granite | Sisters Supersuite | GSWA/GA (unpubl.) | 2930 |
| 26218 | 119.3346 | 21.6486 | ?Pinnacle Well | | Sisters Supersuite | McCulloch (1987) | 2930 |
| 141977 | 117.98115 | 21.202876 | Satirist Monzogranite | monzogranite | Sisters Supersuite | GSWA/GA (unpubl.) | 2930 |
| 98049174B | 118.8026 | 20.6819 | Chillerina Granodiorite | granite | Sisters Supersuite | GSWA/GA (unpubl.) | 2940 |
| 98049136 | 118.9956 | 20.5802 | Donald Well granite | granite | Sisters Supersuite | GSWA/GA (unpubl.) | 2940 |
| 160678 | 118.7198 | 21.7635 | Yule Granitic Complex | tonalite | Sisters Supersuite | GSWA/GA (unpubl.) | 2940 |
| 160685 | 118.6195 | 21.8125 | Yule Granitic Complex | granite | Sisters Supersuite | GSWA/GA (unpubl.) | 2940 |
| 160794 | 118.9706 | 21.5950 | Yule Granitic Complex | granite | Sisters Supersuite | GSWA/GA (unpubl.) | 2940 |
| 160797 | 118.8503 | 21.5736 | Yule Granitic Complex | granite | Sisters Supersuite | GSWA/GA (unpubl.) | 2940 |
| 174312 | 118.7919 | 21.7569 | Yule Granitic Complex | tonalite | Sisters Supersuite | GSWA/GA (unpubl.) | 2940 |
| 174318 | 118.7015 | 21.6273 | Yule Granitic Complex | monzogranite | Sisters Supersuite | GSWA/GA (unpubl.) | 2940 |
| 160794#2 | 118.9706 | 21.5950 | Yule Granitic Complex | granite | Sisters Supersuite | GSWA/GA (unpubl.) | 2940 |
| 141986 | 117.9283 | 20.8281 | Portree Granite | syenite | Portree Suite | GSWA/GA (unpubl.) | 2946 |
| 169025 | 119.4236 | 20.2675 | unknown | rhyolite | Croydon Group | GSWA/GA (unpubl.) | 2948 |
| 118967 | 117.9927 | 20.9873 | Peawah Granodiorite | hornblende–biotite tonalite | Indee Suite | GSWA/GA (unpubl.) | 2948 |
| 142260 | 118.0202 | 21.0970 | Peawah Granodiorite | diorite | Indee Suite | GSWA/GA (unpubl.) | 2948 |
| 142347 | 118.0977 | 20.9987 | Peawah Granodiorite | diorite | Indee Suite | GSWA/GA (unpubl.) | 2948 |
| 174391 | 119.4303 | 20.3482 | Bookingarra Formation | basalt | Croydon Group | GSWA/GA (unpubl.) | 2950 |
| 142359 | 118.0634 | 21.2379 | Bookingarra Formation | boninite | Croydon Group | GSWA/GA (unpubl.) | 2950 |

## Nd-isotopic data

| Method | Sm | Nd | $^{147}Sm/Nd$ | $Sm^{143}/Nd^{144}$ | Error ($\times 10^{-6}$) | $Sm^{143}/Nb^{144}$ (normalized)[a] | Nd/Nd T | CHUR T | $E_{Nd}$ T | Model CHUR | Model DM | Model 2DM[b] |
|---|---|---|---|---|---|---|---|---|---|---|---|---|
| assumed | 6.070 | 31.52 | 0.1165 | 0.511023 | 7 | 0.511035 | 0.508967 | 0.509159 | -3.76 | 3.05 | 3.31 | 3.28 |
| assumed | 4.300 | 19.56 | 0.1329 | 0.511386 | 9 | 0.511398 | 0.509039 | 0.509159 | -2.35 | 2.97 | 3.31 | 3.18 |
| assumed | 3.190 | 11.84 | 0.1628 | 0.511995 | 11 | 0.512007 | 0.509107 | 0.509146 | -0.77 | 2.87 | 3.44 | 3.07 |
| assumed | 3.250 | 12.07 | 0.1625 | 0.512040 | 10 | 0.512052 | 0.509157 | 0.509146 | 0.22 | 2.65 | 3.29 | 2.99 |
| assumed | 3.760 | 13.23 | 0.1718 | 0.512171 | 9 | 0.512183 | 0.509122 | 0.509146 | -0.46 | 2.84 | 3.54 | 3.04 |
| assumed | 3.890 | 14.86 | 0.1584 | 0.511940 | 10 | 0.511952 | 0.509130 | 0.509146 | -0.31 | 2.76 | 3.32 | 3.03 |
| assumed | 3.040 | 11.63 | 0.1582 | 0.511970 | 9 | 0.511982 | 0.509164 | 0.509146 | 0.35 | 2.63 | 3.23 | 2.98 |
| assumed | 1.060 | 3.93 | 0.1622 | 0.512040 | 10 | 0.512052 | 0.509162 | 0.509146 | 0.33 | 2.63 | 3.27 | 2.98 |
| assumed | 3.330 | 15.81 | 0.1272 | 0.511223 | 12 | 0.511235 | 0.508952 | 0.50912 | -3.29 | 3.08 | 3.37 | 3.27 |
| assumed | 3.300 | 15.84 | 0.1258 | 0.511229 | 11 | 0.511241 | 0.508983 | 0.50912 | -2.68 | 3.01 | 3.31 | 3.23 |
| assumed | 6.243 | 32.876 | 0.11477 | 0.511036 | 7 | 0.511036 | 0.508942 | 0.509061 | -2.34 | 2.98 | 3.26 | 3.24 |
| assumed | 4.060 | 19.19 | 0.1279 | 0.511265 | 8 | 0.511277 | 0.508930 | 0.509041 | -2.17 | 3.02 | 3.33 | 3.24 |
| assumed | 6.200 | 30.89 | 0.1213 | 0.511111 | 7 | 0.511123 | 0.508897 | 0.509041 | -2.82 | 3.07 | 3.34 | 3.29 |
| assumed | 4.150 | 19.58 | 0.1281 | 0.511283 | 9 | 0.511295 | 0.508945 | 0.509041 | -1.89 | 2.99 | 3.30 | 3.22 |
| assumed | 4.070 | 19.18 | 0.1284 | 0.511278 | 8 | 0.511290 | 0.508934 | 0.509041 | -2.10 | 3.01 | 3.33 | 3.23 |
| assumed | 2.530 | 11.65 | 0.1313 | 0.511328 | 11 | 0.511340 | 0.508931 | 0.509041 | -2.16 | 3.03 | 3.35 | 3.24 |
| Pb–Pb isochron | 5.278 | 26.07 | 0.1224 | 0.510943 | 28 | 0.510943 | 0.508643 | 0.508953 | -6.10 | 3.47 | 3.68 | 3.59 |
| Pb–Pb isochron | 4.774 | 32.04 | 0.0900 | 0.510236 | 22 | 0.510236 | 0.508545 | 0.508953 | -8.03 | 3.42 | 3.58 | 3.74 |
| Pb–Pb isochron | 5.100 | 29.60 | 0.1039 | 0.509880 | 20 | 0.510694 | 0.508739 | 0.508949 | -4.13 | 3.19 | 3.40 | 3.44 |
| Pb–Pb isochron | 9.100 | 35.00 | 0.1563 | 0.511641 | 20 | 0.511641 | 0.508701 | 0.508949 | -4.88 | 3.77 | 4.01 | 3.50 |
| Pb–Pb isochron | 6.700 | 29.00 | 0.1386 | 0.511280 | 10 | 0.511280 | 0.508673 | 0.508949 | -5.43 | 3.56 | 3.79 | 3.54 |
| Pb–Pb isochron | 4.200 | 16.00 | 0.1620 | 0.511748 | 10 | 0.511748 | 0.508701 | 0.508949 | -4.88 | 3.92 | 4.13 | 3.50 |
| assumed | 4.345 | 19.15 | 0.1372 | 0.511576 | 9 | 0.511568 | 0.508987 | 0.508949 | 0.74 | 2.75 | 3.16 | 3.08 |
| assumed | 5.336 | 32.00 | 0.1008 | 0.510937 | 9 | 0.510929 | 0.509033 | 0.508949 | 1.64 | 2.72 | 3.00 | 3.01 |
| assumed | 3.353 | 16.64 | 0.1218 | 0.511221 | 7 | 0.511200 | 0.508908 | 0.508949 | -0.81 | 2.93 | 3.24 | 3.19 |
| assumed | 11.340 | 74.85 | 0.0916 | 0.510648 | 9 | 0.510640 | 0.508917 | 0.508949 | -0.63 | 2.90 | 3.13 | 3.18 |
| assumed | 3.370 | 13.91 | 0.1464 | 0.511589 | 20 | 0.511601 | 0.508847 | 0.508949 | -2.02 | 3.16 | 3.51 | 3.28 |
| Pb–Pb isochron | 7.506 | 47.89 | 0.0947 | 0.510520 | 18 | 0.510520 | 0.508702 | 0.508873 | -3.37 | 3.16 | 3.36 | 3.44 |
| Pb–Pb isochron | 8.079 | 48.36 | 0.1010 | 0.510650 | 12 | 0.510650 | 0.508711 | 0.508873 | -3.19 | 3.16 | 3.38 | 3.42 |
| assumed | 5.343 | 20.57 | 0.1571 | 0.511870 | 6 | 0.511870 | 0.508836 | 0.508851 | -0.30 | 2.98 | 3.46 | 3.22 |
| assumed | 1.209 | 4.305 | 0.1698 | 0.512107 | 7 | 0.512107 | 0.508828 | 0.508851 | -0.46 | 3.06 | 3.64 | 3.23 |
| assumed | 3.746 | 18.36 | 0.1233 | 0.511225 | 7 | 0.511225 | 0.508844 | 0.508851 | -0.15 | 2.94 | 3.25 | 3.21 |
| assumed | 0.985 | 3.466 | 0.1717 | 0.512145 | 6 | 0.512145 | 0.508829 | 0.508851 | -0.44 | 3.06 | 3.67 | 3.23 |
| assumed | 1.066 | 3.99 | 0.1615 | 0.511952 | 7 | 0.511952 | 0.508833 | 0.508851 | -0.36 | 3.00 | 3.51 | 3.22 |
| assumed | 2.245 | 9.427 | 0.1440 | 0.511596 | 7 | 0.511596 | 0.508815 | 0.508851 | -0.71 | 3.03 | 3.40 | 3.25 |
| assumed | 2.290 | 9.608 | 0.1441 | 0.511602 | 7 | 0.511602 | 0.508819 | 0.508851 | -0.63 | 3.02 | 3.40 | 3.24 |
| assumed | 0.117 | 0.27 | 0.2635 | 0.513931 | 10 | 0.513931 | 0.508842 | 0.508851 | -0.18 | 2.90 | 2.34 | 3.21 |
| assumed | 3.329 | 14.66 | 0.1372 | 0.511490 | 6 | 0.511490 | 0.508840 | 0.508851 | -0.21 | 2.95 | 3.31 | 3.21 |
| assumed | 3.240 | 14.26 | 0.1374 | 0.511484 | 7 | 0.511484 | 0.508830 | 0.508851 | -0.41 | 2.98 | 3.33 | 3.23 |
| assumed | 0.544 | 2.11 | 0.1558 | 0.511838 | 6 | 0.511838 | 0.508829 | 0.508851 | -0.43 | 3.01 | 3.47 | 3.23 |
| assumed | 0.568 | 2.205 | 0.1558 | 0.511850 | 7 | 0.511850 | 0.508841 | 0.508851 | -0.20 | 2.96 | 3.43 | 3.21 |
| assumed | 0.980 | 3.985 | 0.1486 | 0.511718 | 7 | 0.511718 | 0.508848 | 0.508851 | -0.06 | 2.93 | 3.36 | 3.20 |
| assumed | 1.666 | 7.299 | 0.1380 | 0.511496 | 6 | 0.511496 | 0.508831 | 0.508851 | -0.40 | 2.98 | 3.33 | 3.23 |
| assumed | 1.689 | 7.491 | 0.1363 | 0.511468 | 7 | 0.511468 | 0.508836 | 0.508851 | -0.30 | 2.96 | 3.32 | 3.22 |
| assumed | 0.539 | 1.677 | 0.1943 | 0.512598 | 6 | 0.512598 | 0.508845 | 0.508851 | -0.11 | 3.28 | 4.41 | 3.20 |
| assumed | 3.902 | 18.48 | 0.1277 | 0.511304 | 7 | 0.511304 | 0.508838 | 0.508851 | -0.26 | 2.95 | 3.27 | 3.21 |
| assumed | 3.878 | 18.67 | 0.1255 | 0.511249 | 6 | 0.511249 | 0.508825 | 0.508851 | -0.51 | 2.98 | 3.29 | 3.23 |
| assumed | 2.584 | 11.6 | 0.1347 | 0.511434 | 6 | 0.511434 | 0.508832 | 0.508851 | -0.36 | 2.97 | 3.31 | 3.22 |
| Pb–Pb isochron | 3.670 | 18.62 | 0.1191 | 0.510887 | 32 | 0.510887 | 0.508587 | 0.508851 | -5.19 | 3.43 | 3.64 | 3.59 |
| Pb–Pb isochron | 5.757 | 41.53 | 0.0837 | 0.510245 | 16 | 0.510245 | 0.508628 | 0.508851 | -4.37 | 3.22 | 3.40 | 3.52 |
| Pb–Pb isochron | 6.964 | 50.08 | 0.0840 | 0.510248 | 16 | 0.510248 | 0.508626 | 0.508851 | -4.43 | 3.22 | 3.40 | 3.53 |
| Pb–Pb isochron | 5.816 | 38.82 | 0.0905 | 0.510432 | 18 | 0.510432 | 0.508684 | 0.508851 | -3.28 | 3.16 | 3.36 | 3.44 |
| assumed | 2.230 | 6.60 | 0.2042 | 0.512745 | 7 | 0.512745 | 0.508802 | 0.508851 | -0.97 | 1.93 | 6.64 | 3.27 |
| assumed | 16.158 | 79.858 | 0.122307 | 0.511219 | 6 | 0.511219 | 0.508857 | 0.508851 | 0.11 | 2.91 | 3.22 | 3.19 |
| assumed | 6.376 | 35.90 | 0.1073 | 0.510998 | 8 | 0.510977 | 0.508901 | 0.508844 | 1.10 | 2.84 | 3.11 | 3.12 |
| assumed | 4.320 | 25.79 | 0.1011 | 0.510848 | 20 | 0.510860 | 0.508904 | 0.508844 | 1.17 | 2.84 | 3.10 | 3.11 |
| assumed | 3.052 | 16.73 | 0.1103 | 0.511009 | 8 | 0.510988 | 0.508855 | 0.508844 | 0.20 | 2.91 | 3.18 | 3.18 |
| assumed | 7.791 | 45.10 | 0.1044 | 0.510814 | 9 | 0.510793 | 0.508773 | 0.508844 | -1.40 | 3.05 | 3.28 | 3.31 |
| Pb–Pb isochron | 4.800 | 33.90 | 0.0855 | 0.509350 | 20 | 0.510163 | 0.508509 | 0.508844 | -6.60 | 3.38 | 3.54 | 3.70 |
| assumed | 4.368 | 23.758 | 0.11114 | 0.510981 | 6 | 0.510981 | 0.508831 | 0.508844 | -0.27 | 2.95 | 3.22 | 3.22 |
| assumed | 9.474 | 43.57 | 0.1314 | 0.511401 | 8 | 0.511393 | 0.508841 | 0.508831 | 0.20 | 2.92 | 3.26 | 3.19 |
| assumed | 2.466 | 16.75 | 0.0890 | 0.510729 | 8 | 0.510721 | 0.508994 | 0.508831 | 3.19 | 2.71 | 2.97 | 2.97 |
| assumed | 1.270 | 10.26 | 0.0749 | 0.510033 | 20 | 0.510045 | 0.508591 | 0.508831 | -4.73 | 3.24 | 3.40 | 3.56 |
| assumed | 1.590 | 12.79 | 0.0752 | 0.510071 | 20 | 0.510083 | 0.508623 | 0.508831 | -4.09 | 3.20 | 3.37 | 3.52 |
| assumed | 6.650 | 47.15 | 0.0852 | 0.510351 | 20 | 0.510363 | 0.508709 | 0.508831 | -2.41 | 3.10 | 3.30 | 3.39 |
| assumed | 6.830 | 38.67 | 0.1067 | 0.510781 | 20 | 0.510793 | 0.508722 | 0.508831 | -2.16 | 3.12 | 3.35 | 3.37 |
| assumed | 1.810 | 6.27 | 0.1747 | 0.512106 | 20 | 0.512118 | 0.508726 | 0.508831 | -2.06 | 3.65 | 4.05 | 3.36 |
| assumed | 1.600 | 11.11 | 0.0873 | 0.510348 | 20 | 0.510360 | 0.508665 | 0.508831 | -3.27 | 3.17 | 3.36 | 3.45 |
| assumed | 6.560 | 46.07 | 0.0861 | 0.510327 | 20 | 0.510339 | 0.508667 | 0.508831 | -3.22 | 3.16 | 3.35 | 3.45 |
| SHRIMP | 5.694 | 34.58 | 0.0995 | 0.510835 | 9 | 0.510814 | 0.508878 | 0.508823 | 1.07 | 2.86 | 3.12 | 3.13 |
| assumed | 10.800 | 50.29 | 0.1299 | 0.511260 | 20 | 0.511272 | 0.508743 | 0.508821 | -1.53 | 3.12 | 3.42 | 3.33 |
| SHRIMP | 3.204 | 19.13 | 0.1012 | 0.510841 | 9 | 0.510820 | 0.508849 | 0.508821 | 0.56 | 2.90 | 3.16 | 3.17 |
| SHRIMP | 5.440 | 32.54 | 0.1011 | 0.510773 | 20 | 0.510785 | 0.508817 | 0.508821 | -0.08 | 2.95 | 3.20 | 3.22 |
| SHRIMP | 9.150 | 56.75 | 0.0975 | 0.510709 | 20 | 0.510721 | 0.508823 | 0.508821 | 0.04 | 2.94 | 3.18 | 3.21 |
| assumed | 4.070 | 18.20 | 0.1350 | 0.511428 | 20 | 0.511440 | 0.508810 | 0.508818 | -0.16 | 2.97 | 3.32 | 3.23 |
| assumed | 0.850 | 4.26 | 0.1199 | 0.511097 | 20 | 0.511109 | 0.508773 | 0.508818 | -0.88 | 3.04 | 3.32 | 3.28 |

## Appendix 2.

| Sample | Easting | Northing | Unit | Lithology | Group/Suite/ Supersuite | Source of isotopic data | Age |
|---|---|---|---|---|---|---|---|
| 98049159 | 118.8167 | 20.7443 | Wallareenya Granodiorite | granite | Indee Suite | GSWA/GA (unpubl.) | 2950 |
| 142492 | unknown | unknown | dyke in Cleaverville | leucogabbro | Sisters Supersuite | GSWA/GA (unpubl.) | 2950 |
| 160705 | 118.7089 | 20.6649 | Wallaringa | tonalite/granodiorite | Sisters Supersuite | GSWA/GA (unpubl.) | 2950 |
| 97045027A | 118.8313 | 21.1533 | Whim Creek | basalt | Comstock | GSWA/GA (unpubl.) | 2970 |
| 142212 | 118.0896 | 21.0303 | Bookingarra Formation | basalt | Croydon Group | GSWA/GA (unpubl.) | 2970 |
| 142223 | 118.0780 | 21.0223 | Bookingarra Formation | basalt | Croydon Group | GSWA/GA (unpubl.) | 2970 |
| 142263 | 118.0446 | 21.0973 | unknown | gabbro | Croydon Group | GSWA/GA (unpubl.) | 2970 |
| 142288 | 118.1758 | 21.0884 | Bookingarra Formation | basalt | Croydon Group | GSWA/GA (unpubl.) | 2970 |
| 98049027A | 117.8561 | 21.0997 | Low-Ti tholeiite | gabbro | Croydon Group | GSWA/GA (unpubl.) | 2970 |
| 98049027AR | 117.8561 | 21.0997 | Low-Ti tholeiite | gabbro | Croydon Group | GSWA/GA (unpubl.) | 2970 |
| l29 | unknown | unknown | Louden Volcanic Member, Bookingarra Formation | basalt | Croydon Group | Arndt et al. (2001) | 2970 |
| l32 | unknown | unknown | Louden Volcanic Member, Bookingarra Formation | basalt | Croydon Group | Arndt et al. (2001) | 2970 |
| l38 | unknown | unknown | Louden Volcanic Member, Bookingarra Formation | basalt | Croydon Group | Arndt et al. (2001) | 2970 |
| l46 | unknown | unknown | Louden Volcanic Member, Bookingarra Formation | basalt | Croydon Group | Arndt et al. (2001) | 2970 |
| l57 | unknown | unknown | Louden Volcanic Member, Bookingarra Formation | basalt | Croydon Group | Arndt et al. (2001) | 2970 |
| l58 | unknown | unknown | Louden Volcanic Member, Bookingarra Formation | basalt | Croydon Group | Arndt et al. (2001) | 2970 |
| l59 | unknown | unknown | Louden Volcanic Member, Bookingarra Formation | basalt | Croydon Group | Arndt et al. (2001) | 2970 |
| l60 | unknown | unknown | Louden Volcanic Member, Bookingarra Formation | basalt | Croydon Group | Arndt et al. (2001) | 2970 |
| l61 | unknown | unknown | Louden Volcanic Member, Bookingarra Formation | basalt | Croydon Group | Arndt et al. (2001) | 2970 |
| l62 | unknown | unknown | Louden Volcanic Member, Bookingarra Formation | basalt | Croydon Group | Arndt et al. (2001) | 2970 |
| l63 | unknown | unknown | Louden Volcanic Member, Bookingarra Formation | basalt | Croydon Group | Arndt et al. (2001) | 2970 |
| l65 | unknown | unknown | Louden Volcanic Member, Bookingarra Formation | basalt | Croydon Group | Arndt et al. (2001) | 2970 |
| l67 | unknown | unknown | Louden Volcanic Member, Bookingarra Formation | basalt | Croydon Group | Arndt et al. (2001) | 2970 |
| l68 | unknown | unknown | Louden Volcanic Member, Bookingarra Formation | basalt | Croydon Group | Arndt et al. (2001) | 2970 |
| n51 | unknown | unknown | Negri Volcanic Member Bookingarra Formation | basalt | Croydon Group | Arndt et al. (2001) | 2970 |
| n52 | unknown | unknown | Negri Volcanic Member, Bookingarra Formation | basalt | Croydon Group | Arndt et al. (2001) | 2970 |
| n54 | unknown | unknown | Negri Volcanic Member, Bookingarra Formation | basalt | Croydon Group | Arndt et al. (2001) | 2970 |
| 142350 | 117.8585 | 20.7741 | Mount Negri Volcanics | basalt | Croydon Group | GSWA/GA (unpubl.) | 2970 |
| 142193 | 117.9210 | 21.3135 | Bookingarra Formation | boninite | Croydon Group | GSWA/GA (unpubl.) | 2970 |
| 142893 | 116.2435 | 21.0448 | 'Eramurra Creek', Dampier Granitic Complex | pegmatite-veined monzogranite | Maitland River Supersuite | GSWA/GA (unpubl.) | 2982 |
| 168934 | 117.0736 | 21.2102 | 'Fish Creek area', Cherratta Granitic Complex | biotite monzogranite | Maitland River Supersuite | GSWA/GA (unpubl.) | 2988 |
| 160501 | 117.7014 | 20.8219 | Caines Well Monzogranite | granite | Maitland River Supersuite | GSWA/GA (unpubl.) | 2990 |
| 160502 | 117.7953 | 20.8240 | Caines Well Monzogranite | granite | Maitland River Supersuite | GSWA/GA (unpubl.) | 2990 |
| 84770115 | 116.8789 | 21.1141 | Cherratta Granitic Complex | granite | Maitland River Supersuite | GSWA/GA (unpubl.) | 2990 |
| 84770083 | 116.8418 | 21.0953 | Cherratta Granitic Complex | granite | Maitland River Supersuite | Sun and Hoatson (1992) | 2990 |
| 136826 | 116.7677 | 20.975611 | near Baynton Hill | granite | Maitland River Supersuite | GSWA/GA (unpubl.) | 2995 |
| 136844 | 116.7227 | 20.7551 | Dampier salt ponds — main phase | granite | Maitland River Supersuite | GSWA/GA (unpubl.) | 2997 |
| 176740 | 120.1840 | 20.5362 | Cooneeina Basalt | basalt | Croydon Group | GSWA/GA (unpubl.) | 3000 |
| 176747 | 120.2046 | 20.5368 | Cooneeina Basalt | basalt | Croydon Group | GSWA/GA (unpubl.) | 3000 |
| 142858 | 121.2955 | 30.3117 | dolerite dyke | dolerite | unknown | GSWA/GA (unpubl.) | 3000 |
| 160642 | 118.3841 | 21.5077 | Yule Granitic Complex | tonalite | unknown | GSWA/GA (unpubl.) | 3000 |
| 176737 | 117.3808 | 20.9467 | Warambie Basalt | basalt | Whim Creek Group | GSWA/GA (unpubl.) | 3000 |
| 70 | unknown | unknown | Warambie Basalt | basalt | Whim Creek Group | Arndt et al. (2001) | 3010 |
| 75 | unknown | unknown | Warambie Basalt | basalt | Whim Creek Group | Arndt et al. (2001) | 3010 |
| 78 | unknown | unknown | Warambie Basalt | basalt | Whim Creek Group | Arndt et al. (2001) | 3010 |
| JS35 | 116.9223 | 21.0954 | Sholl Terrane | undeformed granite | Orpheus Supersuite | Smith et al. (1998) | 3013 |
| 127320 | 117.16385 | 20.915357 | quartz granophyre | granite | Orpheus Supersuite | GSWA/GA (unpubl.) | 3014 |
| 118966 | 117.6969 | 20.744796 | Forestier Bay Granodiorite | gneissic granodiorite | Orpheus Supersuite | GSWA/GA (unpubl.) | 3014 |
| 86330008 | 117.0777 | 20.8418 | Andover Intrusion | websterite | Orpheus Supersuite | Sun and Hoatson (1992) | 3015 |
| 86330020 | 117.0869 | 20.8480 | Andover Intrusion | mafic dyke | Orpheus Supersuite | Sun and Hoatson (1992) | 3015 |
| 86330069 | 117.1241 | 20.8300 | Andover Intrusion | gabbronorite | Orpheus Supersuite | Sun and Hoatson (1992) | 3015 |
| 87330127 | 117.1052 | 20.8410 | Andover Intrusion | gabbronorite | Orpheus Supersuite | Sun and Hoatson (1992) | 3015 |
| 88330196 | 117.1465 | 20.8375 | Andover Intrusion | norite | Orpheus Supersuite | Sun and Hoatson (1992) | 3015 |
| 88330213 | 117.1585 | 20.8024 | Andover Intrusion | clinopyroxenite | Orpheus Supersuite | Sun and Hoatson (1992) | 3015 |
| 83330172 | 117.1388 | 20.8181 | Andover Intrusion | gabbronorite | Orpheus Supersuite | Sun and Hoatson (1992) | 3015 |
| 168936 | 117.1116 | 20.8602 | 'Andover Mine area' | monzodiorite | Orpheus Supersuite | GSWA/GA (unpubl.) | 3016 |
| 142430 | 117.0750 | 20.8778 | Black Hill Well Monzogranite | monzogranite | Orpheus Supersuite | GSWA/GA (unpubl.) | 3018 |

(continued)

| Method | Sm | Nd | $^{147}Sm/Nd$ | $Sm^{143}/Nd^{144}$ | Error ($\times 10^{-6}$) | $Sm^{143}/Nb^{144}$ (normalized)[a] | Nd/Nd T | CHUR T | $E_{Nd}$ T | Model CHUR | Model DM | Model 2DM[b] |
|---|---|---|---|---|---|---|---|---|---|---|---|---|
| assumed | 5.587 | 36.63 | 0.0966 | 0.510747 | 11 | 0.510739 | 0.508857 | 0.508818 | 0.75 | 2.89 | 3.14 | 3.16 |
| assumed | 2.480 | 11.19 | 0.1338 | 0.511347 | 5 | 0.511347 | 0.508741 | 0.508818 | -1.53 | 3.14 | 3.44 | 3.33 |
| assumed | 5.610 | 27.35 | 0.1239 | 0.511212 | 20 | 0.511224 | 0.508810 | 0.508818 | -0.15 | 2.97 | 3.27 | 3.23 |
| assumed | 3.540 | 15.61 | 0.1372 | 0.511330 | 20 | 0.511385 | 0.508694 | 0.508792 | -1.93 | 3.22 | 3.52 | 3.38 |
| assumed | 5.040 | 24.09 | 0.1264 | 0.511178 | 20 | 0.511233 | 0.508754 | 0.508792 | -0.75 | 3.05 | 3.35 | 3.29 |
| assumed | 5.160 | 24.72 | 0.1261 | 0.511178 | 20 | 0.511233 | 0.508760 | 0.508792 | -0.64 | 3.04 | 3.34 | 3.28 |
| assumed | 2.280 | 10.43 | 0.1320 | 0.511354 | 20 | 0.511366 | 0.508777 | 0.508792 | -0.29 | 3.00 | 3.33 | 3.25 |
| assumed | 5.000 | 23.89 | 0.1266 | 0.511177 | 20 | 0.511232 | 0.508749 | 0.508792 | -0.85 | 3.06 | 3.36 | 3.30 |
| assumed | 0.850 | 2.17 | 0.2383 | 0.513478 | 20 | 0.513490 | 0.508816 | 0.508792 | 0.47 | 3.06 | 2.01 | 3.20 |
| assumed | 0.896 | 2.27 | 0.2384 | 0.513476 | 20 | 0.513488 | 0.508812 | 0.508792 | 0.40 | 3.04 | 1.99 | 3.20 |
| assumed | 1.400 | 6.05 | 0.1403 | 0.511460 | 11 | 0.511472 | 0.508720 | 0.508792 | -1.41 | 3.16 | 3.49 | 3.34 |
| assumed | 1.430 | 6.1 | 0.1419 | 0.511474 | 6 | 0.511486 | 0.508703 | 0.508792 | -1.75 | 3.21 | 3.54 | 3.36 |
| assumed | 1.980 | 9.09 | 0.1315 | 0.511245 | 12 | 0.511257 | 0.508678 | 0.508792 | -2.24 | 3.23 | 3.51 | 3.40 |
| assumed | 1.980 | 8.52 | 0.1405 | 0.511442 | 7 | 0.511454 | 0.508698 | 0.508792 | -1.84 | 3.22 | 3.53 | 3.37 |
| assumed | 1.420 | 6.03 | 0.1427 | 0.511463 | 9 | 0.511475 | 0.508676 | 0.508792 | -2.28 | 3.29 | 3.60 | 3.40 |
| assumed | 2.020 | 8.88 | 0.1375 | 0.511399 | 8 | 0.511411 | 0.508714 | 0.508792 | -1.53 | 3.17 | 3.48 | 3.35 |
| assumed | 2.050 | 8.87 | 0.1394 | 0.511412 | 8 | 0.511424 | 0.508690 | 0.508792 | -2.01 | 3.24 | 3.54 | 3.38 |
| assumed | 1.900 | 8.08 | 0.1423 | 0.511497 | 9 | 0.511509 | 0.508718 | 0.508792 | -1.45 | 3.17 | 3.51 | 3.34 |
| assumed | 1.630 | 6.99 | 0.1405 | 0.511436 | 8 | 0.511448 | 0.508692 | 0.508792 | -1.96 | 3.24 | 3.55 | 3.38 |
| assumed | 1.510 | 6.36 | 0.1431 | 0.511472 | 6 | 0.511484 | 0.508677 | 0.508792 | -2.25 | 3.29 | 3.60 | 3.40 |
| assumed | 1.470 | 6.17 | 0.1439 | 0.511500 | 10 | 0.511512 | 0.508690 | 0.508792 | -2.01 | 3.26 | 3.58 | 3.38 |
| assumed | 1.660 | 7.16 | 0.1404 | 0.511453 | 6 | 0.511465 | 0.508711 | 0.508792 | -1.59 | 3.18 | 3.51 | 3.35 |
| assumed | 1.210 | 5.25 | 0.1394 | 0.511397 | 6 | 0.511409 | 0.508675 | 0.508792 | -2.30 | 3.28 | 3.57 | 3.41 |
| assumed | 1.150 | 4.99 | 0.1396 | 0.511434 | 8 | 0.511446 | 0.508708 | 0.508792 | -1.65 | 3.19 | 3.51 | 3.36 |
| assumed | 3.470 | 16.11 | 0.1300 | 0.511263 | 10 | 0.511275 | 0.508725 | 0.508792 | -1.31 | 3.12 | 3.41 | 3.33 |
| assumed | 3.990 | 18.37 | 0.1316 | 0.511227 | 9 | 0.511239 | 0.508658 | 0.508792 | -2.64 | 3.28 | 3.55 | 3.43 |
| assumed | 3.900 | 17.92 | 0.1316 | 0.511272 | 9 | 0.511284 | 0.508703 | 0.508792 | -1.75 | 3.18 | 3.46 | 3.36 |
| assumed | 3.540 | 16.30 | 0.1312 | 0.511276 | 20 | 0.511288 | 0.508715 | 0.508792 | -1.52 | 3.15 | 3.44 | 3.35 |
| assumed | 1.090 | 5.42 | 0.1217 | 0.511090 | 20 | 0.511102 | 0.508715 | 0.508792 | -1.51 | 3.12 | 3.39 | 3.35 |
| SHRIMP | 4.590 | 35.30 | 0.0786 | 0.510254 | 20 | 0.510266 | 0.508718 | 0.508776 | -1.14 | 3.06 | 3.25 | 3.33 |
| SHRIMP | 2.800 | 8.93 | 0.1895 | 0.510481 | 20 | 0.510493 | 0.506753 | 0.508768 | -39.60 | 40.07 | 16.07 | 6.23 |
| assumed | 2.830 | 20.06 | 0.0852 | 0.510395 | 20 | 0.510407 | 0.508725 | 0.508766 | -0.81 | 3.05 | 3.25 | 3.31 |
| assumed | 1.900 | 14.74 | 0.0780 | 0.510226 | 20 | 0.510238 | 0.508698 | 0.508766 | -1.34 | 3.08 | 3.26 | 3.35 |
| assumed | 2.853 | 21.28 | 0.081024 | 0.510382 | 7 | 0.510382 | 0.508782 | 0.508766 | 0.32 | 2.97 | 3.17 | 3.23 |
| assumed | 4.257 | 26.837 | 0.0959 | 0.510669 | 5 | 0.510669 | 0.508775 | 0.508766 | 0.19 | 2.98 | 3.21 | 3.24 |
| assumed | 5.883 | 26.149 | 0.13601 | 0.511495 | 6 | 0.511495 | 0.508805 | 0.508759 | 0.89 | 2.88 | 3.25 | 3.19 |
| SHRIMP | 2.580 | 14.32 | 0.1087 | 0.510823 | 20 | 0.510835 | 0.508683 | 0.508757 | -1.44 | 3.12 | 3.36 | 3.36 |
| assumed | 2.650 | 11.45 | 0.1401 | 0.511408 | 20 | 0.511420 | 0.508644 | 0.508753 | -2.13 | 3.29 | 3.58 | 3.42 |
| assumed | 1.420 | 5.37 | 0.1599 | 0.511805 | 20 | 0.511817 | 0.508649 | 0.508753 | -2.04 | 3.42 | 3.79 | 3.41 |
| assumed | 5.080 | 30.42 | 0.1010 | 0.511011 | 20 | 0.511023 | 0.509022 | 0.508753 | 5.29 | 2.58 | 2.88 | 2.86 |
| assumed | 4.120 | 37.48 | 0.0664 | 0.509809 | 20 | 0.509821 | 0.508505 | 0.508753 | -4.86 | 3.28 | 3.43 | 3.62 |
| assumed | 4.500 | 21.17 | 0.1286 | 0.511283 | 20 | 0.511295 | 0.508747 | 0.508753 | -0.11 | 3.01 | 3.32 | 3.27 |
| assumed | 4.610 | 22.64 | 0.1231 | 0.511177 | 9 | 0.511189 | 0.508742 | 0.50874 | 0.04 | 3.01 | 3.30 | 3.26 |
| assumed | 4.190 | 18.82 | 0.1346 | 0.511404 | 10 | 0.511416 | 0.508740 | 0.50874 | 0.01 | 3.01 | 3.34 | 3.27 |
| assumed | 2.080 | 9.36 | 0.1341 | 0.511325 | 9 | 0.511337 | 0.508671 | 0.50874 | -1.35 | 3.17 | 3.47 | 3.37 |
| SHRIMP | 2.476 | 13.97 | 0.1071 | 0.510884 | 11 | 0.510884 | 0.508752 | 0.508736 | 0.32 | 2.99 | 3.24 | 3.24 |
| assumed | 4.511 | 28.982 | 0.094066 | 0.510708 | 7 | 0.510708 | 0.508835 | 0.508734 | 1.99 | 2.87 | 3.11 | 3.12 |
| assumed | 4.270 | 23.914 | 0.10791 | 0.510861 | 7 | 0.510861 | 0.508713 | 0.508734 | -0.42 | 3.05 | 3.29 | 3.30 |
| assumed | 0.961 | 4.161 | 0.1397 | 0.511492 | 6 | 0.511492 | 0.508710 | 0.508733 | -0.45 | 3.08 | 3.42 | 3.30 |
| assumed | 5.001 | 20.18 | 0.1499 | 0.512195 | 6 | 0.512195 | 0.509210 | 0.508733 | 9.38 | 1.48 | 2.31 | 2.56 |
| assumed | 1.224 | 4.483 | 0.1651 | 0.512035 | 5 | 0.512035 | 0.508747 | 0.508733 | 0.28 | 2.95 | 3.52 | 3.25 |
| assumed | 3.531 | 14.06 | 0.1518 | 0.511789 | 7 | 0.511789 | 0.508766 | 0.508733 | 0.65 | 2.90 | 3.36 | 3.22 |
| assumed | 1.782 | 7.911 | 0.1362 | 0.511403 | 5 | 0.511403 | 0.508691 | 0.508733 | -0.83 | 3.12 | 3.44 | 3.33 |
| assumed | 1.858 | 5.712 | 0.1966 | 0.512636 | 6 | 0.512636 | 0.508721 | 0.508733 | -0.24 | 20.03 | 4.67 | 3.29 |
| assumed | 3.775 | 17.84 | 0.1279 | 0.511261 | 5 | 0.511261 | 0.508714 | 0.508733 | -0.37 | 3.06 | 3.36 | 3.30 |
| SHRIMP | 8.820 | 40.50 | 0.1317 | 0.511360 | 20 | 0.511372 | 0.508748 | 0.508732 | 0.33 | 2.98 | 3.31 | 3.25 |
| SHRIMP | 7.710 | 46.45 | 0.1003 | 0.510672 | 20 | 0.510684 | 0.508685 | 0.508729 | -0.87 | 3.09 | 3.31 | 3.34 |

## Appendix 2.

| Sample | Easting | Northing | Unit | Lithology | Group/Suite/ Supersuite | Source of isotopic data | Age |
|---|---|---|---|---|---|---|---|
| JS25 | 116.9501 | 20.8964 | Sholl Shear zone | mylonitic tonalite | Orpheus Supersuite | Smith et al. (1998) | 3024 |
| 142661 | 116.8695 | 21.1454 | Cliff Pool Tonalite | foliated tonalite | Elizabeth Hill Supersuite | GSWA/GA (unpubl.) | 3068 |
| 142534 | 116.5775 | 21.1025 | Pinderi–Cherratta | granite | Cherratta | GSWA/GA (unpubl.) | 3100 |
| 142536 | 116.9141 | 21.2454 | Pinderi–Cherratta | granite | Cherratta | GSWA/GA (unpubl.) | 3100 |
| JS44 | 116.7273 | 20.9161 | Cherratta Granitic Complex | undeformed granite | Railway Supersuite | Smith et al. (1998) | 3114 |
| JS20 | 116.8406 | 20.8946 | Sholl Terrane | foliated granite | Railway Supersuite | Smith et al. (1998) | 3114 |
| JS33 | 116.8988 | 21.1100 | Sholl Terrane | foliated granodiorite band in migmatite | Railway Supersuite | Smith et al. (1998) | 3114 |
| 174489 | 117.0434 | 20.9475 | Bradley Basalt | calc-alkaline basalt | Whundo Group | GSWA/GA (unpubl.) | 3115 |
| 114305 | 117.01389 | 20.925 | Whundo Group | felsic tuff | Whundo Group | GSWA/GA (unpubl.) | 3115 |
| 114356 | 116.9275 | 20.9525 | Whundo Group | rhyolite | Whundo Group | GSWA/GA (unpubl.) | 3115 |
| 174460 | 116.9489 | 20.9755 | Bradley Basalt | calc-alkaline basalt | Whundo Group | GSWA/GA (unpubl.) | 3115 |
| 174463 | 116.9501 | 20.9769 | Bradley Basalt | MORB | Whundo Group | GSWA/GA (unpubl.) | 3115 |
| 174497 | 117.0557 | 20.9392 | Bradley Basalt | calc-alkaline basalt | Whundo Group | GSWA/GA (unpubl.) | 3115 |
| 127378 | 117.0930 | 20.9181 | Woodbrook Formation | welded felsic tuff | Whundo Group | GSWA/GA (unpubl.) | 3117 |
| 174438 | 116.8479 | 20.9057 | Whundo Group | boninite | Whundo Group | GSWA/GA (unpubl.) | 3120 |
| 180229 | 116.8477 | 20.9065 | Whundo Group | calc-alkaline basalt | Whundo Group | GSWA/GA (unpubl.) | 3120 |
| 180232 | 116.8597 | 20.9319 | Whundo Group | boninite | Whundo Group | GSWA/GA (unpubl.) | 3120 |
| 174445 | 116.8621 | 20.9657 | dyke in Nallana basalt | basalt | Whundo Group | GSWA/GA (unpubl.) | 3120 |
| 174442 | 116.8675 | 20.9319 | Nallana Basalt | basalt | Whundo Group | GSWA/GA (unpubl.) | 3120 |
| 174451 | 116.9271 | 20.9536 | Tozer Formation | basalt | Whundo Group | GSWA/GA (unpubl.) | 3120 |
| 174454 | 116.9295 | 20.9647 | Tozer Formation | basalt | Whundo Group | GSWA/GA (unpubl.) | 3120 |
| 114358 | 116.92222 | 20.995833 | Whundo Group | porphyritic rhyolite | Whundo Group | GSWA/GA (unpubl.) | 3122 |
| 114350 | 116.91889 | 20.936389 | Whundo Group | metadacite | Whundo Group | GSWA/GA (unpubl.) | 3125 |
| 142019 | 117.8736 | 21.6794 | Nunyerry | granite | Mount Billroth Supersuite | GSWA/GA (unpubl.) | 3170 |
| 142020 | 117.8736 | 21.6794 | Nunyerry | granite | Mount Billroth Supersuite | GSWA/GA (unpubl.) | 3170 |
| 160760#2 | 119.0071 | 21.97267 | Yule Granitic Complex | granodiorite | ?Cleland Supersuite | GSWA/GA (unpubl.) | 3200 |
| 176712 | 117.0602 | 20.7240 | Regal Formation | basalt | Regal Terrane | GSWA/GA (unpubl.) | 3200 |
| 176722 | 116.7488 | 20.8057 | Regal Formation | basalt | Regal Terrane | GSWA/GA (unpubl.) | 3200 |
| 160235 | 116.8834 | 20.7430 | Regal Formation | basalt | Regal Terrane | GSWA/GA (unpubl.) | 3200 |
| 160238 | 116.8824 | 20.7523 | Regal Formaion | komatiite | Regal Terrane | GSWA/GA (unpubl.) | 3200 |
| 174479 | 118.6613 | 21.1608 | Wodgina gsb | basalt | unknown | GSWA/GA (unpubl.) | 3200 |
| 174430 | 118.2767 | 21.2185 | Pilbara Well gsb | basalt | unknown | GSWA/GA (unpubl.) | 3200 |
| 174431 | 118.2754 | 21.2179 | Pilbara Well gsb | basalt | unknown | GSWA/GA (unpubl.) | 3200 |
| 174477 | 118.6619 | 21.1599 | Wodgina gsb | basalt | unknown | GSWA/GA (unpubl.) | 3200 |
| 174434 | 118.2649 | 21.2022 | Pilbara Well gb | basalt | unknown | GSWA/GA (unpubl.) | 3200 |
| 160646 | 118.3669 | 21.6183 | Yule Granitic Complex | monzogranite | unknown | GSWA/GA (unpubl.) | 3200 |
| 160650 | 118.5385 | 21.5554 | Yule Granitic Complex | tonalite | unknown | GSWA/GA (unpubl.) | 3200 |
| 160760 | 119.0071 | 21.9727 | Yule Granitic Complex | granodiorite | unknown | GSWA/GA (unpubl.) | 3200 |
| 142535 | 116.5044 | 21.3880 | Tarlwa Pool Tonalite | foliated hornblende–biotite tonalite | Cleland Supersuite | GSWA/GA (unpubl.) | 3236 |
| 207186 | 119.2076 | 21.1743 | unknown | mafic microdiorite | Cleland Supersuite | Brauhart et al. (2000) | 3240 |
| 203368 | 119.1942 | 21.2120 | Strelley Monzogranite | inner phase | Cleland Supersuite | Brauhart et al. (2000) | 3240 |
| 203366 | 119.1058 | 21.2771 | Strelley Monzogranite | outer phase | Cleland Supersuite | Brauhart et al. (2000) | 3240 |
| 207334 | 119.2199 | 21.2452 | Kangaroo Caves Formation | rhyolite | Sulphur Springs Group | Brauhart et al. (2000) | 3240 |
| 142874 | 120.5257 | 20.8258 | Ninety Mile | granodiorite | Cleland Supersuite | GSWA/GA (unpubl.) | 3242 |
| 142869 | 120.5688 | 20.8131 | Warrawagine Granitic Complex | granodiorite | Cleland Supersuite | GSWA/GA (unpubl.) | 3244 |
| 143810 | 120.4181 | 20.7947 | Wolline Monzogranite | monzogranite | Cleland Supersuite | GSWA/GA (unpubl.) | 3244 |
| 143805 | 120.0414 | 20.6042 | Wolline Monzogranite | monzogranite | Cleland Supersuite | GSWA/GA (unpubl.) | 3252 |
| JS17 | 116.8512 | 20.8295 | Karratha Granodiorite | undeformed tonalite | Cleland Supersuite | Smith et al. (1998) | 3261 |
| JS43 | 116.9729 | 20.8792 | Harding Granitic Complex | undeformed granodiorite | Cleland Supersuite | Smith et al. (1998) | 3265 |
| 142431 | 116.8308 | 20.8233 | Dampier–Karratha | granite | Cleland Supersuite | GSWA/GA (unpubl.) | 3270 |
| 142432 | 116.8133 | 20.8364 | Dampier–Karratha | granite | Cleland Supersuite | GSWA/GA (unpubl.) | 3270 |
| 142433 | 116.7803 | 20.8328 | Karratha Granodiorite | tonalite | Cleland Supersuite | GSWA/GA (unpubl.) | 3270 |
| 148881 | 116.3355 | 20.9981 | Preston–Dampier | granite | Cleland Supersuite | GSWA/GA (unpubl.) | 3270 |
| 1 | unknown | unknown | Ruth Well Formation | basalt | Roebourne Group | Arndt et al. (2001) | 3270 |
| 21 | unknown | unknown | Ruth Well Formation | basalt | Roebourne Group | Arndt et al. (2001) | 3270 |
| 174185 | 119.3242 | 20.9029 | Carlindi Granitic Complex | | ?Emu Pool Supersuite | GSWA/GA (unpubl.) | 3300 |
| 160240 | 116.8482 | 20.8576 | Ruth Well Formation | basalt | Roebourne Group | GSWA/GA (unpubl.) | 3300 |
| 59244 | 119.9135 | 21.5645 | Carbana Pool Monzogranite | monzogranite | Emu Pool Supersuite | GSWA/GA (unpubl.) | 3307 |
| 59244#2 | 119.9135 | 21.5645 | Carbana Pool Monzogranite | monzogranite | Emu Pool Supersuite | GSWA/GA (unpubl.) | 3307 |
| 59270 | 119.8402 | 21.7156 | Mondana Monzogranite | monzogranite | Emu Pool Supersuite | GSWA/GA (unpubl.) | 3317 |
| 59363 | 119.8249 | 21.4766 | Corunna Downs Granitic Complex | tonalite | Tambina Supersuite | GSWA/GA (unpubl.) | 3420 |
| 59363#2 | 119.8249 | 21.4766 | Corunna Downs Granitic Complex | tonalite | Tambina Supersuite | GSWA/GA (unpubl.) | 3420 |
| 142170 | 118.5138 | 21.0900 | Kangan homestead | foliated monzogranite | Tambina Supersuite | GSWA/GA (unpubl.) | 3421 |
| 179871 | 120.0430 | 21.4634 | Panorama Formation | rhyolite | Warrawoona Group | GSWA/GA (unpubl.) | 3430 |
| 179873 | 120.0556 | 21.4614 | Panorama Formation | rhyolite | Warrawoona Group | GSWA/GA (unpubl.) | 3430 |
| 168915 | 119.7335 | 21.5684 | Panorama Formation | rhyolite | Warrawoona Group | GSWA/GA (unpubl.) | 3432 |
| 26218 | 119.3346 | 21.6486 | ?Pinnacle Well | | Sisters Supersuite | McCulloch (1987) | 3440 |
| 179737 | 119.5234 | 20.8037 | Apex Basalt | basalt | Warrawoona Group | GSWA/GA (unpubl.) | 3460 |
| SB611 | unknown | unknown | North Shaw Suite | foliated biotite granodiorite | Callina Supersuite | Bickle et al. (1993) | 3470 |
| SB615 | unknown | unknown | North Shaw Suite | foliated biotite granodiorite | Callina Supersuite | Bickle et al. (1993) | 3470 |
| SB616 | unknown | unknown | North Shaw Suite | foliated biotite granodiorite | Callina Supersuite | Bickle et al. (1993) | 3470 |
| A11-4 | 119.4575 | 21.3624 | North Shaw Tonalite | tonalite | Callina Supersuite | Bickle et al. (1993) | 3470 |
| A171-4 | 119.5632 | 21.4533 | Coolyia Creek Granodiorite | granodiorite | Callina Supersuite | Bickle et al. (1993) | 3470 |
| A195-1 | 119.3859 | 21.4388 | Coolyia Creek Granodiorite | granite | Callina Supersuite | Bickle et al. (1993) | 3470 |

(continued)

| Method | Sm | Nd | $^{147}Sm/Nd$ | $Sm^{143}/Nd^{144}$ | Error ($\times 10^{-6}$) | $Sm^{143}/Nb^{144}$ (normalized)[a] | Nd/Nd T | CHUR T | $E_{Nd}$ T | Model CHUR | Model DM | Model 2DM[b] |
|---|---|---|---|---|---|---|---|---|---|---|---|---|
| SHRIMP | 2.922 | 15.66 | 0.1128 | 0.510890 | 9 | 0.510890 | 0.508637 | 0.508721 | -1.65 | 3.17 | 3.41 | 3.40 |
| SHRIMP | 2.010 | 11.98 | 0.1013 | 0.510763 | 20 | 0.510775 | 0.508722 | 0.508663 | 1.15 | 2.98 | 3.22 | 3.23 |
| assumed | 2.210 | 17.14 | 0.0779 | 0.510288 | 20 | 0.510300 | 0.508704 | 0.508621 | 1.63 | 3.00 | 3.19 | 3.22 |
| assumed | 3.890 | 28.04 | 0.0838 | 0.510396 | 20 | 0.510408 | 0.508692 | 0.508621 | 1.38 | 3.01 | 3.21 | 3.24 |
| assumed | 1.938 | 15.11 | 0.0775 | 0.510295 | 8 | 0.510295 | 0.508700 | 0.508603 | 1.91 | 2.99 | 3.19 | 3.21 |
| SHRIMP | 15.344 | 69.81 | 0.1328 | 0.511418 | 7 | 0.511418 | 0.508685 | 0.508603 | 1.61 | 2.92 | 3.27 | 3.23 |
| SHRIMP | 6.495 | 32.06 | 0.1225 | 0.511154 | 9 | 0.511154 | 0.508635 | 0.508603 | 0.62 | 3.05 | 3.33 | 3.31 |
| SHRIMP | 2.930 | 12.53 | 0.1411 | 0.511573 | 20 | 0.511585 | 0.508681 | 0.508602 | 1.56 | 2.90 | 3.29 | 3.24 |
| assumed | 12.580 | 57.61 | 0.13205 | 0.511454 | 5 | 0.511454 | 0.508736 | 0.508602 | 2.65 | 2.80 | 3.17 | 3.15 |
| assumed | 8.074 | 39.12 | 0.12476 | 0.511254 | 5 | 0.511254 | 0.508686 | 0.508602 | 1.66 | 2.94 | 3.25 | 3.23 |
| SHRIMP | 2.030 | 9.07 | 0.1352 | 0.511448 | 20 | 0.511460 | 0.508677 | 0.508602 | 1.49 | 2.93 | 3.29 | 3.24 |
| SHRIMP | 3.730 | 11.69 | 0.1927 | 0.512666 | 20 | 0.512678 | 0.508712 | 0.508602 | 2.17 | -1.07 | 3.51 | 3.19 |
| SHRIMP | 3.530 | 18.79 | 0.1135 | 0.510964 | 20 | 0.510976 | 0.508640 | 0.508602 | 0.75 | 3.05 | 3.30 | 3.30 |
| SHRIMP | 5.330 | 23.93 | 0.1346 | 0.511442 | 20 | 0.511454 | 0.508682 | 0.508599 | 1.63 | 2.92 | 3.27 | 3.23 |
| assumed | 0.470 | 1.93 | 0.1467 | 0.511711 | 20 | 0.511723 | 0.508699 | 0.508595 | 2.04 | 2.81 | 3.26 | 3.20 |
| assumed | 4.690 | 20.06 | 0.1414 | 0.511579 | 20 | 0.511591 | 0.508676 | 0.508595 | 1.59 | 2.90 | 3.29 | 3.24 |
| assumed | 0.490 | 1.94 | 0.1516 | 0.511797 | 20 | 0.511809 | 0.508684 | 0.508595 | 1.74 | 2.83 | 3.30 | 3.23 |
| assumed | 3.330 | 10.48 | 0.1919 | 0.512610 | 20 | 0.512622 | 0.508666 | 0.508595 | 1.40 | 0.89 | 3.77 | 3.25 |
| assumed | 2.730 | 11.80 | 0.1397 | 0.511893 | 20 | 0.511905 | 0.509025 | 0.508595 | 8.46 | 1.99 | 2.58 | 2.72 |
| SHRIMP | 4.200 | 13.96 | 0.1817 | 0.512433 | 20 | 0.512445 | 0.508699 | 0.508595 | 2.05 | 2.08 | 3.40 | 3.20 |
| SHRIMP | 3.450 | 10.83 | 0.1926 | 0.512661 | 20 | 0.512673 | 0.508703 | 0.508595 | 2.11 | -0.86 | 3.53 | 3.20 |
| assumed | 7.501 | 34.959 | 0.1297 | 0.511336 | 6 | 0.511336 | 0.508661 | 0.508593 | 1.34 | 2.97 | 3.29 | 3.26 |
| assumed | 6.665 | 32.78 | 0.12289 | 0.511308 | 6 | 0.511308 | 0.508771 | 0.508589 | 3.58 | 2.76 | 3.10 | 3.09 |
| assumed | 7.450 | 43.55 | 0.1034 | 0.510667 | 20 | 0.510679 | 0.508513 | 0.508529 | -0.33 | 3.20 | 3.41 | 3.42 |
| assumed | 3.880 | 24.13 | 0.0973 | 0.510613 | 20 | 0.510625 | 0.508587 | 0.508529 | 1.13 | 3.08 | 3.30 | 3.31 |
| assumed | 7.530 | 57.41 | 0.0793 | 0.510053 | 20 | 0.510065 | 0.508388 | 0.50849 | -2.01 | 3.33 | 3.49 | 3.58 |
| assumed | 3.190 | 10.06 | 0.1915 | 0.512704 | 20 | 0.512716 | 0.508666 | 0.50849 | 3.46 | -1.95 | 3.06 | 3.16 |
| assumed | 0.310 | 0.76 | 0.2473 | 0.513375 | 20 | 0.513387 | 0.508157 | 0.50849 | -6.55 | 2.21 | 1.01 | 3.92 |
| assumed | 4.290 | 13.62 | 0.1906 | 0.512584 | 20 | 0.512596 | 0.508565 | 0.50849 | 1.48 | 1.35 | 3.72 | 3.31 |
| assumed | 0.470 | 1.24 | 0.2284 | 0.513337 | 20 | 0.513349 | 0.508519 | 0.50849 | 0.56 | 3.34 | 1.91 | 3.38 |
| assumed | 1.320 | 3.98 | 0.1999 | 0.512790 | 20 | 0.512802 | 0.508574 | 0.50849 | 1.66 | 7.10 | 3.98 | 3.30 |
| assumed | 3.380 | 14.09 | 0.1451 | 0.511518 | 20 | 0.511530 | 0.508461 | 0.50849 | -0.57 | 3.28 | 3.60 | 3.47 |
| assumed | 4.790 | 19.64 | 0.1473 | 0.511516 | 20 | 0.511528 | 0.508413 | 0.50849 | -1.52 | 3.43 | 3.73 | 3.54 |
| assumed | 1.250 | 3.75 | 0.2010 | 0.512859 | 20 | 0.512871 | 0.508620 | 0.50849 | 2.56 | 7.66 | 3.50 | 3.23 |
| assumed | 0.220 | 0.69 | 0.1964 | 0.512699 | 20 | 0.512711 | 0.508557 | 0.50849 | 1.32 | -34.77 | 3.97 | 3.32 |
| assumed | 6.190 | 35.02 | 0.1069 | 0.510824 | 20 | 0.510836 | 0.508575 | 0.50849 | 1.67 | 3.06 | 3.30 | 3.30 |
| assumed | 2.120 | 12.36 | 0.1038 | 0.510645 | 20 | 0.510657 | 0.508462 | 0.50849 | -0.56 | 3.25 | 3.45 | 3.47 |
| assumed | 7.200 | 54.75 | 0.0795 | 0.509999 | 20 | 0.510011 | 0.508330 | 0.50849 | -3.16 | 3.40 | 3.55 | 3.66 |
| SHRIMP | 2.400 | 16.43 | 0.0885 | 0.510388 | 20 | 0.510400 | 0.508507 | 0.508443 | 1.26 | 3.15 | 3.34 | 3.36 |
| assumed | 3.420 | 12.98 | 0.1591 | 0.511824 | 6 | 0.511824 | 0.508417 | 0.508438 | -0.41 | 3.32 | 3.71 | 3.49 |
| assumed | 5.140 | 27.54 | 0.1127 | 0.510827 | 6 | 0.510827 | 0.508413 | 0.508438 | -0.48 | 3.28 | 3.50 | 3.49 |
| assumed | 5.640 | 23.94 | 0.1425 | 0.511438 | 5 | 0.511438 | 0.508387 | 0.508438 | -1.00 | 3.38 | 3.66 | 3.53 |
| assumed | 6.180 | 26.97 | 0.1384 | 0.511378 | 6 | 0.511378 | 0.508413 | 0.508438 | -0.48 | 3.30 | 3.59 | 3.49 |
| SHRIMP | 2.940 | 14.95 | 0.1191 | 0.510981 | 20 | 0.510993 | 0.508441 | 0.508435 | 0.12 | 3.23 | 3.47 | 3.45 |
| SHRIMP | 6.340 | 45.82 | 0.0837 | 0.510201 | 20 | 0.510213 | 0.508418 | 0.508432 | -0.28 | 3.26 | 3.43 | 3.48 |
| SHRIMP | 6.290 | 43.74 | 0.0869 | 0.510219 | 20 | 0.510231 | 0.508368 | 0.508432 | -1.27 | 3.33 | 3.50 | 3.56 |
| SHRIMP | 3.870 | 27.06 | 0.0864 | 0.510226 | 20 | 0.510238 | 0.508381 | 0.508422 | -0.81 | 3.31 | 3.48 | 3.53 |
| SHRIMP | 2.851 | 15.95 | 0.1080 | 0.510710 | 9 | 0.510710 | 0.508382 | 0.50841 | -0.55 | 3.31 | 3.51 | 3.52 |
| SHRIMP | 2.508 | 13.40 | 0.1131 | 0.510837 | 7 | 0.510837 | 0.508397 | 0.508405 | -0.16 | 3.28 | 3.50 | 3.49 |
| assumed | 3.420 | 20.23 | 0.1021 | 0.510638 | 20 | 0.510650 | 0.508443 | 0.508398 | 0.88 | 3.20 | 3.41 | 3.42 |
| assumed | 2.960 | 17.11 | 0.1047 | 0.510673 | 20 | 0.510685 | 0.508422 | 0.508398 | 0.47 | 3.23 | 3.44 | 3.45 |
| SHRIMP | 3.190 | 18.43 | 0.1045 | 0.510645 | 20 | 0.510657 | 0.508398 | 0.508398 | 0.00 | 3.27 | 3.47 | 3.48 |
| assumed | 3.090 | 16.94 | 0.1101 | 0.510834 | 20 | 0.510846 | 0.508466 | 0.508398 | 1.34 | 3.15 | 3.39 | 3.38 |
| assumed | 0.670 | 1.77 | 0.2302 | 0.513407 | 12 | 0.513419 | 0.508443 | 0.508398 | 0.88 | 3.47 | 2.34 | 3.42 |
| assumed | 4.770 | 16.05 | 0.1796 | 0.512290 | 8 | 0.512302 | 0.508420 | 0.508398 | 0.43 | 3.08 | 3.82 | 3.45 |
| assumed | 2.680 | 15.17 | 0.1070 | 0.510664 | 20 | 0.510676 | 0.508342 | 0.508359 | -0.34 | 3.33 | 3.53 | 3.53 |
| assumed | 3.880 | 15.43 | 0.1521 | 0.511687 | 20 | 0.511699 | 0.508381 | 0.508359 | 0.43 | 3.23 | 3.60 | 3.48 |
| SHRIMP | 3.200 | 16.89 | 0.1147 | 0.510858 | 20 | 0.510870 | 0.508362 | 0.508349 | 0.25 | 3.28 | 3.50 | 3.50 |
| SHRIMP | 3.260 | 16.93 | 0.1163 | 0.510901 | 20 | 0.510913 | 0.508370 | 0.508349 | 0.41 | 3.27 | 3.50 | 3.48 |
| SHRIMP | 2.260 | 11.56 | 0.1180 | 0.510988 | 20 | 0.511000 | 0.508412 | 0.508336 | 1.49 | 3.17 | 3.42 | 3.41 |
| assumed | 4.680 | 32.20 | 0.0878 | 0.510282 | 20 | 0.510294 | 0.508308 | 0.508201 | 2.11 | 3.27 | 3.45 | 3.45 |
| assumed | 4.660 | 32.30 | 0.0872 | 0.510255 | 20 | 0.510267 | 0.508295 | 0.508201 | 1.84 | 3.29 | 3.46 | 3.47 |
| SHRIMP | 8.020 | 45.67 | 0.1061 | 0.510520 | 20 | 0.510532 | 0.508131 | 0.5082 | -1.34 | 3.53 | 3.70 | 3.71 |
| assumed | 4.150 | 29.99 | 0.0836 | 0.510115 | 20 | 0.510127 | 0.508230 | 0.508188 | 0.84 | 3.37 | 3.53 | 3.55 |
| assumed | 3.480 | 19.85 | 0.1060 | 0.510642 | 20 | 0.510654 | 0.508249 | 0.508188 | 1.21 | 3.33 | 3.52 | 3.53 |
| SHRIMP | 5.880 | 34.61 | 0.1028 | 0.510543 | 20 | 0.510555 | 0.508222 | 0.508185 | 0.72 | 3.37 | 3.56 | 3.56 |
| Pb–Pb isochron | 4.800 | 33.90 | 0.0855 | 0.509350 | 20 | 0.510163 | 0.508218 | 0.508175 | 0.85 | 3.38 | 3.54 | 3.56 |
| assumed | 1.270 | 3.90 | 0.1965 | 0.512677 | 20 | 0.512689 | 0.508192 | 0.508148 | 0.86 | -33.19 | 4.18 | 3.58 |
| Pb–Pb isochron | 4.275 | 28.07 | 0.0920 | 0.510208 | 16 | 0.510208 | 0.508095 | 0.508135 | -0.78 | 3.53 | 3.67 | 3.71 |
| Pb–Pb isochron | 5.430 | 35.33 | 0.0929 | 0.510191 | 28 | 0.510191 | 0.508059 | 0.508135 | -1.49 | 3.58 | 3.72 | 3.76 |
| Pb–Pb isochron | 4.983 | 32.43 | 0.0929 | 0.510319 | 12 | 0.510319 | 0.508188 | 0.508135 | 1.04 | 3.39 | 3.56 | 3.57 |
| SHRIMP | 5.794 | 40.63 | 0.0862 | 0.510154 | 14 | 0.510154 | 0.508176 | 0.508135 | 0.81 | 3.41 | 3.57 | 3.59 |
| SHRIMP | 5.384 | 34.11 | 0.0954 | 0.510410 | 12 | 0.510410 | 0.508221 | 0.508135 | 1.69 | 3.34 | 3.52 | 3.52 |
| SHRIMP | 4.957 | 21.38 | 0.1401 | 0.511324 | 18 | 0.511324 | 0.508108 | 0.508135 | -0.53 | 3.54 | 3.78 | 3.69 |

## Appendix 2.

| *Sample* | *Easting* | *Northing* | *Unit* | *Lithology* | *Group/Suite/ Supersuite* | *Source of isotopic data* | *Age* |
|---|---|---|---|---|---|---|---|
| A207-1 | 119.4351 | 21.3519 | North Shaw Tonalite | tonalite | Callina Supersuite | Bickle et al. (1993) | 3470 |
| EM59 | unknown | unknown | Euro Basalt | basalt | Kelly Group | Arndt et al. (2001) | 3470 |
| EM69 | unknown | unknown | Euro Basalt | basalt | Kelly Group | Arndt et al. (2001) | 3470 |
| EM70 | unknown | unknown | Euro Basalt | basalt | Kelly Group | Arndt et al. (2001) | 3470 |
| EM71 | unknown | unknown | Euro Basalt | basalt | Kelly Group | Arndt et al. (2001) | 3470 |
| EM82 | unknown | unknown | Euro Basalt | basalt | Kelly Group | Arndt et al. (2001) | 3470 |
| 179711 | 119.8374 | 20.9424 | Duffer Formation | dacite | Warrawoona Group | GSWA/GA (unpubl.) | 3470 |
| 179713 | 119.8374 | 20.9329 | Duffer Formation | dacite | Warrawoona Group | GSWA/GA (unpubl.) | 3470 |
| 179718 | 119.9300 | 20.9324 | Duffer Formation | andesite | Warrawoona Group | GSWA/GA (unpubl.) | 3470 |
| 49250 | 120.1513 | 21.4486 | Duffer Formation | dacite | Warrawoona Group | McCulloch (1987) | 3470 |
| 168920 | 119.6019 | 21.3653 | Duffer Formation – 'Pidgeon Rock' | | Warrawoona Group | GSWA/GA (unpubl.) | 3470 |
| 179731 | 119.5336 | 20.8076 | Mount Ada Basalt | basalt | Warrawoona Group | GSWA/GA (unpubl.) | 3475 |
| 153188 | 119.0848 | 21.0450 | Carlindi Granitic Complex | granodiorite | Callina Supersuite | GSWA/GA (unpubl.) | 3484 |
| 15255 | 119.4180 | 21.4819 | North Shaw Suite | granite | Callina Supersuite | McCulloch (1987) | 3493 |
| 179760 | 119.0948 | 21.0866 | Coonterunah Subgroup | basalt | Warrawoona Group | GSWA/GA (unpubl.) | 3515 |
| 179775 | 119.0924 | 21.1031 | Coonterunah Subgroup | andesite | Warrawoona Group | GSWA/GA (unpubl.) | 3515 |
| 179806 | 119.0420 | 21.1151 | Coonterunah Subgroup | basalt | Warrawoona Group | GSWA/GA (unpubl.) | 3515 |
| 179782 | 119.0879 | 21.1104 | Coonterunah Subgroup | basalt | Warrawoona Group | GSWA/GA (unpubl.) | 3515 |
| 179791 | 119.0770 | 21.1231 | Coucal Formation | andesite | Warrawoona Group | GSWA/GA (unpubl.) | 3515 |
| 168995 | 119.4524 | 20.8343 | Coucal Formation | rhyolite | Warrawoona Group | GSWA/GA (unpubl.) | 3515 |
| 142870 | 120.5688 | 20.8114 | Warrawagine Granitic Complex | tonalite gneiss | unknown | GSWA/GA (unpubl.) | 3576 |
| 142870r | 120.5688 | 20.8112 | Warrawagine Granitic Complex | tonalite gneiss | unknown | GSWA/GA (unpubl.) | 3576 |

**NOTES:** (a) Normalized to BCR-1 =0.512653 and La Jolla=0.511872
(b) $Sm^{147}/Nd^{144}$ assumed to be 0.11 in the source

(continued)

| Method | Sm | Nd | $^{147}Sm/Nd$ | $Sm^{143}/Nd^{144}$ | Error ($\times 10^{-6}$) | $Sm^{143}/Nb^{144}$ (normalized)[a] | Nd/Nd T | CHUR T | $E_{Nd}$ T | Model CHUR | Model DM | Model 2DM[b] |
|---|---|---|---|---|---|---|---|---|---|---|---|---|
| SHRIMP | 4.645 | 31.44 | 0.0893 | 0.510224 | 14 | 0.510224 | 0.508175 | 0.508135 | 0.78 | 3.41 | 3.57 | 3.59 |
| SHRIMP | 0.980 | 2.87 | 0.2066 | 0.512881 | 16 | 0.512893 | 0.508151 | 0.508135 | 0.31 | 3.71 | 5.79 | 3.63 |
| SHRIMP | 0.970 | 2.96 | 0.1972 | 0.512679 | 10 | 0.512691 | 0.508165 | 0.508135 | 0.58 | 12.06 | 4.34 | 3.61 |
| SHRIMP | 0.920 | 2.97 | 0.1952 | 0.512656 | 11 | 0.512668 | 0.508188 | 0.508135 | 1.03 | -1.85 | 4.06 | 3.57 |
| SHRIMP | 0.820 | 2.53 | 0.1959 | 0.512672 | 11 | 0.512684 | 0.508187 | 0.508135 | 1.03 | -6.64 | 4.08 | 3.57 |
| SHRIMP | 1.120 | 3.77 | 0.1803 | 0.512330 | 6 | 0.512342 | 0.508204 | 0.508135 | 1.35 | 2.84 | 3.72 | 3.55 |
| assumed | 2.770 | 16.83 | 0.0997 | 0.510476 | 20 | 0.510488 | 0.508200 | 0.508135 | 1.27 | 3.37 | 3.55 | 3.55 |
| assumed | 3.750 | 20.81 | 0.1090 | 0.510713 | 20 | 0.510725 | 0.508223 | 0.508135 | 1.73 | 3.32 | 3.52 | 3.52 |
| assumed | 3.080 | 17.23 | 0.1082 | 0.510660 | 20 | 0.510672 | 0.508188 | 0.508135 | 1.05 | 3.38 | 3.57 | 3.57 |
| SHRIMP | 5.200 | 28.90 | 0.1083 | 0.509830 | 20 | 0.510644 | 0.508158 | 0.508135 | 0.45 | 3.43 | 3.62 | 3.62 |
| SHRIMP | 3.170 | 18.25 | 0.1050 | 0.510572 | 20 | 0.510584 | 0.508174 | 0.508135 | 0.76 | 3.41 | 3.59 | 3.59 |
| assumed | 2.601 | 8.69 | 0.1809 | 0.512314 | 20 | 0.512326 | 0.508168 | 0.508129 | 0.77 | 3.10 | 3.86 | 3.60 |
| SHRIMP | 2.030 | 12.18 | 0.1007 | 0.510489 | 20 | 0.510501 | 0.508180 | 0.508117 | 1.25 | 3.39 | 3.56 | 3.57 |
| SHRIMP | 5.900 | 37.80 | 0.0949 | 0.509520 | 20 | 0.510333 | 0.508140 | 0.508105 | 0.70 | 3.44 | 3.60 | 3.62 |
| assumed | 3.300 | 11.63 | 0.1717 | 0.512128 | 20 | 0.512140 | 0.508147 | 0.508076 | 1.40 | 3.09 | 3.69 | 3.58 |
| assumed | 3.710 | 17.27 | 0.1300 | 0.511174 | 20 | 0.511186 | 0.508163 | 0.508076 | 1.71 | 3.32 | 3.57 | 3.56 |
| assumed | 5.360 | 23.71 | 0.1367 | 0.511288 | 20 | 0.511300 | 0.508121 | 0.508076 | 0.89 | 3.40 | 3.66 | 3.62 |
| assumed | 6.180 | 25.25 | 0.1481 | 0.511555 | 20 | 0.511567 | 0.508123 | 0.508076 | 0.93 | 3.37 | 3.68 | 3.62 |
| assumed | 7.550 | 33.97 | 0.1344 | 0.511222 | 20 | 0.511234 | 0.508109 | 0.508076 | 0.64 | 3.44 | 3.68 | 3.64 |
| SHRIMP | 6.680 | 31.55 | 0.1281 | 0.511091 | 20 | 0.511103 | 0.508124 | 0.508076 | 0.95 | 3.41 | 3.64 | 3.62 |
| SHRIMP | 6.480 | 34.56 | 0.1134 | 0.510730 | 20 | 0.510742 | 0.508059 | 0.507996 | 1.24 | 3.46 | 3.65 | 3.65 |
| SHRIMP | 6.620 | 35.80 | 0.1118 | 0.510705 | 20 | 0.510717 | 0.508071 | 0.507996 | 1.49 | 3.44 | 3.63 | 3.63 |

This Report draws together geochemical studies emanating from the mapping of the 3.65 to 2.83 Ga Pilbara Craton by the Geological Survey of Western Australia and Geoscience Australia between 1994 and 2004. New geochemical data are presented for 438 whole-rock samples of volcanic rocks from the East Pilbara Terrane, the West Pilbara Superterrane, and the De Grey Superbasin. Results show the basaltic rocks of the East Pilbara Terrane were derived from sources apparently unrelated to subduction processes. By contrast, the younger basaltic rocks of the West Pilbara Superterrane and De Grey Superbasin were derived from an enriched-mantle source formed during a 3.2 to 3.1 Ga subduction event.
The new geochemical dataset is included as an Appendix to the Report.

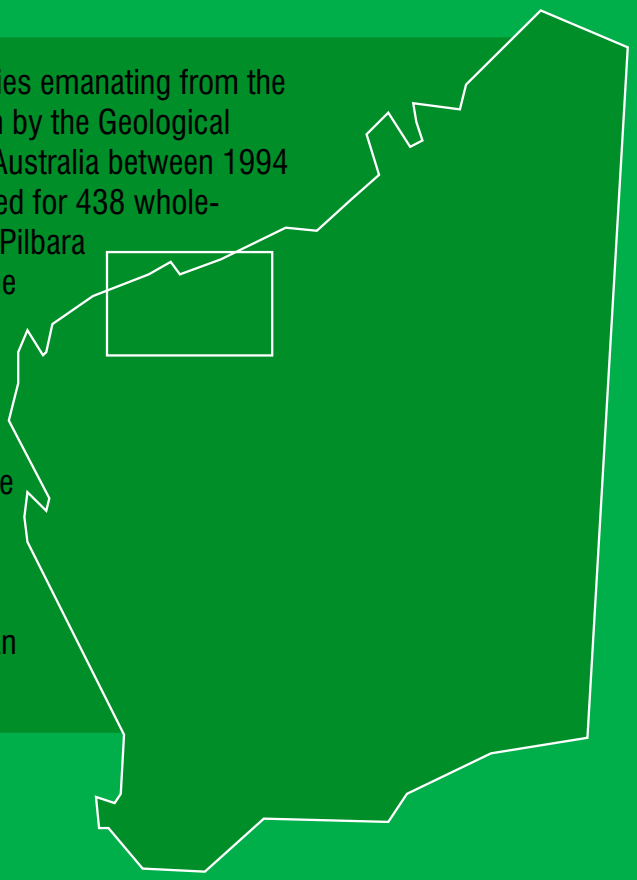

SMITHIES et al.

Geochemistry of volcanic rocks of the northern Pilbara Craton, Western Australia

REPORT 104

**This Report is published in digital format (PDF) and is available online at: www.doir.wa.gov.au/GSWA/publications. Laser-printed copies can be ordered from the Information Centre for the cost of printing and binding.**

**Further details of geological publications and maps produced by the Geological Survey of Western Australia are available from:**

**Information Centre**
**Department of Industry and Resources**
**100 Plain Street**
**East Perth, WA 6004**
**Phone: (08) 9222 3459 Fax: (08) 9222 3444**

**www.doir.wa.gov.au/GSWA/publications**